SOLID STATE PHYSICS, VOLUME 42

The Structure of $Y_1Ba_2Cu_3O_{7-\delta}$ and Its Derivatives

R. BEYERS

IBM Research Division
Almaden Research Center
San Jose, California

T. M. SHAW

IBM Research Division
Thomas J. Watson Research Center
Yorktown Heights, New York

I. Introduction

In 1986, Georg Bednorz and Alex Müller discovered superconductivity above 30 K in the La–Ba–Cu–O system.[1,2] Several groups quickly

[1]J. G. Bednorz and K. A. Müller, *Z. Phys. B* **64**, 189 (1986).
[2]J. G. Bednorz, M. Takashige, and K. A. Müller, *Europhys. Lett.* **3**, 379 (1987).

ISBN 0-12-607742-8
ISBN 0-12-607790-8 (pbk.)

reproduced their results and identified the superconducting phase as $La_{2-x}Ba_xCuO_4$. Many researchers then began to determine the effects of elemental substitutions and different processing conditions on the structure and superconducting properties of this oxide. Following this approach, in 1987, Paul Chu, Maw-Kuen Wu, and coworkers discovered superconductivity above 90 K in the Y–Ba–Cu–O system.[3] As before, the discovery was quickly reproduced, the 90 K phase was identified as $Y_1Ba_2Cu_3O_7$, and studies of the effects of substitutions and processing conditions were initiated. This cycle has been repeated twice in 1988 with the independent discoveries of superconductivity above 100 K in the Bi–Ca–Sr–Cu–O system by Hiroshi Maeda and coworkers[4] and in the Tl–Ca–Ba–Cu–O system by Allen Hermann and Zhengzhi Sheng.[5,6]

The purpose of this article is to give an overview of the structural studies performed on these superconducting oxides. We focus primarily on $Y_1Ba_2Cu_3O_{7-\delta}$, nicknamed the 123 structure, because this structure has been the most extensively studied to date. In the first two sections, we describe the basic atomic arrangements in $Y_1Ba_2Cu_3O_{7-\delta}$ and how these arrangements change as a function of processing. We then discuss the defects that are commonly found in the 123 structure, some of which play a dominant role in controlling superconducting properties. Next, we summarize the studies of elemental substitutions for Y, Ba, Cu and/or O in 123, and we compare 123 with the other families of superconducting oxides. These studies have both theoretical and practical interest because they provide clues to the roles that various structural features play in the mechanism of high-temperature superconductivity, which, in turn, may aid in the discovery of even higher temperature superconductors. Finally, we draw some conclusions and make suggestions for future structural studies. In all but the final section, we try to emphasize what is known and generally agreed upon about these oxides. The last section, however, is largely our own opinion and more speculative in nature.

II. Basic Structure

Soon after the discovery and confirmation of superconductivity in the Y–Ba–Cu–O system,[3,7–10] the phase responsible for the 90 K transition

[3]W. K. Wu, J. R. Ashburn, C. J. Torng, P. H. Hor, R. L. Meng, L. Gao, Z. J. Huang, Y. Q. Wang, and C. W. Chu, *Phys. Rev. Lett.* **58,** 908 (1987).

[4]M. Maeda, Y. Tanaka, M. Fukutomi, and A. Asano, *Jpn. J. Appl. Phys.* **27,** L209 (1988).

[5]Z. Z. Sheng and A. M. Hermann, *Nature* **332,** 55 (1988).

[6]Z. Z. Sheng and A. M. Hermann, *Nature* **332,** 138 (1988).

was found to have a cation stoichiometry of 1Y:2Ba:3Cu. The unit cell dimensions determined by electron and x-ray diffraction identified the structure as being related to a cubic perovskite with one of the cube axes tripled.[11–23] In the basic perovskite structure ABO_3, there are two cation sites.[24] The A site lies at the center of a cage formed by corner-sharing anion octahedra and accommodates the larger cations in the structure. The B site lies at the centers of the anion octahedra and accommodates the smaller cations. It was therefore natural to place the larger Y and Ba ions in the A sites and the smaller Cu ions in the B sites. The tripling of

[7]Z. Zhao, L. Chen, Q. Yang, Y. Huang, G. Chen, R. Tang, G. Liu, C. Cui, L. Chen, L. Wang, S. Guo, S. Li, and J. Bi, *Kexue Tongbao* **32,** 1098 (1987).

[8]P. Ganguly, R. A. Mohan Ram, K. Sreedhar, and C. N. R. Rao, *Pramana J. Phys.* **28,** L321 (1987).

[9]J. M. Tarascon, L. H. Greene, W. R. McKinnon, and G. W. Hull, *Phys. Rev. B.* **35,** 7115 (1987).

[10]S. J. Hwu, S. N. Song, J. Thiel, K. R. Poeppelmeier, J. B. Ketterson, and A. J. Freeman, *Phys. Rev. B* **35,** 7119 (1987).

[11]R. J. Cava, B. Batlogg, R. B. van Dover, D. W. Murphy, S. Sunshine, T. Siegrist, J. P. Remeika, E. A. Rietman, S. Zahurak, and G. P. Espinosa, *Phys. Rev. Lett.* **58,** 1676 (1987).

[12]P. M. Grant, R. B. Beyers, E. M. Engler, G. Lim, S. S. P. Parkin, M. L. Ramirez, V. Y. Lee, A. Nazzal, J. E. Vazquez, and R. J. Savoy, *Phys. Rev. B.* **35,** 7242 (1987).

[13]R. M. Hazen, L. W. Finger, R. J. Angel, C. T. Prewitt, N. L. Ross, H. K. Mao, C. G. Hadidiacos, P. H. Hor, R. L. Meng, and C. W. Chu, *Phys. Rev. B* **35,** 7238 (1987).

[14]W. R. McKinnon, J. M. Tarascon, L. H. Greene, G. W. Hull, and D. A. Hwang, *Phys. Rev. B* **35,** 7245 (1987).

[15]W. J. Gallagher, R. L. Sandstrom, T. R. Dinger, T. M. Shaw, and D. A. Chance, *Solid State Commun.* **63,** 147 (1987).

[16]D. G. Hinks, L. Soderholm, D. W. Capone II, J. D. Jorgensen, and Ivan K. Schuller, *Appl. Phys. Lett.* **50,** 1688 (1987).

[17]T. Hatano, A. Matsushita, K. Nakamura, K. Honda, T. Matsumoto, and K. Ogawa, *Jpn. J. Appl. Phys.* **26,** L374 (1987).

[18]Y. Kitano, K. Kifune, I. Mukouda, H. Kamimura, J. Sakurai, Y. Komura, K. Hoshino, M. Suzuki, A. Minami, Y. Maeno, M. Kato, and T. Fujita, *Jpn. J. Appl. Phys.* **26,** L394 (1987).

[19]M. Hirabayashi, H. Ihara, N. Tereda, K. Senzaki, K. Hayashi, S. Waki, K. Murata, M. Tomumoto, and Y. Kimura, *Jpn. J. Appl. Phys.* **26,** L454 (1987).

[20]E. Takayama-Muromachi, Y. Uchida, Y. Matsui, and K. Kato, *Jpn. J. Appl. Phys.* **26,** L476 (1987).

[21]Y. Syono, M. Kikuchi, K. Ohishi, K. Hiraga, H. Arai, Y. Matsui, N. Kobayashi, T. Sasaoka, and Y. Muto, *Jpn. J. Appl. Phys.* **26,** L498 (1987).

[22]K. Semba, S. Tsurumi, M. Hikita, T. Iwata, J. Noda, and S. Kurihara, *Jpn. J. Appl. Phys.* **26,** L429 (1987).

[23]S. B. Qadri, L. E. Toth, M. Osofsky, S. Lawrence, D. U. Gubser, and S. A. Wolf, *Phys. Rev. B* **35,** 7235 (1987).

[24]J. B. Goodenough and M. Longo, *in* "Landolt-Börnstein" (K.-H. Hellwege and A. M. Hellwege, eds.), Group II.Vol. 4a, Chapter 3a, Springer-Verlag, New York, 1970.

the perovskite unit cell could then be accounted for by ordering the Y and Ba ions in the *A* sites such that the top and bottom cells in a stack of three contained Ba ions, while the middle cell contained a Y ion. This basic cation arrangement was not only consistent with the 1Y:2Ba:3Cu stoichiometry but also provided a reasonable fit to x-ray powder diffraction data obtained from nearly single-phase materials[11–14] and accounted for contrast seen in high-resolution images of the structure.[25–29] These results confirmed that the alternative suggestion[19,23] that the structure was related to the $La_3Ba_3Cu_6O_{14}$ structure proposed by Er-Rakho[30] was incorrect.

There are 3 anions per unit cell in the ideal perovskite structure, corresponding to 9 possible oxygen sites in a tripled perovskite unit cell. Formal balancing of the charges on the cations requires a maximum of 8 oxygen ions per unit cell if all of the copper is assumed to be in a +3 state, and 6.5 and 5 oxygen ions per unit cell if charges of +2 and +1 are assumed for all the copper cations. It was therefore clear that the 123 structure was oxygen deficient relative to the ideal perovskite structure. X-ray diffraction from small single crystals extracted from sintered polycrystalline material confirmed and refined the basic positions of the cations and also identified where the oxygen deficiency was accommodated in the structure.[13,14,31,32] The x-ray data clearly showed that the Y ion was surrounded by only 8 oxygen ions rather than by 12 as in the ideal perovskite structure. Oxygen deficiency was also noted in the basal copper plane between the Ba ions. Anion sites in this plane, which lie along the cell edges, were found to be only half occupied.[14,31,32] Refinements of the cell parameters in several studies[11,12,14,20,21,31] indicated that the unit cell was orthorhombic with *b* slightly larger than *a*, even though some single crystal studies[13,14,31,32] observed a tetragonal distribution of diffracted intensities. It was noted later that this apparent

[25]R. Beyers, G. Lim, E. M. Engler, R. J. Savoy, T. M. Shaw, T. R. Dinger, W. J. Gallagher, and R. L. Sandstrom, *Appl. Phys. Lett.* **50,** 1918 (1987).

[26]A. Ourmazd, J. A. Rentschler, J. C. H. Spence, M. O'Keeffe, R. J. Graham, D. W. Johnson Jr., and W. W. Rhodes, *Nature* **327,** 308 (1987).

[27]E. A. Hewat, M. Dupuy, A. Bourret, J. J. Capponi, and M. Marezio, *Nature* **327,** 400 (1987).

[28]Y. Matsui, E. Takayama-Muromachi, A. Ono, S. Horiuchi, and K. Kato, *Jpn. J. Appl. Phys.* **26,** L777 (1987).

[29]K. Hiraga, D. Shindo, M. Hirabayashi, M. Kikuchi, K. Oh-Ishi, and Y. Syono, *Jpn. J. Appl. Phys.* **26,** L1071 (1987).

[30]L. Er-Rakho, C. Michel, J. Provost, and B. Raveau, *J. Solid State Chem.* **37,** 151 (1981).

[31]T. Siegrist, S. Sunshine, D. W. Murphy, R. J. Cava, and S. M. Zahurak, *Phys. Rev. B* **35,** 7137 (1987).

[32]F. P. Okamura, S. Sueno, I. Nakai, and A. Ono, *Mat. Res. Bull.* **22,** 1081 (1987).

discrepancy was probably caused by microdomain twinning which prevented oxygen ordering in the single crystals from being observed by x-ray diffraction techniques. The twinning was readily apparent in transmission electron microscope (TEM) images of the material.[21,25]

The source of the orthorhombic distortion in the 123 structure was finally revealed by neutron diffraction data refined using the Rietveld technique.[33–41] The advantage of Rietveld refinement[42] is that the structure can be deduced directly from neutron powder diffraction data by fitting the data with calculated diffraction scans. Thus the larger scattering cross-section for oxygen by neutrons relative to x-rays can be taken advantage of without the need for large single crystals. The neutron diffraction experiments showed unambiguously that the oxygens in the basal copper plane of the unit cell were ordered in the orthorhombic structure and that the 90 K material contained nearly seven oxygens per unit cell.

The essential features of the orthorhombic structure are shown in Fig. 1, and atomic coordinates and thermal parameters for each atom, which agree well with those originally determined by Seigrest *et al.*,[31] are given in Table I.[43] The effect of oxygen ordering in the basal plane of the structure is to occupy one of the oxygen sites along a cell edge and to leave the other site vacant. The cell edge with the occupied site is thus lengthened relative to the cell edge with the vacant oxygen site, producing an orthorhombic unit cell. The ordering puts the copper ions in the basal plane of the structure, at the center of square arrangements

[33]J. J. Capponi, C. Chaillout, A. W. Hewat, P. Lejay, M. Marezio, N. Nguyen, B. Raveau, J. L. Soubeyroux, J. L. Tholence, and R. Tournier, *Europhys. Lett.* **3,** 1301 (1987).

[34]M. A. Beno, L. Soderholm, D. W. Capone, D. G. Hinks, J. D. Jorgensen, I. K. Schuller, C. U. Segre, K. Zhan, and J. D. Grace, *Appl. Phys. Lett.* **51,** 57 (1987).

[35]F. Beech, S. Miraglia, A. Santoro, and R. S. Roth, *Phys. Rev. B* **35,** 8778 (1987).

[36]J. E. Greedan, A. O'Reilly, and C. V. Stager, *Phys. Rev. B* **35,** 8770 (1987).

[37]F. Izumi, H. Asano, T. Ishigaki, E. Takayama-Muromachi, Y. Uchida, N. Watanabe, and T. Nishikawa, *Jpn. J. Appl. Phys.* **26,** L649 (1987).

[38]M. Francois, E. Walker, J. L. Jorda, and K. Yvon, *Solid State Commun.* **63,** 1149 (1987).

[39]T. Kajitani, K. Oh-Ishi, M. Kikuchi, Y. Syono, and M. Hirabayashi, *Jpn. J. Appl. Phys.* **26,** L1144 (1987).

[40]Q. W. Yan, P. L. Zhang, Z. G. Shen, J. K. Zhao, Y. Ren, Y. N. wei, T. D. Mao, C. X. Liu, T. S. Ning, K. Sun, and Q. S. Yang, *Phys. Rev. B* **36,** 5599 (1987).

[41]W. I. F. David, W. T. A. Harrison, J. M. F. Gunn, O. Moze, A. K. Soper, P. Day, J. D. Jorgensen, D. G. Hinks, M. A. Beno, L. Solderholm, D. W. Capone II, I. K. Schuller, C. U. Segres, K. Zhang, and J. D. Grace, *Nature* **327,** 310 (1987).

[42]L. M. Rietveld, *J. Appl. Cryst.* **2,** 65 (1969).

[43]A. Williams, G. H. Kwei, R. B. Von Dreele, A. C. Larson, I. D. Raistrick, and D. L. Bish, *Phys. Rev. B* **37,** 7960 (1988).

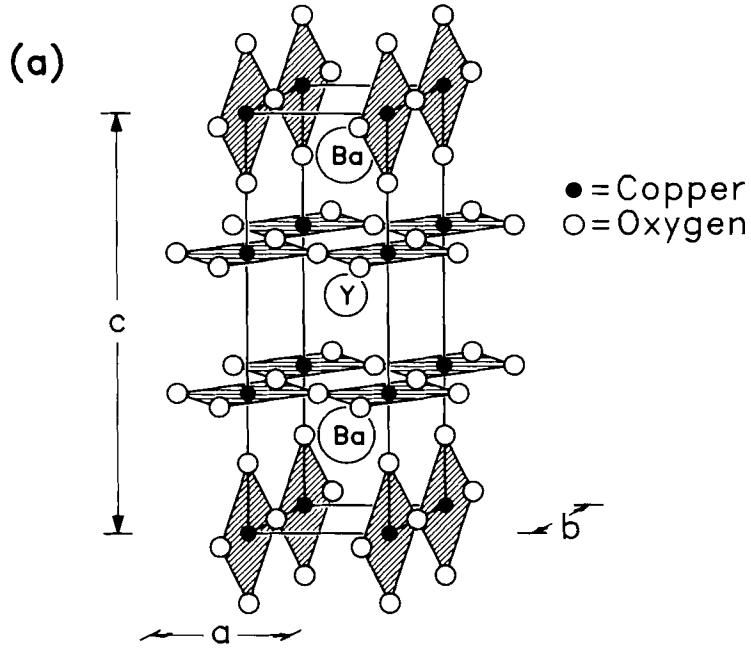

FIG. 1. The structure of $Y_1Ba_2Cu_3O_{7-\delta}$. In (a) the coordination of copper with oxygen is emphasized to show the location of copper-oxygen planes and chains in the structure. In (b) nearest-neighbor bonds are drawn in to show the puckering of the copper-oxygen planes. The notation used for the oxygen positions in this figure is used consistently throughout the remainder of this review. Note, however, that the oxygen site designations are often interchanged in the literature, especially the O(1) and O(4) sites.

of oxygen ions. The square planar arrangements of copper and oxygen ions are then linked together by sharing their corners to form "linear chains" along the *b* axis of the structure. A recent neutron diffraction study suggests that the chains may not be perfectly linear.[44] The effect of vacant oxygen sites around the Y ion can also be seen in Fig. 1. The absence of oxygen from the Y plane places the copper ions in five-fold coordinated square pyramidal sites. Linking of the square bases of the pyramids at their corners results in two-dimensional puckered sheets of copper-oxygen bonds that extend in the a-b plane of the structure. The chains and planes in the structure are linked through the oxygens that lie

[44]M. Francois, A. Junod, K. Yvon, A. W. Hewat, J. J. Capponi, P. Strobel, M. Marezio and P. Fischer, *Solid State Commun.* **66**, 1117 (1988).

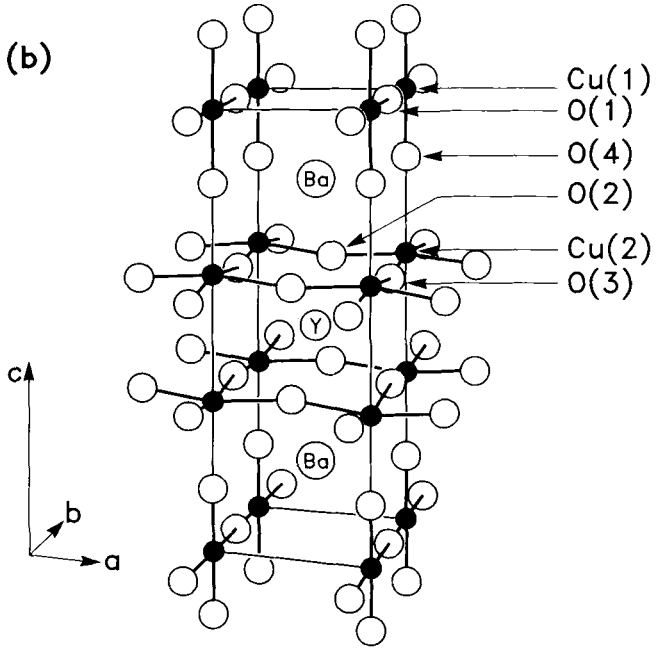

FIG. 1. (*Continued*)

at the apices of the square pyramids. The Y ion, which lies at the center of the cell, is coordinated by 8 oxygens that form a slightly distorted square prism. The Ba ion is 10-fold coordinated and is shifted slightly towards the Y ion relative to its position in the ideal perovskite structure.

Selected bond lengths and angles for the structure are given in Table II.[45] The Y–O and Ba–O distances are typical and compare well with distances observed in other structures. The Cu(2)–O(2) and Cu(2)–O(3) distances in the planes are 1.929 and 1.961, respectively, whereas the Cu(2)–O(4) bond, which joins the copper atom in the plane to the apical oxygen, is much longer, with a value of 2.341 Å. The Cu(1) atom in the chain has a bond length of 1.947 Å to the O(1) atom in the chain. The shortest Cu–O bond length, 1.834 Å, is between the Cu(1) atom in the chain and the apical O(4) atom. The long Cu(2)–O(4) distance suggests that the coppers in the planes are only weakly linked to those in the chains via the apical oxygen. It has been suggested that the short

[45]G. Calestani and C. Rizzoli, *Nature* **328,** 606 (1987).

TABLE I. STRUCTURAL PARAMETERS FOR ORTHORHOMBIC $Y_1Ba_2Cu_3O_{6.91}$ DETERMINED FROM A JOINT REFINEMENT OF X-RAY AND NEUTRON POWDER DIFFRACTION DATA TAKEN AT 297 K. THE NUMBERS IN PARENTHESES ARE THE ESTIMATED STANDARD DEVIATIONS IN THE LAST SIGNIFICANT DIGIT(S). (WILLIAMS *et al.*[43])

ATOM	SPACE GROUP *Pmmm*, $a = 3.82030(8)$ Å, $b = 3.88548(10)$ Å, $c = 11.68349(23)$ Å						
	x	y	z	U_{11}(Å^2)	U_{22}(Å^2)	U_{33}(Å^2)	OCCUPANCY
Y	$\frac{1}{2}$	$\frac{1}{2}$	$\frac{1}{2}$	0.0085(8)	0.0106(8)	0.0085(6)	1
Ba	$\frac{1}{2}$	$\frac{1}{2}$	0.18393(6)	0.0078(6)	0.0096(7)	0.0198(5)	1
Cu(1)	0	0	0	0.0080(9)	0.0115(9)	0.0150(7)	1
Cu(2)	0	0	0.35501(8)	0.0033(5)	0.0036(5)	0.0207(5)	1
O(1)	0	$\frac{1}{2}$	0	0.0161(16)	0.0104(11)	0.0080(14)	0.910(8)
O(2)	$\frac{1}{2}$	0	0.37819(15)	0.0039(6)	0.0068(7)	0.0203(11)	1
O(3)	0	$\frac{1}{2}$	0.37693(16)	0.0109(8)	0.0084(7)	0.0056(11)	1
O(4)	0	0	0.15840(13)	0.0162(11)	0.0123(9)	0.0097(7)	1

TABLE II. SELECTED BOND LENGTHS (Å) AND ANGLES (°) IN ORTHORHOMBIC $Y_1Ba_2Cu_3O_7$. THE NUMBERS IN PARENTHESES ARE ESTIMATED STANDARD DEVIATIONS. (CALESTANI AND RIZZOLI[45])

Y–O(2)	4 × 2.418(15)	Cu(1)–O(1)	2 × 1.947(5)
Y–O(3)	4 × 2.399(15)	Cu(1)–O(4)	2 × 1.834(27)
Ba–O(1)	2 × 2.891(2)	Cu(2)–O(2)	2 × 1.929(3)
Ba–O(2)	2 × 2.980(19)	Cu(2)–O(3)	2 × 1.961(3)
Ba–O(3)	2 × 2.948(19)	Cu(2)–O(4)	2.341(28)
Ba–O(4)	4 × 2.750(3)		
O(1)–Cu(1)–O(4)	90.0(5)		
O(4)–Cu(1)–O(4)	180.0(7)		
O(1)–Cu(1)–O(1)	180.0(0)		
O(3)–Cu(2)–O(3)	166.3(1)		
O(2)–Cu(2)–O(2)	165.3(7)		
O(2)–Cu(2)–O(3)	89.1(0)		
O(4)–Cu(2)–O(3)	96.9(6)		
O(4)–Cu(2)–O(2)	97.4(6)		

Cu(1)–O(4) bond distance is a consequence of preferential location of Cu^{3+} ions in the chain sites.

In addition to the refinements done at room temperature, a number of refinements were conducted at lower temperatures in order to investigate any structural changes that occur on cooling.[33,35,36,40] As will be discussed in Section 4, these initial studies found no substantial changes in the basic orthorhombic structure down to temperatures as low as 5 K, but several anomalies were reported in subsequent studies.

The oxygen content in the 123 structure depends strongly on the processing conditions used to form the material. An O_7 stoichiometry is only reached if samples are slowly cooled in oxygen. Quenching from high temperatures or cooling in a reducing atmosphere results in a more oxygen deficient structure. If sufficient oxygen is removed, the structure undergoes an orthorhombic-to-tetragonal phase transformation. This transformation will be described in greater detail in Section 1. Variability in oxygen content due to different heat treatments can account for many of the differences in unit cell dimensions and atomic positions reported in early x-ray refinements. For example, the report of a tetragonal unit cell by Hazen *et al.*[13] is consistent with an oxygen deficient structure.

Rietveld refinements of neutron diffraction data taken from oxygen deficient materials show that oxygen is lost primarily from the O(1) site in

TABLE III. ATOM POSITIONS AND OCCUPANCIES FOR TETRAGONAL $Y_1Ba_2Cu_3O_{6.06}$. THE O(2) AND O(3) POSITIONS ARE EQUIVALENT IN THE TETRAGONAL STRUCTURE. (SANTORO *et al.*[48])

	SPACE GROUP $P4/mmm$, $a = b = 3.8570(1)$ Å, $c = 11.8194(3)$ Å				
ATOM	x	y	z	B_{iso} (Å^2)	OCCUPANCY
Y	$\frac{1}{2}$	$\frac{1}{2}$	$\frac{1}{2}$	0.73(4)	1
Ba	$\frac{1}{2}$	$\frac{1}{2}$	0.1952(2)	0.50(4)	1
Cu(1)	0	0	0	1.00(4)	1
Cu(2)	0	0	0.3607(1)	0.49(3)	1
O(1)	0	$\frac{1}{2}$	0	0.9	0.028(4)
O(2)	0	$\frac{1}{2}$	0.3791(1)	0.73(4)	1
O(4)	0	0	0.1518(2)	1.25(6)	0.990(6)

the chains.[39,46–50] In reduced material with six oxygens per unit cell the chain site is completely empty, which reduces the coordination of the Cu(1) atom to two. This copper coordination is similar to that found in delafossites, which has led to the suggestion that reduced 123 contains Cu^{2+} ions in the planes and Cu^{1+} ions in the two-fold coordinated sites.[48,49] Refined cell parameters, atom coordinates, and selected bond lengths for the reduced 123 structure are given in Tables III and IV.[48] As can be seen by comparing the bond length data in Tables II and IV, the long bond length between the Cu(2) and O(4) atoms lengthens and the short bond length between the Cu(1) and O(4) atoms shortens in the reduced material. This indicates a further decrease in the coupling between Cu(2) planes and the Cu(1) site. The bond length changes are reflected in the unit cell dimensions as a lengthening of the c axis of the cell. Because the average of the a and b axes in the orthorhombic structure is about the same as the a axis of the tetragonal structure, the volume of the unit cell for the O_6 material is also increased. Two structural studies[39,49] reported cation disorder on the Ba and Y sites in

[46]A. Renault, G. J. McIntyre, G. Collin, J. P. Pouget, and R. Comes, *J. de Phys.* **48,** 1407 (1987).

[47]J. D. Jorgensen, M. A. Beno, D. G. Hinks, L. Soderholm, K. J. Volin, R. L. Hitterman, J. D. Grace, I. K. Schuller, C. U. Segre, K. Zhang, and M. S. Kleefisch, *Phys. Rev. B* **36,** 3608 (1987).

[48]A. Santoro, S. Miraglia, F. Beech, S. A. Sunshine, D. W. Murphy, L. F. Schneemeyer, and J. V. Waszczak, *Mat. Res. Bull.* **22,** 1007 (1987).

[49]P. Bordet, C. Chaillout, J. J. Capponi, J. Chenavas, and M. Marezio, *Nature* **327,** 687 (1987).

[50]C. C. Torardi, E. M. McCarron, P. E. Bierstedt, A. W. Sleight, and D. E. Cox, *Solid State Commun.* **64,** 497 (1987).

TABLE IV. SELECTED BOND LENGTHS (Å) IN TETRAGONAL $Y_1Ba_2Cu_3O_{6.06}$. (SANTORO *et al.*[48])

Y–O(2)	$8 \times 2.4004(8)$
Ba–O(2)	$4 \times 2.905(1)$
Ba–O(4)	$4 \times 2.7751(5)$
Cu(1)–O(4)	$2 \times 1.795(2)$
Cu(2)–O(2)	$4 \times 1.9406(3)$
Cu(2)–O(4)	2.469(2)

reduced 123, but there have been no subsequent investigations of this possibility.

One final point regarding the basic structure of 123 that has not been fully resolved concerns the space group of the structure. The final refinements in x-ray and neutron diffraction studies[25,51–56] of the orthorhombic structure have all been conducted in the space group *Pmmm*. Attempts to refine in other space groups including the *Pmm2* space group give either comparable or poorer fits to the data.[34,35,41] A number of studies[25,51–56] of the space group have been conducted using convergent beam electron diffraction,[57] which is sensitive to even small deviations from symmetry. These studies have led to conflicting results. Several authors have found evidence for the absence of one of the mirror planes parallel to the *c* axis of the structure, which would reduce the space group to *Pmm2*.[25,51,52,56] In one study this absence was attributed to the presence of defects in the crystals being studied.[52] However, in cases where care was taken to avoid such artifacts the *Pmm2* space group was still observed in some crystals.[25,26] Moodie and Whitfield[54] suggest that the loss of a mirror plane normal to the *a* axis could be caused by the presence of oxygen vacancy strings along the *b* axis in oxygen deficient material. The distinction between the two space groups is of considerable interest as the *Pmm2* space group is not centrosymmetric and therefore

[51]C. H. Chen, D. J. Werder, S. H. Liou, J. R. Kwo, and M. Hong, *Phys. Rev. B* **35,** 8767 (1987).

[52]D. J. Eaglesham, C. J. Humphreys, N. McN. Alford, W. J. Clegg, M. A. Harmer, and J. D. Birchall, *Appl. Phys. Lett.* **51,** 457 (1987).

[53]M. Tanaka, M. Terauchi, K. Tsuda, and A. Ono, *Jpn. J. Appl. Phys.* **26,** L1237 (1987).

[54]A. F. Moodie and H. J. Whitfield, *Ultramicroscopy* **24,** 329 (1988).

[55]X. D. Zou, C. Y. Yang and Y. Q. Zhou, *J. Electron Microsc. Tech.* **7,** 269 (1987).

[56]J. Zou, D. J. H. Cockayne, G. J. Auchterlonie, D. R. McKenzie, S. X. Dou, A. J. Bourdillon, C. C. Sorrell, K. E. Easterling, and A. W. S. Johnson, *Phil. Mag. Lett.* **57,** 157 (1988).

[57]B. F. Buxton, J. A. Eades, J. W. Steeds, and G. M. Rackham, *Phil. Trans. Roy. Soc. A* **281,** 171, (1976).

allows for phenomena such as ferroelectricity, which has been speculated to occur in the 123 structure.[58–60]

III. Phase Transformations and Oxygen Arrangements

The structure and properties of $Y_1Ba_2Cu_3O_{7-\delta}$ that are observed at and below room temperature depend critically on how the material is processed at higher temperatures. This situation arises because the superconducting properties are largely controlled by the oxygen content and arrangement in $Y_1Ba_2Cu_3O_{7-\delta}$, which, in turn, are controlled by the annealing times and temperatures, the oxygen partial pressures, and the quench rates used in preparing the material. In this section we review the many studies of the orthorhombic-to-tetragonal phase transition in 123 and summarize the oxygen arrangements that have been observed. We then use theoretical phase diagrams to try to tie these two areas together. Lastly, we briefly discuss some of the structural changes that have been reported to occur below room temperature.

1. The Orthorhombic-to-Tetragonal Phase Transition

The orthorhombic-to-tetragonal phase transition in 123 was initially identified by electron beam heating in a transmission electron microscope[25] (TEM) and was subsequently studied in situ by numerous techniques.[47,61–71] Hot-stage x-ray diffraction[61,62] showed that the lattice

[58]Z. Yang, J. Zhu, and Y. Xu, *J. Phys. C* **20,** L843 (1987).

[59]Z. J. Yang, J. Zhu, and Y. H. Xu, *Mater. Lett.* **6,** 19 (1987).

[60]S. K. Kurtz, L. E. Cross, N. Setter, D. Knight, A. Bhalla, W. W. Cao, and W. N. Lawless, *Mater. Lett.* **6,** 317 (1988).

[61]I. K. Schuller, D. G. Hinks, M. A. Beno, D. W. Capone II, L. Soderholm, J. P. Locquet, Y. Bruynserade, C. U. Segre, and K. Zhang, *Solid State Commun.* **63,** 385 (1987).

[62]R. Beyers, G. Lim, E. M. Engler, V. Y. Lee, M. L. Ramirez, R. J. Savoy, R. D. Jacowitz, T. M. Shaw, S. LaPlaca, R. Boehme, C. C. Tsuei, S. I. Park, M. W. Shafer, and W. J. Gallagher, *Appl. Phys. Lett.* **51,** 614 (1987).

[63]P. K. Gallagher, H. M. O'Bryan, S. A. Sunshine, and D. W. Murphy, *Mat. Res. Bull.* **22,** 995 (1987).

[64]J. M. Tarascon, W. R. McKinnon, L. H. Greene, G. W. Hull, B. G. Bagley, E. M. Vogel, and Y. LePage, *in* "Extended Abstracts on High Temperature Superconductors," (D. U. Gubser and M. Schluter, eds.), p. 65. Materials Research Society, Pittsburgh, PA, 1987.

[65]K. Kishio, J. Shimoyama, T. Hasegawa, K. Kitazawa, and K. Fueki, *Jpn. J. Appl. Phys.* **26,** L1228 (1987).

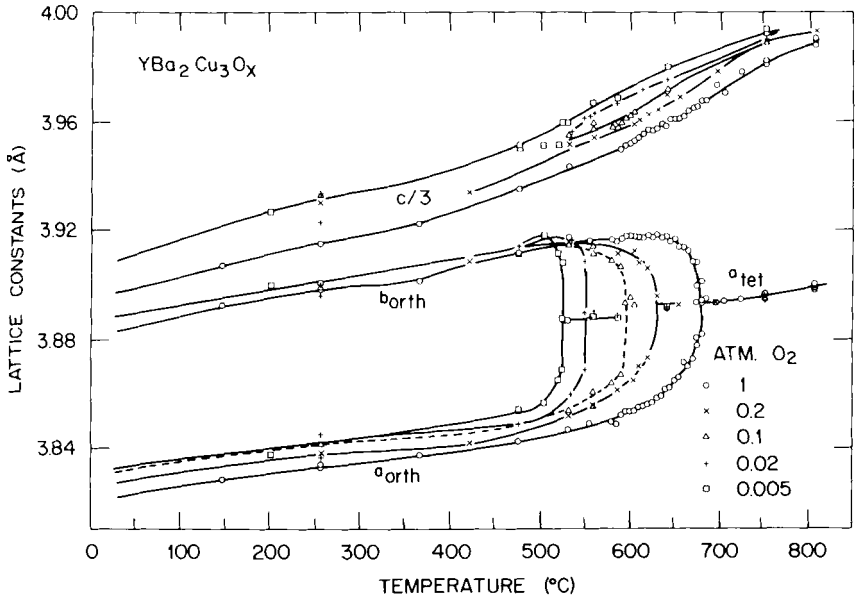

FIG. 2. Lattice constants versus temperature for various oxygen partial pressures. The orthorhombic-to-tetragonal transformation temperature decreases with decreasing oxygen pressure. The lines are to guide the eye. (Specht *et al.*[67])

parameters of 123 expanded linearly up to 500°C, with a thermal expansion along the *c* axis that is nearly twice that along the *a* and *b* axes. Above 500°C, however, the *b* axis contracts and the *a* axis expands at a supralinear rate. Finally, the *a* and *b* axes become equal and 123 is tetragonal. The temperatures at which the thermal expansion deviates from linearity and at which the orthorhombic-to-tetragonal transition occur are very dependent on the oxygen partial pressure[47,67] (Fig. 2). Thermogravimetric studies[62–67] have shown that O_7 starting material begins to lose oxygen reversibly above ~350–400°C. The

[66]S. Yamaguchi, K. Terabe, A. Saito, S. Yahagi, and Y. Iguchi, *Jpn. J. Appl. Phys* **27,** L179 (1988).

[67]E. D. Specht, C. J. Sparks, A. G. Dhere, J. Brynestad, O. B. Cavin, D. M. Kroeger, and H. A. Oye, *Phys. Rev. B* **37,** 7426 (1988).

[68]P. P. Freitas and T. S. Plaskett, *Phys. Rev. B* **36,** 5723 (1987).

[69]G. Van Tendeloo, H. W. Zandbergen, and S. Amelinckx, *Solid State Commun.* **63,** 389 (1987).

[70]G. Van Tendeloo, H. W. Zandbergen, and S. Amelinckx, *Solid State Commun.* **63,** 603 (1987).

[71]G. Van Tendeloo and S. Amelinckx, *Phys. Stat. Sol.* (*a*) **103,** K1 (1987).

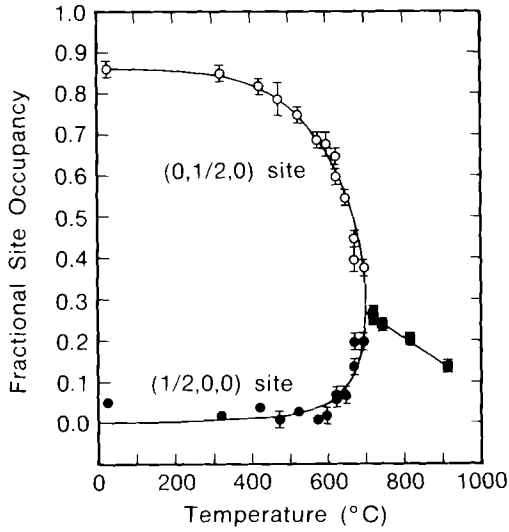

FIG. 3. Fractional oxygen site occupancies in the basal copper plane versus temperature for a sample heated in one atmosphere oxygen. (Jorgensen *et al.*[47])

orthorhombic-to-tetragonal transition is assumed to occur where there is a discontinuity in the curvature of weight loss versus temperature plots.[63]

In situ neutron diffraction[47] showed that the observed temperature-dependent changes in lattice parameters are caused by changes in oxygen content and order on the basal copper plane (between the barium layers) (Fig. 3). The oxygen that is lost above ~400°C comes primarily from the O(1) [= (0, 1/2, 0)] site, resulting in the negative thermal expansion of the *b* axis before the transition. Part of the oxygen that is removed from the O(1) site goes on the normally vacant (1/2, 0, 0) site, resulting in the enhanced expansion along the *a* axis just below the transition. These results show that the oxygen arrangement changes from fully ordered at room temperature, to partially ordered at elevated temperatures in the orthorhombic phase, to completely disordered at still higher temperatures in the tetragonal phase. Oxygen continues to be depleted from the basal copper plane above the transition. The first neutron diffraction study[47] found that the transition always occurs near an oxygen stoichiometry of 6.5. More recent studies[66,67] have concluded that the oxygen stoichiometry at the transition varies with oxygen partial pressure. An in situ x-ray diffraction and thermogravimetric study[67] found that the oxygen content at the transition decreases from 6.66 ± 0.01 to 6.59 ± 0.02 as the oxygen partial pressure is reduced from 1.0 atm to 5×10^{-3} atm

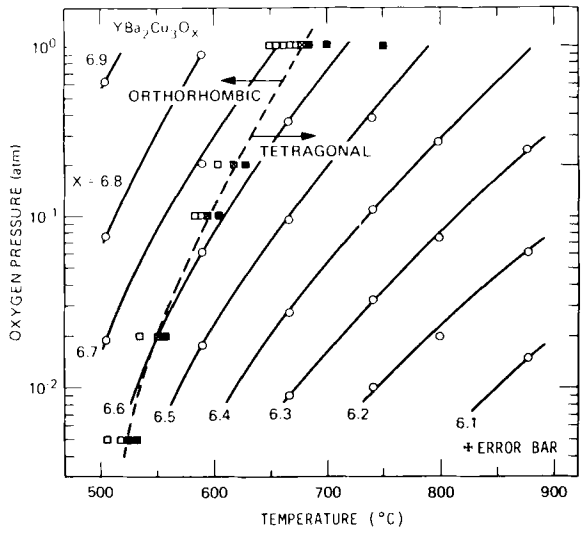

FIG. 4. Structural phase diagram for 123. Open squares indicate orthorhombic x-ray diffraction pattern, filled squares indicate tetragonal, and x-filled squares indicate the point of transformation. The oxygen content at the orthorhombic-to-tetragonal transition and the transition temperature both decrease with decreasing oxygen partial pressure. (Specht *et al.*[67])

(Fig. 4). Concurrently, the transition temperature decreases from 676 ± 5 to 621 ± 10°C. Lower oxygen pressures can reduce further the oxygen content at the transition. For example, samples prepared in 5×10^{-4} atm oxygen at 500°C by a solid-state ionic technique remained orthorhombic with an oxygen content of just 6.41 ± 0.02.[72]

There is no doubt that the orthorhombic-to-tetragonal transition is an order-disorder transformation. However, it is not yet clear whether the phase change is a classical Gibbsian first-order phase change or is a second-order transformation. Hysteresis observed in early hot-stage x-ray diffraction studies was interpreted as evidence for a first-order phase change.[61] Moreover, several x-ray diffraction studies found evidence for coexistence of orthorhombic and tetragonal 123, again indicative of a first-order phase change.[63] Conversely, others saw little or no hysteresis in their x-ray diffraction,[67] neutron diffraction,[47] or resistivity[68] studies of the transition and concluded that the phase change is second-order.

[72]R. Beyers, E. M. Engler, P. M. Grant, S. S. P. Parkin, G. Lim, M. L. Ramirez, K. P. Roche, J. E. Vazquez, V. Y. Lee, R. D. Jacowitz, B. T. Ahn, T. M. Gür, and R. A. Huggins, *Mater. Res. Soc. Symp. Proc.* **99**, 77 (1987).

Differential scanning calorimetry studies did not detect a latent heat at the transition. The difficulties encountered here in determining the order of the transition are analogous to those encountered in studies of order-disorder transformations in metal alloys. Rhines and Newkirk[73] provide an excellent discussion of the difficulties in making such a determination for metal alloys and conclude that order-disorder transformations in alloys are normal first-order phase changes if studied under true equilibrium conditions. More careful studies than those performed to date are required before the order of the transition can be definitively determined for 123.

2. Ordered Oxygen Arrangements

Soon after the orthorhombic $Y_1Ba_2Cu_3O_7$ and tetragonal $Y_1Ba_2Cu_3O_6$ phases were identified, researchers began to investigate the structures and properties of $Y_1Ba_2Cu_3O_{7-\delta}$ samples with intermediate oxygen contents. Many studies[74–79] prepared these samples by rapidly quenching the high-temperature, low-oxygen-content tetragonal phase from 600–1000°C to room temperature or liquid nitrogen temperature. These studies usually found a smooth variation of T_c with oxygen content with the samples becoming insulators near $O_{6.5}$, corresponding to the orthorhombic-to-tetragonal phase transition.[74] Alternatively, intermediate oxygen content samples were prepared by removing oxygen at lower temperatures (typically 500°C) from O_7 starting material. These studies employed a variety of methods to remove the oxygen, including annealing in reducing atmospheres,[79,80] equilibrating O_6 and O_7 123 mixtures in sealed quartz tubes,[81] gettering with zirconium in a sealed

[73]F. N. Rhines and J. B. Newkirk, *Trans. ASME* **45,** 1029 (1953).

[74]J. D. Jorgensen, B. W. Veal, W. K. Kwok, G. W. Crabtree, A. Umezawa, L. J. Nowicki, and A. P. Paulikas, *Phys. Rev. B* **36,** 5731 (1987).

[75]E. Takayama-Muromachi, Y. Uchida, M. Ishi, T. Tanaka, and K. Kato, *Jpn. J. Appl. Phys.* **26,** L1156 (1987).

[76]H. Nozaki, Y. Ishizawa, O. Fukunaga, and H. Wada, *Jpn. J. Appl. Phys.* **26,** L1180 (1987).

[77]M. Tokumoto, H. Ihara, T. Matsubara, M. Hirabayashi, N. Terada, H. Oyanagi, K. Murata, and Y. Kimura, *Jpn. J. Appl. Phys.* **26,** L1565 (1987).

[78]S. Nakanishi, M. Kogachi, H. Sasakura, N. Fukuoka, S. Minamigawa, K. Nakahigashi, and A. Yanase, *Jpn. J. Appl. Phys.* **27,** L329 (1988).

[79]W. E. Farneth, R. K. Borida, E. M. McCarron III, M. K. Crawford, and R. B. Flippen, *Solid State Commun.* **66,** 953 (1988).

[80]P. Monod, M. Ribault, F. D'Yvoire, J. Jegoudez, G. Collin, and A. Revcolevschi, *J. de Physique* **48,** 1369 (1987).

[81]D. C. Johnston, A. J. Jacobson, J. M. Newsam, J. T. Lewandowski, D. P. Goshorn, D. Xie, and W. B. Yelon, *ACS Symposium Series* **351:** "Chemistry of High-Temperature Superconductors," 136 (1987).

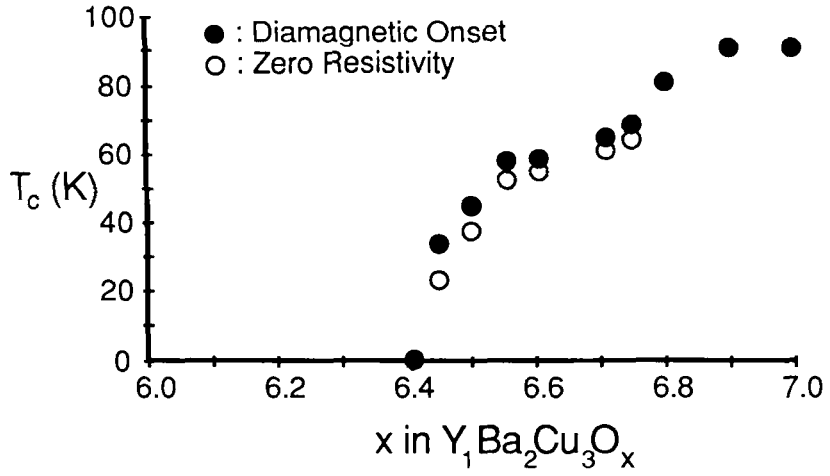

FIG. 5. Superconducting transition temperature vs oxygen content for samples prepared at 500°C by a solid-state ionic technique. (Beyers *et al.*[83])

tube,[82] and titrating electrochemically in a solid-state ionic cell.[72,83] The variation of T_c with oxygen content in samples prepared at lower temperatures is different from that observed in samples quenched from the tetragonal phase. The superconducting transition temperature does not vary smoothly with oxygen content in these samples (Fig. 5). Instead, T_c remains at 91 K between O_7 and $O_{6.9}$, then falls to a ~60 K "plateau" between $O_{6.7}$ and $O_{6.6}$, and finally drops to zero (i.e., not superconducting) between $O_{6.5}$ and $O_{6.4}$.

Complementary structural studies have tried to establish a link between the variations in T_c and variations in the oxygen structure. Numerous electron diffraction studies[70–72,84–88] found evidence for addi-

[82]R. J. Cava, B. Batlogg, C. H. Chen, E. A. Rietman, S. M. Zahurak, and D. Werder, *Phys. Rev. B* **36,** 5719 (1987).

[83]R. Beyers, G. Gorman, P. M. Grant, V. Y. Lee, R. M. Macfarlane, S. S. P. Parkin, S. J. LaPlaca, B. T. Ahn, T. M. Gür, and R. A. Huggins (unpublished).

[84]C. Chaillout, M. A. Alario-Franco, J. J. Capponi, J. Chenavas, J. L. Hodeau, and M. Marezio, *Phys. Rev. B* **36,** 7118 (1987).

[85]S. S. P. Parkin, E. M. Engler, V. Y. Lee, and R. B. Beyers, *Phys. Rev. B* **37,** 131 (1988).

[86]M. A. Alario-Franco, J. J. Capponi, C. Chaillout, J. Chenavas, and M. Marezio, *Mater. Res. Soc. Symp. Proc.* **99,** 41 (1988).

[87]Y. Kubo, T. Ichihashi, T. Manako, K. Baba, J. Tabuchi, and H. Igarashi, *Phys. Rev. B* **37,** 7858 (1988).

[88]C. H. Chen, D. J. Werder, L. F. Schneemeyer, P. K. Gallagher, and J. V. Waszczak, *Phys. Rev. B* **38,** 2888 (1988).

tional oxygen vacancy ordering near $O_{6.5}$. In [001] zone axis patterns, superlattice spots appear with wave vector $q = [1/2, 0, 0]$, corresponding to a doubling of the unit cell along the a axis in real space (Fig. 6(a)). The superlattice spots elongate into bands along the a^* direction in rapidly quenched samples. Tilting experiments revealed that the extra spots are in fact diffuse streaks running parallel to the c^* axis (Fig. 6(b)). The observed diffraction effects are consistent with an $O_{6.5}$ structure in

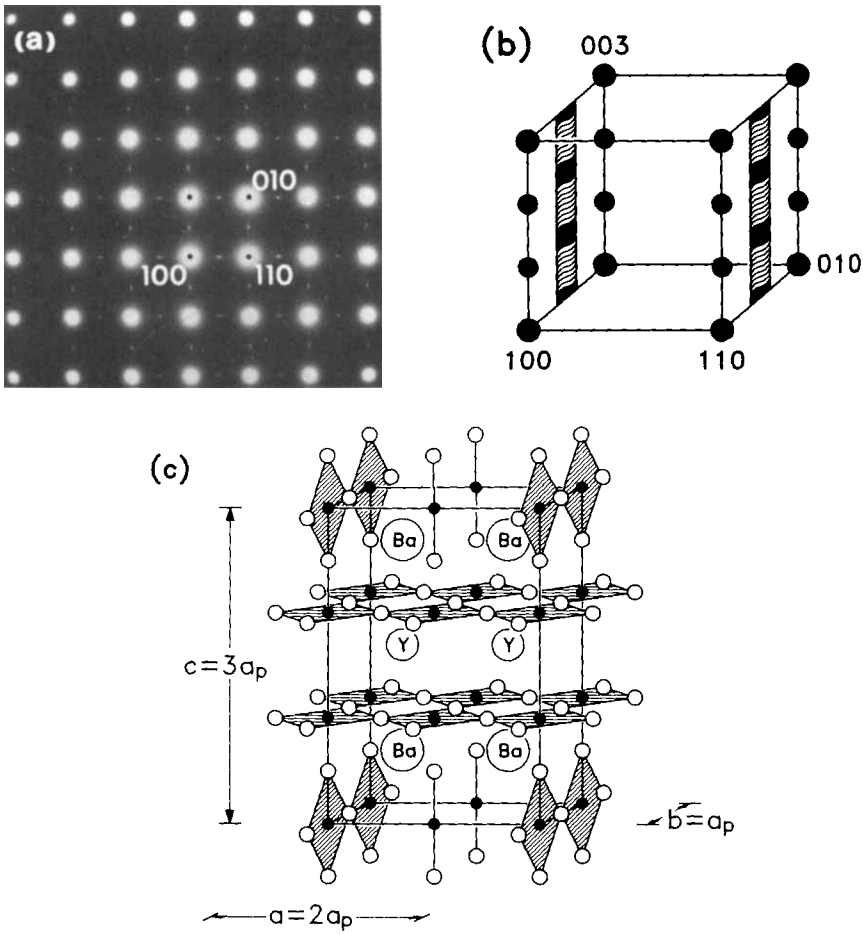

FIG. 6. (a) Typical [001] zone axis pattern from a twinned $O_{6.5}$ sample prepared at 500°C by a solid-state ionic technique. Sharp $q = [1/2, 0, 0]$ superlattice reflections are present along a^*. (Beyers *et al.*[83]) (b) Schematic of the reciprocal lattice obtained by electron diffraction tilting experiments and (c) proposed real space structure for the $O_{6.5}$ phase. (Alario-Franco *et al.*[86])

which oxygen is removed from the O(1) position in every other Cu(1)–O(1) linear chain in the 123 structure, thereby creating strings of oxygen vacancies along the *b* axis in the basal copper plane and doubling the unit cell along the *a* axis (Fig. 6(c)). Presumably the vacancy strings are not perfectly ordered in rapidly quenched material or in material that is off the $O_{6.5}$ stoichiometry, thus causing the superlattice spots to elongate into bands along the a^* direction in diffraction patterns from these samples. The diffuse streaking parallel to c^* indicates that the vacancy strings are uncorrelated between adjacent basal copper planes, which is not surprising given the layered nature of the 123 structure. These electron diffraction patterns have been observed in samples with overall oxygen contents ranging from $O_{6.4}$ to $O_{6.7}$, and it is widely believed that this structure is responsible for the "plateau" in T_c between $O_{6.6}$ and $O_{6.7}$. This speculation will be discussed in greater detail in the next section.

Three additional types of superlattices have been observed in electron diffraction studies. Alario-Franco *et al.*[86,89] observed continuous rods running parallel to c^* that give superlattice reflections with wave vector $q = [\pm 1/4, \pm 1/4, 0]$ in [001] zone axis patterns of orthorhombic $O_{6.85}$ and tetragonal $O_{6.15}$ samples. For the $O_{6.85}$ crystals, the superlattice was attributed to the ordered removal of every fourth O(1) atom from every other Cu(1)–O(1) linear chain in the basal copper plane, with the ordering being uncorrelated between the basal copper planes (Fig. 7). The ordering scheme is the same in the $O_{6.15}$ crystals, but the roles of oxygen and oxygen vacancies are reversed. Werder et al.[90] observed a superlattice with wave vector $q = [2/5, 0, 0]$ in $O_{6.72}$ material in addition to the more commonly reported $q = [1/2, 0, 0]$ superlattice, and Mitchell *et al.*[91] found a transient superlattice with wave vector $q = [1/3, 0, 0]$ in reduced samples. The electron diffraction patterns provide an existence proof for each of these superlattices. However, because they have not been studied as extensively as the $q = [1/2, 0, 0]$ superlattice, the precise conditions needed to form these superstructures reproducibly have yet to be determined. All of the superlattices observed indicate that intermediate oxygen stoichiometries in 123 are accommodated by ordered oxygen vacancy arrangements if the material is given time to equilibrate. A simplistic chemical explanation for this behavior is that the ordered

[89]M. A. Alario-Franco, C. Chaillout, J. J. Capponi, and J. Chenavas, *Mat. Res. Bull.* **22,** 1685 (1987).

[90]D. J. Werder, C. H. Chen, R. J. Cava, and B. Batlogg, *Phys. Rev. B* **37,** 2317 (1988).

[91]T. E. Mitchell, T. Roy, R. B. Schwarz, J. F. Smith, and D. Wohlleben, *J. Electron Microsc. Tech.* **8,** 317 (1988).

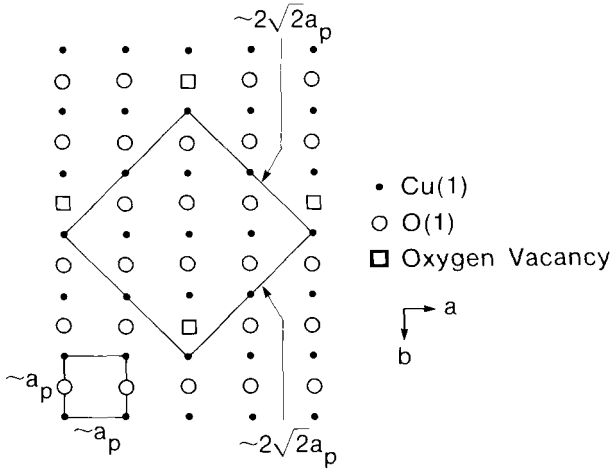

FIG. 7. Proposed oxygen arrangement in the basal copper plane of $O_{6.875}$ material. (Alario-Franco *et al.*[89])

arrangements minimize the number of copper atoms that are three-fold coordinated to oxygen, which is an energetically unfavorable state.[92]

When oxygen is removed from O_7 starting material at low temperatures, the loss of superconductivity does not coincide precisely with the orthorhombic-to-tetragonal phase transition. In these samples, T_c typically drops to zero between $O_{6.5}$ and $O_{6.4}$, but the orthorhombic-to-tetragonal transition does not occur until $O_{6.40-6.35}$. Several bond lengths change rapidly just before the transition, such as the Cu(1)–O(4) and Cu(2)–O(4) bonds. Consequently, it has been suggested that these bonds may play a role in superconductivity. However, because several distances are changing simultaneously, it is not clear at the present time which, if any, is critical for high T_c. A comparison with bond length changes in related superconducting structures may help to determine if there is more to these empirical observations. Finally, we note that a solid-state ionic study[72] concluded that oxygen inhomogeneity is essential for observing small amounts of superconductivity in samples with average oxygen contents below 6.5. It is currently speculated that these inhomogeneities arise from stress-induced oxygen diffusion, which in turn results from the anisotropic thermal expansion in 123.

[92]J. L. Hodeau, C. Chaillout, J. J. Capponi, and M. Marezio, *Solid State Commun.* **64,** 1349 (1987).

3. Phase Diagrams

The many structural changes that occur in 123 as a function of processing are most simply understood and discussed using phase diagrams. Pseudoternary[93–95] and quaternary[96,97] phase diagrams describing the equilibria between 123 and the other phases in the Y–Ba–Cu–O system have been determined by several groups. In this section, we restrict our discussion to the theoretical pseudobinary phase diagrams that have been used to explain variations in the oxygen substructure that occur with processing.[98–105] Most of these calculated diagrams use two-dimensional Ising models to explain the oxygen arrangements in the basal copper plane as a function of oxygen content and temperature. They neglect any changes in the remainder of the 123 structure.

Treating only nearest-neighbor interactions between oxygen atoms, Bakker *et al.*[98] derived an open-system order-disorder model of the orthorhombic-to-tetragonal phase transition that explained the observed variations in lattice constants with temperature. By incorporating a concentration-dependent heat of oxygen solution, Salomons *et al.*[99] extended Bakker's treatment to explain oxygen pressure-composition isotherms in 123. Wille and de Fontaine[102] analyzed the stability of a two-dimensional Ising model with one nearest-neighbor interaction, V_1, and two second-nearest-neighbor interactions, V_2 and V_3 (Fig. 8(a)). Stable oxygen arrangements for average oxygen stoichiometries of 7.0 and 6.5 were derived as a function of two phenomenological parameters, the ratios V_2/V_1 and V_3/V_1 (Fig. 8(b) and (c)). Assuming the effective pair

[93]K. G. Frase, E. G. Liniger, and D. R. Clarke, *J. Amer. Ceram. Soc.* **70,** C204 (1987).
[94]R. S. Roth, K. L. Davis, and J. R. Dennis, *Adv. Ceram. Mater.* **2,** 303 (1987).
[95]G. Wang, S. J. Hwu, S. N. Song, J. B. Ketterson, L. D. Marks, K. R. Poeppelmeier, and T. O. Mason, *Adv. Ceram. Mater.* **2,** 313 (1987).
[96]B. T. Ahn, T. M. Gür, R. A. Huggins, R. Beyers, and E. M. Engler, *Mater. Res. Soc. Symp. Proc.* **99,** 171 (1987).
[97]B. T. Ahn, T. M. Gür, R. A. Huggins, R. Beyers, E. M. Engler, P. M. Grant, S. S. P. Parkin, G. Lim, M. L. Ramirez, K. P. Roche, J. E. Vazquez, V. Y. Lee, and R. D. Jacowitz, *Physica C.* **153-155,** 590 (1988).
[98]H. Bakker, D. O. Welch, and O. W. Lazareth, Jr., *Solid State Commun.* **64,** 237 (1987).
[99]E. Salomons, N. Koeman, R. Brouwer, D. G. de Groot, and R. Griessen, *Solid State Commun.* **64,** 1141 (1987).
[100]J. M. Bell, *Phys. Rev. B.* **37,** 541 (1988).
[101]D. de Fontaine, L. T. Wille, and S. C. Moss, *Phys. Rev. B* **36,** 5709 (1987).
[102]L. T. Wille and D. de Fontaine, *Phys. Rev. B* **37,** 2227 (1988).
[103]L. T. Wille, A. Berera, and D. de Fontaine, *Phys. Rev. Lett.* **60,** 1065 (1988).
[104]A. G. Khachaturyan, S. V. Semenovskaya, and J. W. Morris, Jr., *Phys. Rev. B* **37,** 2243 (1988).
[105]A. G. Khachaturyan and J. W. Morris, Jr., *Phys. Rev. Lett.* **61,** 215 (1988).

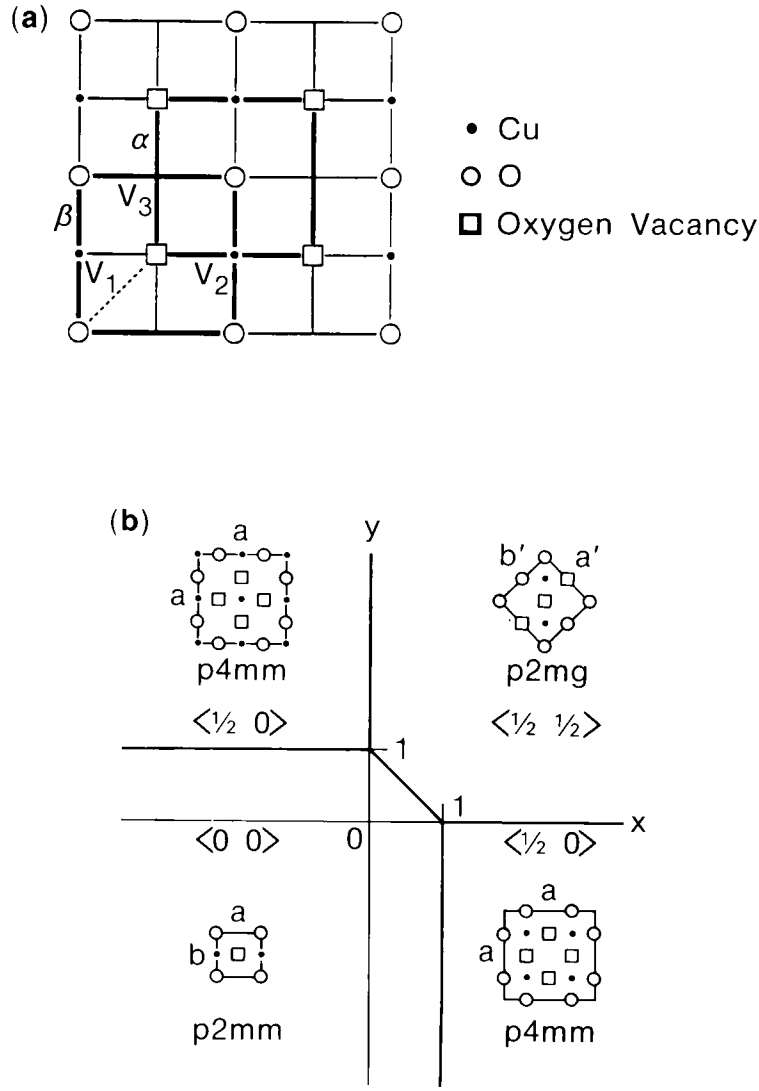

FIG. 8. (a) Ising model for the basal copper plane in $Y_1Ba_2Cu_3O_7$. V_2 and V_3 are second-nearest-neighbor interactions, with V_2 mediated by copper. (Willie *et al.*[103]) Stable ground states as a function of $x = V_2/V_1$ and $y = V_3/V_1$ for (b) O_7 and (c) $O_{6.5}$ (Wille and de Fontaine[102]).

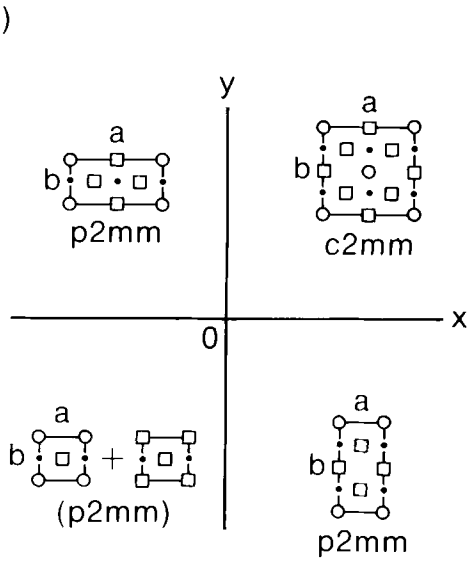

FIG. 8. (c)

interactions do not depend on oxygen content, the following restrictions must be placed on V_1, V_2, and V_3 to agree with the experimentally observed oxygen arrangements at $O_{6.5}$ and O_7: $V_1 > 0$, $V_2 < 0$, and $0 < V_3 < V_1$.

Wille *et al.*[103] arbitrarily set $V_1 = 1$, $V_2 = -0.5$, and $V_3 = 0.5$ to meet these restrictions and used the cluster variation method to calculate the phase diagram shown in Fig. 9. This diagram predicts that the orthorhombic-to-tetragonal transition is a second-order transition between points *b* and *c*, but is a first-order transition to the left of point *b* (i.e., for the transformation from the orthorhombic cell doubled along the *a* axis, *p2mm II*, to the disordered tetragonal phase, *p4mm*). Thus, the observation of a first-order or a second-order orthorhombic-to-tetragonal transition depends on how the phase diagram is traversed. The open circles in the diagram are the data reported by Specht *et al.*[67] One of these points was used to fit the estimated temperature scale on the right side of the drawing. The dotted phase boundaries below $kT/V_1 \sim 0.8$ are conjectured extrapolations. This diagram comes closest to matching the oxygen arrangements observed in 123 to date because it includes the orthorhombic phase near $O_{6.5}$ with the doubled unit cell.

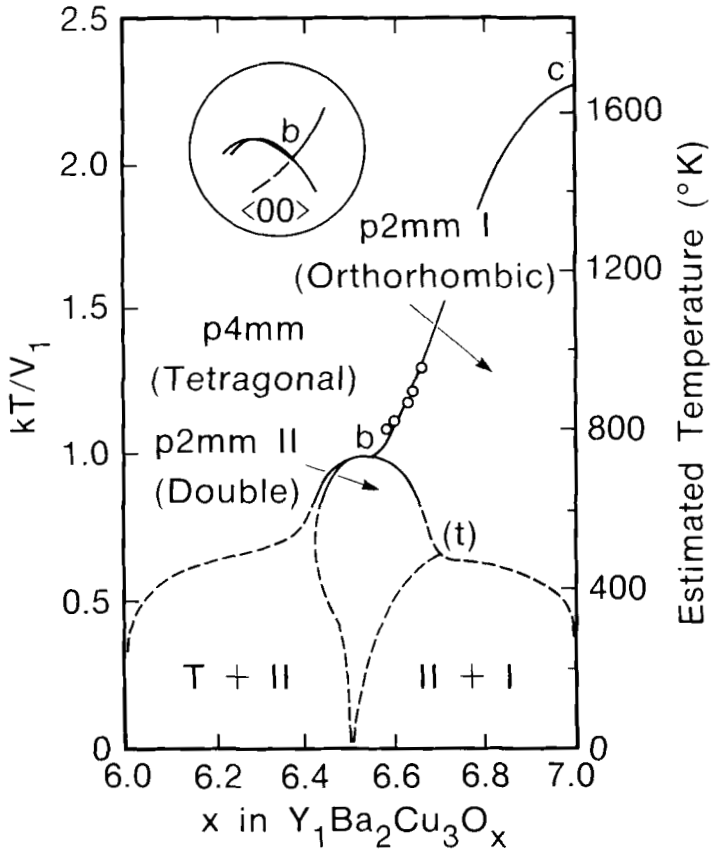

FIG. 9. Phase diagram obtained by the cluster variation method. Dotted lines are conjectured extensions. The diagram contains a bicritical point, *b*, and a tricritical point, *t*. Open circles are experimental data from Fig. 4. (Wille *et al.*[103])

Previous analyses equated the two second-nearest-neighbor interactions ($V_2 = V_3$) and thus predicted a miscibility gap between tetragonal O_6 and orthorhombic O_7 phases at low temperatures and no distinct phase at $O_{6.5}$. Such a miscibility gap has never been observed, whereas there is widespread agreement on the existence of the $O_{6.5}$ phase. However, the phase diagram in Fig. 9 cannot be considered completely correct either, given the electron diffraction evidence for additional superstructures. It seems likely that some of these superstructures exist between $O_{6.5}$ and

O_7. Higher order interactions must be included in the Ising models to stabilize such structures. Alternatively, using a "maximum amplitude principle," Khachaturyan and Morris[105] explain all of the observed superstructures except that reported by Alario-Franco *et al.*[89] Khachaturyan and Morris[105] also propose that these superstructures are metastable transients that precede a spinodal decomposition into the O_6 and O_7 phases. As noted above, however, separation into O_6 and O_7 phases has never been observed experimentally.

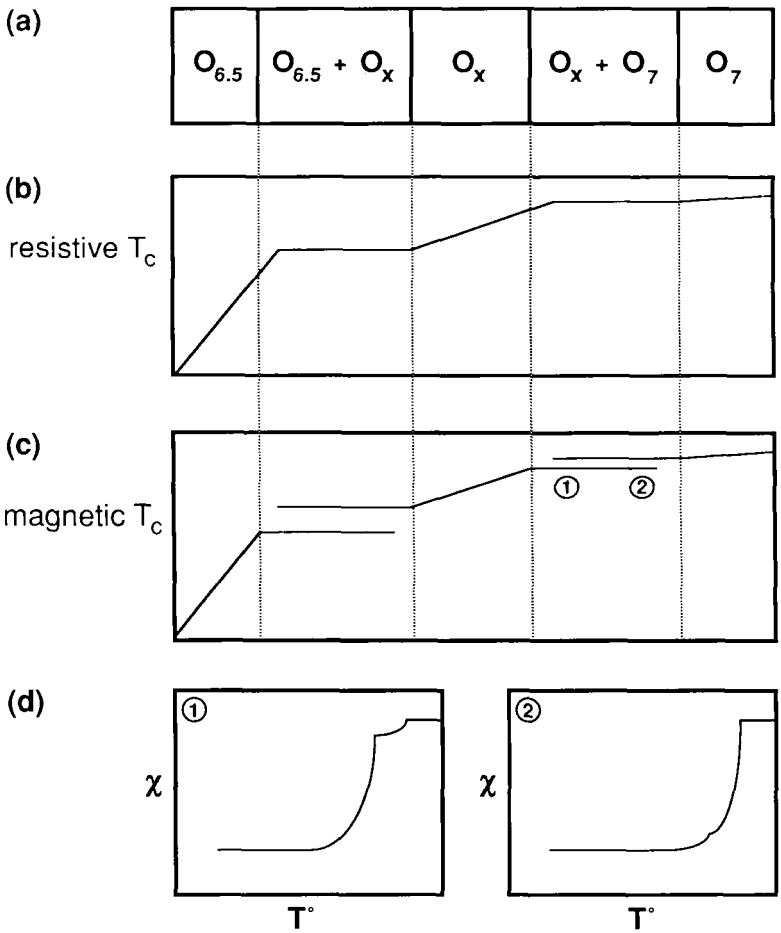

FIG. 10. For the pseudobinary diagram in (a), the expected variations in T_c measured by (b) resistivity and (c) susceptibility. In (d) susceptibility versus temperature plots are shown for points 1 and 2 in (c).

The variation of T_c with oxygen content in samples prepared at low temperatures may also point to the existence of additional phases between $O_{6.5}$ and O_7. If the "plateaus"[106] at 91 and ~60 K in the T_c-versus-O_x curve arise from crossing two-phase regions in the pseudobinary diagram, then there must be at least one additional ordered oxygen phase between $O_{6.5}$ and O_7. Figure 10 shows the expected variations in T_c measured by resistivity and susceptibility if an additional phase exists in the pseudobinary phase diagram at low temperature and the samples are prepared under equilibrium conditions. In the single-phase regions, T_c is allowed to vary as the oxygen content within the single phase varies. In the two-phase regions, however, the properties of the coexisting phases are fixed because the oxygen contents in the coexisting phases are fixed by the Gibbs phase rule (assuming that the pseudobinary approximation is valid). Consequently, the T_c measured resistively in the two-phase regions would be that of the higher oxygen content phase if there were connectivity between grains of this phase (Fig. 10(b)). Susceptibility data in the two-phase regions would show evidence for two phases with different T_c (Fig. 10(c)). The diamagnetic contributions of each phase would vary according to the lever rule as the two-phase region was crossed (Fig. 10(d)). If this pseudobinary interpretation is valid, then the "plateau" at ~60 K could be caused by either the additional phase between $O_{6.5}$ and O_7 or the $O_{6.5}$ phase. Moreover, it is also possible that the additional phase is in fact a series of phases with only small differences in oxygen content and superstructure.

4. Low-Temperature Structure Changes

High superconducting transition temperatures are often associated with lattice instabilities brought on by strong electron-phonon coupling.[107] Consequently, many investigators have looked for structural changes in 123 below room temperature. While no substantial changes have been found, there have been a number of anomalies reported. A high-resolution x-ray scattering study by Horn *et al.*[108] detected an anomaly in the orthorhombic splitting, *b-a*, near the superconducting transition. They suggested that uniaxial anisotropy within the *ab* plane in the

[106]The word 'plateau' is put in quotes because the observed T_c varies somewhat in these regions, possibly due to insufficient equilibration time. Alternatively, the T_c variation in the "plateaus" could indicate that this simple phase rule explanation for the shape of the T_c versus oxygen curve is not correct.

[107]J. C. Phillips, *Phys. Rev. Lett.* **26,** 543 (1971).

[108]P. M. Horn, D. T. Keane, G. A. Held, J. L. Jordan-Sweet, D. L. Kaiser, F. Holtzberg, and T. M. Rice, *Phys. Rev. Lett.* **59,** 2772 (1987).

superconducting wave function might be the cause of this distortion. David *et al.*[109] also found an anomaly in the volume expansivity at T_c with neutron powder diffraction, but tentatively associated this anomaly with a change in the *c* axis, rather than with a change in the *ab* plane. Conversely, Francois *et al.*[44] verified the enhancement in the orthorhombic splitting at T_c with neutron powder diffraction and found evidence for a second anomaly at 240 K. Laegreid *et al.*[110] observed a specific heat anomaly at 90 K. Using ultrasound propagation, Bhattacharya *et al.*[111] found evidence for a phase transition at 120–130 K, probably occurring in the *ab* planes. In a related material with the 123 structure, $CaLaBaCu_3O_x$, both electron and neutron diffraction[112] found a phase transition between 160 and 230 K that increases the basic unit cell from a $1a_p \times 1a_p \times 3a_p$ cell to a $2a_p \times 2a_p \times 6a_p$ cell, where $a_p \sim 3.85$ Å (Fig. 11). The reproducibility of these effects, their root causes, and the implications for pairing mechanisms remain largely unresolved.

There is definitely a second type of phase transition occurring in 123 that may be important for pairing mechanisms not involving electron-phonon coupling, namely antiferromagnetic ordering of the magnetic moments on the copper ions. Antiferromagnetism was first detected by Nishida *et al.*[113] using muon spin relaxation and was subsequently studied by several groups using neutron diffraction.[114–118] There are differences in the magnetic structures derived by these groups. Tranquada *et al.*[114,115]

[109]W. I. F. David, P. P. Edwards, M. R. Harrison, R. Jones, and C. C. Wilson, *Nature* **331,** 245 (1988).

[110]T. Laegreid, K. Fossheim, E. Sandvold, and S. Julsrud, *Nature* **330,** 637 (1987).

[111]S. Bhattacharya, M. J. Higgins, D. C. Johnston, A. J. Jacobson, J. P. Stokes, D. P. Goshorn, and J. T. Lewandowski, *Phys. Rev. Lett.* **60,** 1181 (1988).

[112]Y. Tokura, S. J. La Placa, T. C. Huang, R. Beyers, R. F. Boehme, A. I. Nazzal, S. S. P. Parkin, and J. B. Torrance (unpublished).

[113]N. Nishida, H. Miyatake, D. Shimada, S. Okuma, M. Ishikawa, T. Takabatake, Y. Nakazawa, Y. Kuno, R. Keitel, J. H. Brewer, T. M. Riseman, D. L. Williams, Y. Watanabe, T. Yamazaki, K. Nishiyama, K. Nagamine, E. J. Ansaldo, and E. Torikai, *Jpn. J. Appl. Phys.* **26,** L1856 (1987).

[114]J. M. Tranquada, D. E. Cox, W. Kunnmann, H. Moudden, G. Shirane, M. Suenaga, P. Zolliker, D. Vaknin, S. K. Sinha, M. S. Alvarez, A. J. Jacobson, and D. C. Johnston, *Phys. Rev. Lett.* **60,** 156 (1988).

[115]J. M. Tranquada, A. H. Moudden, A. I. Goldman, P. Zolliker, D. E. Cox, G. Shirane, S. K. Sinha, D. Vaknin, D. C. Johnston, M. S. Alvarez, A. J. Jacobson, J. T. Kewandowski, and J. M. Newsam, *Phys. Rev. B* **38,** 2477 (1988).

[116]W. J. Li, J. W. Lynn, H. A. Mook, B. C. Sales, and Z. Fisk, *Phys. Rev. B* **37,** 9844 (1988).

[117]H. Kadowaki, M. Nishi, Y. Yamada, H. Takeya, H. Takei, S. M. Shapiro, and G. Shirane, *Phys. Rev. B* **37,** 7932 (1988).

[118]J. W. Lynn, W. H. Li, H. A. Mook, B. C. Sales, and Z. Fisk, *Phys. Rev. Lett.* **60,** 2781 (1988).

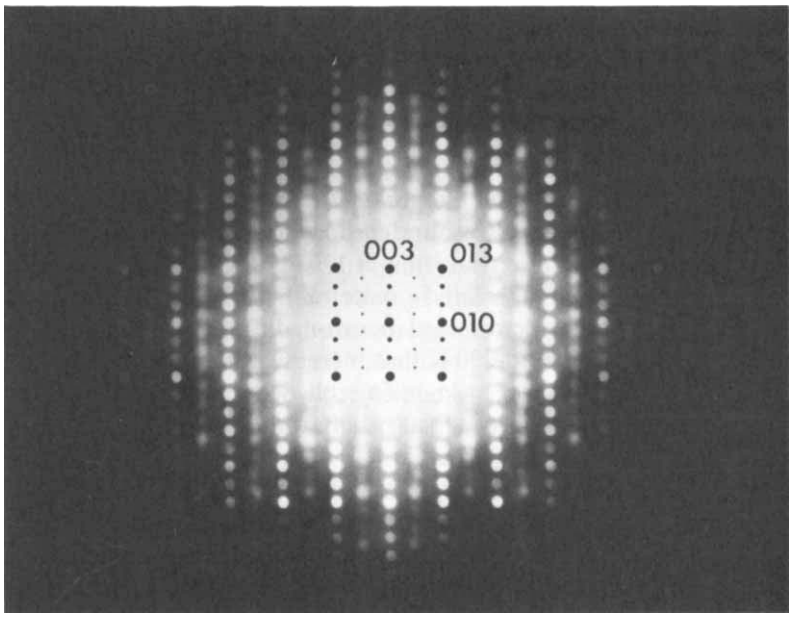

FIG. 11. [100] electron diffraction pattern from tetragonal $CaLaBaCu_3O_x$ at 77 K. The superlattice spots arise from a low-temperature phase transformation that doubles the unit cell along all three axes. (Tokura *et al.*[112]).

found that copper spins order antiferromagnetically in the CuO_2 planes, but not in the linear chains (i.e., not in the basal copper plane). More recent studies by Kadowaki *et al.*[117] and Lynn *et al.*[118] observed a second transition at lower temperature that they attributed to ordering of the spins in the basal copper plane, but the spin structures that these two groups deduced are not the same. All groups agree that the antiferromagnetic properties depend strongly on oxygen content. The Néel temperature for three-dimensional ordering in the CuO_2 planes varies from ~500 K at $O_{6.0}$ to ~0 K at $O_{6.4}$. Local antiferromagnetic ordering may exist in the superconducting state, but this has not been proven experimentally. A more detailed discussion of the magnetic properties of 123 and its derivatives is beyond the scope of this review.

IV. Defect Structures

X-ray and neutron diffraction are widely used to examine the average structure of 123 and its derivatives. Microscopic examination, however, shows that nearly all 123 materials contain defects. Transmission electron

microscopy (TEM) has played a central role in determining the structure of these defects, but has some inherent limitations. High-resolution TEM has shown that while the location of the cations can be readily identified under the proper focus conditions,[25–29] the local oxygen structure is much more difficult to determine. Image simulations indicate that the images are only sensitive to the presence of oxygen in the basal copper plane over a narrow range of focus and are highly sensitive to the thickness of the crystal.[27,119–122] Moreover, the electron beam used to obtain the images can change the oxygen substructure.[25] In practice, these difficulties make analysis of the local oxygen distribution all but impossible. High-resolution studies have thus focussed on the analysis of defects in the cation sublattice. (However, as discussed in Section 2, ordered oxygen arrangements have been inferred from electron diffraction studies.) In this section we describe the structures of the various defects and briefly examine their effects on superconducting properties.

5. Twins

The most commonly observed defects in 123 are the twins that arise from the orthorhombic-to-tetragonal phase transformation.[21,25,51–55,69,92,123–135] The twins form when oxygen ordering in the

[119]A. Ourmazd and J. C. H. Spence, *Nature* **329,** 425 (1987).
[120]A. Ourmazd, J. C. H. Spence, J. M. Zuo, and C. H. Li, *J. Electron Microsc. Tech.* **8,** 251 (1988).
[121]W. Krakow and T. M. Shaw, *J. Electron Microsc. Tech.* **8,** 273 (1988).
[122]N. P. Huxford, D. J. Eaglesham, and C. J. Humphreys, *Nature* **329,** 812 (1987).
[123]S. Nakahara, T. Boone, M. F. Yan, G. J. Fisanick, and D. W. Johnson, Jr., *J. Appl. Phys.* **63,** 451 (1988).
[124]E. A. Hewat, M. Dupuy, A. Bourret, J. J. Capponi, and M. Marezio, *Solid State Commun.* **64,** 517 (1987).
[125]M. Hervieu, B. Domenges, C. Michel, G. Heger, J. Provost, and B. Raveau, *Phys. Rev. B* **36,** 3920 (1987).
[126]A. I. Kingon, S. Chevacharoenkul, J. Mansfield, J. Brynestad, and D. G. Haase, *Adv. Ceram. Mater.* **2,** 678 (1987).
[127]M. Sarikaya, B. L. Thiel, I. A. Aksay, W. J. Weber, and W. S. Frydrych, *J. Mater. Res.* **2,** 736 (1987).
[128]S. Iijima, T. Ichihashi, Y. Kubo, and J. Tabuchi, *Jpn. J. Appl. Phys.* **26,** L1478 (1987).
[129]S. Iijima, T. Ichihashi, Y. Kubo, and J. Tabuchi, *Jpn. J. Appl. Phys.* **26,** L1790 (1987).
[130]J. C. Barry, *J. Electron Microsc. Tech.* **8,** 325 (1988).
[131]A. Brokman, *Solid State Commun.* **64,** 257 (1987).
[132]K. Lukaszewicz, J. Stepiendamm, R. Horyn, Z. Bukowski, and M. Kowalski, *J. Appl. Cryst.* **20,** 505 (1987).
[133]M. M. Fang, V. G. Kogan, D. K. Finnemore, J. R. Clem, L. S. Chumbley, and D. E. Farrell, *Phys. Rev. B* **37,** 2334 (1988).
[134]S. Takeda and S. Hikami, *Jpn. J. Appl. Phys.* **26,** L848 (1987).
[135]M. Sarikaya, R. Kikuchi, and I. A. Aksay, *Physica C* **152,** 161 (1988).

basal copper plane causes elongation of the b axis and contraction of the a axis. At the twin boundaries the cell edge with the enhanced oxygen content switches from one cell edge to the other, effectively rotating the unit cell through almost 90°. The two orientations share a common (110) plane in the twin boundary. Dense arrays of parallel twins with spacings from 20 nm to over 100 nm are observed. A typical example of parallel twins formed in 123 is shown in Fig. 12. Arrangements in which both {110} variants occur in the same grain are also frequently seen.[25,54,69,70,125,129,135] The misorientation across the twin boundary deviates from 90° by an amount ϕ, where $\phi = 2\arctan(b/a) - \pi/2$, which is on the order of 1° for the O_7 structure.

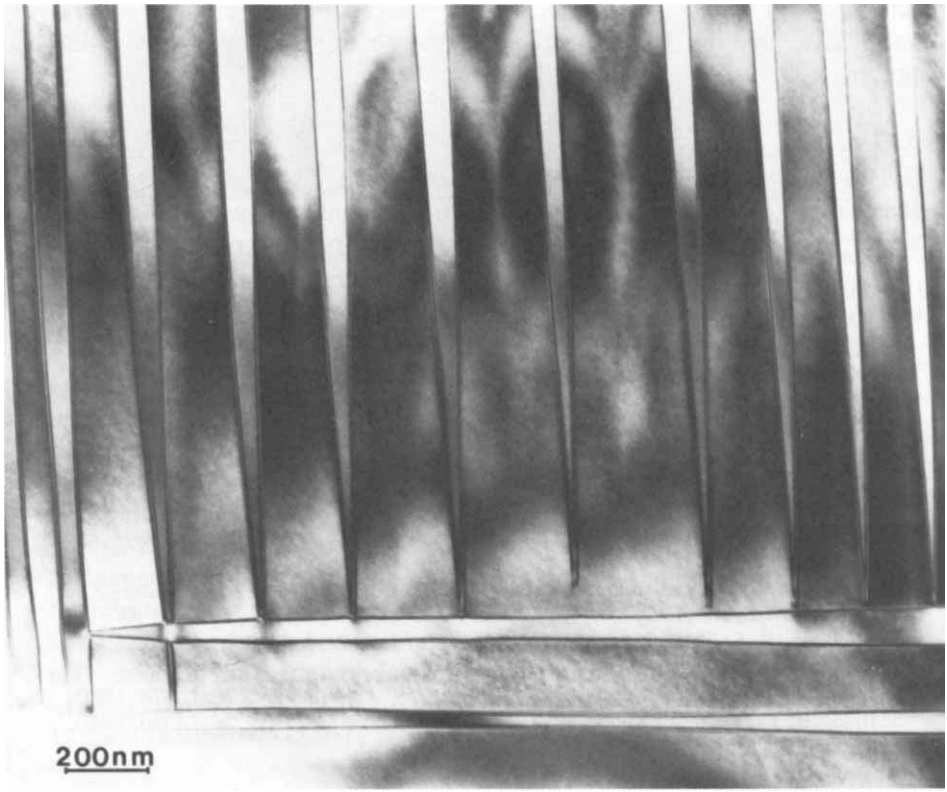

FIG. 12. Transmission electron micrograph of parallel twins formed on the {110} planes in $Y_1Ba_2Cu_3O_7$.

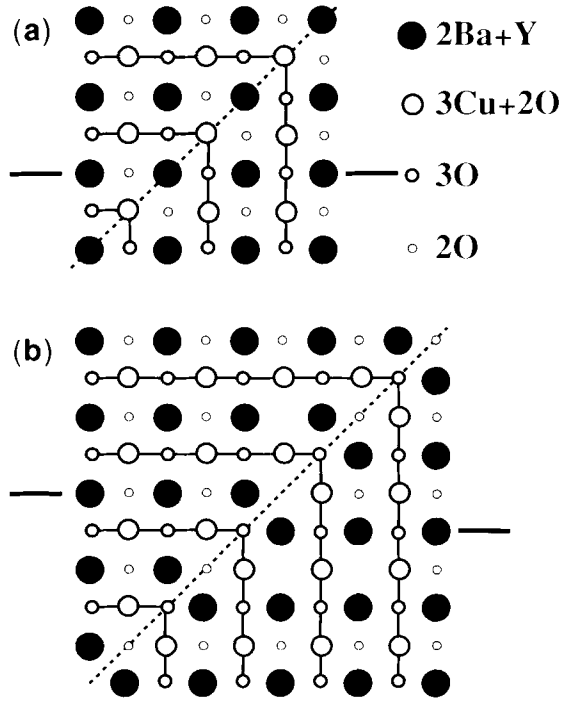

FIG. 13. Two models for twin boundaries in 123. In (a) both copper and oxygen ions are shared at the twin boundary whereas in (b) only oxygen ions are shared. Note the offset in the rows of (2Ba + Y) columns in model (b). (Hewat *et al.*[124]) Only model (a) is consistent with high-resolution TEM images of the twin boundaries.

Two models for the twin boundary structure have been proposed, one in which the twin plane contains both copper and oxygen and one in which it contains only oxygen.[54,124,125] Both models are shown schematically in Fig. 13. High-resolution images show that the planes containing columns of cations bend slightly on crossing the twin boundary but remain continuous.[54,124,130,136] The observation of continuous lattice planes is only consistent with the model in which the twin plane contains both copper and oxygen (Fig. 13(a)). Examination of the lattice plane bending in well-annealed material indicates that the lattice distortion associated with the twin boundary is confined to one or two unit cells at the boundary.[130,136] The high-resolution images do not reveal the location

[136]H. W. Zandbergen, G. Van Tendeloo, T. Okabe, and S. Amelinckx, *Phys. Stat. Sol.* (*a*) **103,** 45 (1987).

of the oxygen ions at the boundary. From the model in Fig. 13(a), however, it is evident that if all the oxygen sites in the two twin-related crystals are occupied, then the oxygens at the boundary share the same cell. Some repositioning of oxygens at the twin boundary plane therefore seems likely. It has also been suggested that the boundary is a likely site for peroxide formation.[131]

It is well known that the strain energy produced in transformations that cause small shear strains can be partially relieved by twinning.[137] The reduction in strain energy is balanced by the energy required to form the twin boundaries. This energy balance leads to an equilibrium spacing for the twins that depends on the size of the transformed region, the magnitude of the shear strain, and the twin boundary energy. For polycrystalline materials, when a complete phase transformation takes place, the relevant scale for the transformed region is the grain size.[138] The twin spacing, d, is then related to the grain size, G, by the relation

$$d = \sqrt{\frac{128\pi\gamma G}{ES_s^2}},$$

where E is the elastic modulus of the material, γ is the twin boundary energy, and S_s is a measure of the transformation strain and is related to the lattice parameters by $S_s = (a/b) - 1$. Measurements of twin spacings in different grain size materials are consistent with this relationship,[139] clearly demonstrating that the twin spacings in 123 are controlled by the transformation strains. This observation also explains why attempts to correlate twin spacings to the local oxygen content of a grain have failed, since the effect of grain size was not taken into consideration in these studies.[135,140]

While the cause of twinning in 123 is clear, the precise mechanism by which the transformation takes place and the twinning develops is not well-established. In samples rapidly quenched to below the transformation temperature, *in situ* observations found that a fine tweed-like microstructure develops that subsequently coarsens into a set of parallel twins.[70,129] On the other hand, in polycrystalline materials cooled slowly through the transformation temperature, dense patches of intersecting twin boundaries form in the final microstructure.[139] Similar twin struc-

[137]A. G. Khachaturyan, "Theory of Structural Transformations in Solids," John Wiley and Sons, New York, 1983.

[138]G. Arlt, D. Hennings, and G. de With, *J. Appl. Phys.* **58,** 1619 (1985).

[139]T. M. Shaw, S. L. Shinde, D. Dimos, R. F. Cook, P. R. Duncombe, and C. Kroll, *J. Mater. Res.* (1988) (in press).

[140]M. Sarikaya and E. A. Stern, *Phys. Rev. B* (1988) (submitted).

tures are seen in single crystals after oxygen treatment.[141-143] Convergent beam electron diffraction patterns and lattice images from twinned crystals also indicate that there are substantial local changes in the *a* and *b* lattice parameters in polycrystalline materials.[129,140,144] These variations have been interpreted as evidence that phase separation[103,104] may accompany the transformation.

Twins may affect a number of superconducting and normal state properties of 123. Several authors suggest that twinning could lead to an enhancement of T_c by either altering the ordering of oxygen in the twin plane,[145] altering the symmetry and periodicity of the crystal,[146] or changing the low-frequency phonon spectrum, which also alters the specific heat and normal state resistivity of the structure.[147] Indirect evidence for the enhancement of T_c by twins, similar to that reported in other superconducting materials,[148] has been obtained from magnetization experiments on field orientated samples[133] of $Y_1Ba_2Cu_3O_{7-\delta}$. The presence of a superconducting glass state, deduced from magnetization and microwave absorption experiments,[149,150] has also been attributed to the twins. In this case the twins are thought to act as weak links. Direct assessment of the effects of twins on superconducting properties, however, is hampered by the difficulty in controlling the twin structure without altering other features of the material, such as the grain size, doping, or oxygen content. In the absence of such controlled experiments, the effects of twins remain uncertain.

6. Stacking Faults

Several different fault structures occur on the (001) planes in 123. In high resolution images of the faults, an offset in the (100) planes of $a/2$ is

[141]H. A. Hoff, A. K. Singh, and C. S. Pande, *Appl. Phys. Lett.* **52,** 669 (1988).
[142]Y. Tajima, M. Hikita, A. Katsui, Y. Hidaka, T. Iwata, and S. Tsurumi, *J. Cryst. Growth* **85,** 665 (1987).
[143]K. Semba, H. Suzuki, A. Katsui, Y. Hidaka, M. Hikita, and S. Tsurumi, *Jpn. J. Appl. Phys.* **26,** L1645 (1987).
[144]Z. Hiroi, M. Takano, Y. Ikeda, Y. Takeda, and Y. Bando, *Jpn. J. Appl. Phys.* **27,** L141 (1988).
[145]A. Robledo and C. Varea, *Phys. Rev. B* **37,** 631 (1988).
[146]F. M. Mueller, S. P. Chen, M. L. Prueitt, J. F. Smith, J. L. Smith, and D. Wohlleben, *Phys. Rev. B* **37,** 5837 (1988).
[147]B. Horovitz, G. R. Barsch, and J. A. Krumhansl, *Phys. Rev. B* **36,** 8895 (1987).
[148]I. N. Khlustikov and A. I. Buzdin, *Adv. Phys.* **36,** 271 (1987).
[149]K. A. Müller, K. W. Blazey, J. G. Bednorz, and M. Takashige, *Physica B & C* **148,** 149 (1987).
[150]K. W. Blazey, K. A. Müller, J. G. Bednorz, W. Berlinger, G. A. Moretti, E. Buluggiu, A. Vera, and F. C. Matacotta, *Phys. Rev. B* **36,** 7241 (1987).

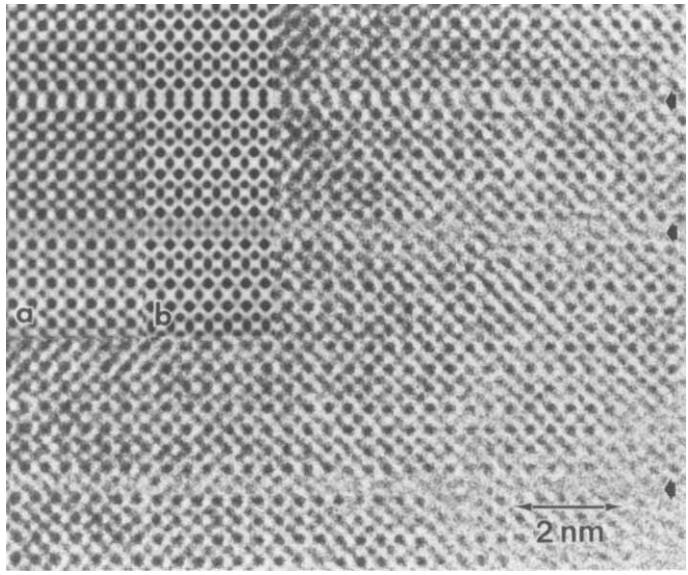

FIG. 14. High-resolution TEM image of $Y_1Ba_2Cu_3O_7$ in [010] orientation showing stacking faults (indicated by black arrows). The uppermost fault shows mirror symmetry while the lower two faults show glide symmetry. Note that the uppermost fault gradually assumes glide character near the right edge, suggesting that the length of the *a* axis is different on both sides of the defect. An averaged experimental image (a) and a calculated image (b) are inset. (Zandbergen *et al.*[152])

observed across some faults and not others.[26,28,151–153] Other faults appear to cause an offset in the {110} planes.[152,153] In each case the fault is accompanied by an increase in the *c* lattice parameter. Different displacement vectors have been assigned to the faults based on the high-resolution images. From diffraction contrast experiments only two faults with similar displacement vectors of $[a/2, 0, c/6]$ and $[0, b/2, c/6]$ were identified.[154] It was shown later that the displacements observed in high-resolution images are consistent with displacement vectors of this type.[152] High-resolution images of the faults (Fig. 14) matched the contrast calculated for a defect in which an extra Cu–O layer is inserted between the Ba–O layers.[152] Examples are also reported of faults where an extra Cu–O layer is inserted between the Y and Ba–O layers.[28,153]

[151]Y. Hirotsu, Y. Nakamura, Y. Murata, S. Nagakura, T. Nishihara, and M. Takata, *Jpn. J. Appl. Phys.* **26,** L1168 (1987).
[152]H. W. Zandbergen, R. Gronsky, K. Wang, and G. Thomas, *Nature* **331,** 596 (1988).
[153]Y. Matsui, E. Takayama-Muromachi, and K. Kato, *Jpn. J. Appl. Phys.* **27,** L350 (1988).
[154]J. Tafto, M. Suenaga, and R. L. Sabatini, *Appl. Phys. Lett.* **52,** 667 (1988).

In bulk material, the faults appear to be extrinsic defects that result from the reaction of 123 with the environment, rather than intrinsic growth defects. The faults can grow in from the surfaces of crystals if they are left exposed to air.[155] The process of ion milling, used to prepare specimens for TEM, can also introduce faults.[127,152] The models for the faults indicate that a local enrichment in copper accompanies fault formation. The copper enrichment might result from copper segregated at the surface diffusing into the crystals.[156] Alternatively, copper enrichment could result from the loss of yttrium or barium from the crystals. It is unclear what role reactive species such as water vapor or carbon dioxide play in fault formation, and it is possible that the defects contain other species such as carbon or OH^- groups. Extensive fault formation has also been observed in 123 crystals heated in a reducing atmosphere and then quenched.[62,157,158] In this case the faults appear to be part of the reaction mechanism through which 123 decomposes to $Y_2Ba_1Cu_1O_5$, $BaCuO_2$, and Cu_2O.

The periodic introduction of stacking faults in the 123 structure gives rise to two new phases, $Y_1Ba_2Cu_4O_8$ and $Y_2Ba_4Cu_7O_{14}$.[159–162] In $Y_1Ba_2Cu_4O_8$, extra Cu–O layers are inserted between the Ba–O layers in *every* 123 unit cell, while in $Y_2Ba_4Cu_7O_{14}$, extra Cu–O layers are inserted between the Ba–O layers in every *other* 123 unit cell. Both structures are orthorhombic with space group *Ammm*. The unit cell parameters for $Y_1Ba_2Cu_4O_8$ are $a \sim b = 3.86(1)$ and $c = 27.24(6)$ Å, and those for $Y_2Ba_4Cu_7O_{14}$ are $a = 3.851(1)$, $b = 3.869(1)$, and $c = 50.29(2)$Å. The thermodynamic stability of these new phases has yet to be determined; $Y_2Ba_4Cu_7O_{14}$ has been produced in bulk samples, but $Y_1Ba_2Cu_4O_8$ has only been made in thin films. The superconducting transition temperature does not change substantially with the periodic introduction of the extra Cu–O layers. $Y_1Ba_2Cu_4O_8$ has a T_c of 81 K and a ytterbium derivative of $Y_2Ba_4Cu_7O_{14}$ has a T_c of 86 K. These results

[155]G. Van Tendeloo and S. Amelinckx, *J. of Electron Microsc. Tech.* **8,** 285 (1988).

[156]H. W. Zandbergen, R. Gronsky, and G. Thomas, *Phys. Stat. Sol.* (*a*) **105,** 207 (1988).

[157]G. Van Tendeloo, H. W. Zandbergen, T. Okabe, and S. Amelinckx, *Solid State Commun.* **63,** 969 (1987).

[158]L. D. Marks, J. P. Zhang, S. J. Hwu, and K. R. Poeppelmeier, *J. Solid State Chem.* **69,** 189 (1987).

[159]A. F. Marshall, R. W. Barton, K. Char, A. Kapitulnik, B. Oh, R. H. Hammond, and S. S. Laderman, *Phys. Rev. B* **37,** 9353 (1988).

[160]P. Marsh, R. M. Fleming, M. L. Mandich, A. M. DeSantolo, J. Kwo, M. Hong, and L. J. Martinez-Miranda, *Nature* **334,** 141 (1988).

[161]T. Kogure, R. Kontra, G. J. Yurek, and J. B. Vander Sander, *Physica C* **156,** 45 (1988).

[162]P. Bordet, C. Chaillout, J. Chenavas, J. L. Hodeau, M. Marezio, J. Karpinski, and E. Kaldis, *Nature* **334,** 596 (1988).

support the view that it is the CuO_2 planes that are essential for obtaining high-temperature superconductivity. In addition, these new phases may aid in understanding the role of the layers that separate the CuO_2 planes. A similar situation occurs in the thallium-containing superconductors (see Section 14) where the CuO_2 planes are separated by either Tl–O monolayers or Tl–O bilayers.

7. Grain Boundaries

Numerous investigations implicate grain boundaries as the cause of the low critical current densities in polycrystalline 123.[163–169] There have been relatively few investigations, however, of intrinsic grain boundary structures. Part of the reason for this is that boundaries in materials processed under typical conditions contain a number of extrinsic features. Photoemission, inverse photoemission, and Auger spectroscopy of fracture surfaces in polycrystalline materials indicate the presence of carbonate phases at the grain boundaries,[170–172] which TEM observations confirm.[173] In many cases a discrete second phase is observed at the grain boundary,[173,174] but even in "clean" materials that show no evidence of second phases in the TEM, evidence of carbon segregation and carbonate formation is still seen in Auger spectra from the boundaries.[172]

[163]J. W. Ekin, *Adv. Ceram. Mater.* **2,** 586 (1987).

[164]S. Jin, R. A. Fastnacht, T. H. Tiefel, and R. C. Sherwood, *Appl. Phys. Lett.* **51,** 203 (1987).

[165]S. Jin, R. C. Sherwood, T. H. Tiefel, R. B. van Dover, D. W. Johnson, and G. S. Grader, *Appl. Phys. Lett.* **51,** 855 (1987).

[166]R. A. Camps, J. E. Evetts, B. A. Glowwaki, S. B. Newcomb, R. E. Somejh, and W. M. Stobbs, *Nature* **329,** 229 (1987).

[167]S. Jin, R. A. Fastnacht, T. H. Tiefel, and R. C. Sherwood, *Phys. Rev. B* **37,** 5828 (1988).

[168]J. W. Ekin, A. I. Braginski, A. J. Panson, M. A. Janocko, D. W. Capone, N. J. Zaluzec, B. Flandermeyer, O. F. Delima, M. Hong, J. Kwo, and S. H. Liou, *J. Appl. Phys.* **62,** 4821 (1987).

[169]R. L. Peterson, and J. W. Ekin, *Phys. Rev. B* **37,** 9848 (1988).

[170]J. A. Yarmoff, D. R. Clarke, W. Drube, U. O. Karlsson, A. Taleb-Ibrahimi, and F. J. Himpsel, *Phys. Rev. B* **36,** 3967 (1987).

[171]A. G. Schrott, S. L. Cohen, T. R. Dinger, F. J. Himpsel, J. A. Yarmoff, K. G. Frase, S. I. Park, and R. Purtell, *in* "Thin Film Processing and Characterization of High Temperature Superconductors," Conference Proceedings No. 165, p. 349 American Institute of Physics, 1987.

[172]S. Nakahara, G. J. Fisanick, M. F. Yan, R. B. van Dover, T. Boone, and R. Moore, *J. Cryst. Growth* **85,** 639 (1987).

[173]M. F. Chisholm (1987) (unpublished work).

[174]Y. Ishida, Y. Takahashi, M. Mori, K. Kishio, K. Kitazawa, K. Fueki, and M. Kawasaki, *J. Electron Microsc.* **36,** 251 (1987).

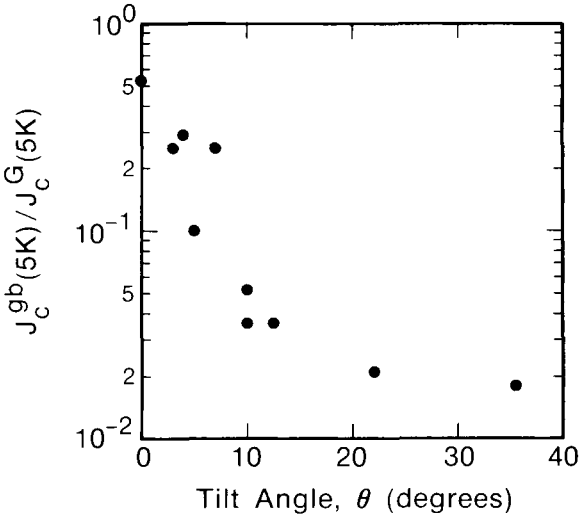

FIG. 15. Ratio of the grain boundary critical current density to the average critical current density in the two grains at 5 K versus the misorientation angle in the basal copper plane. (Dimos *et al.*[176])

Moreover, the thermal expansion anisotropy in the 123 structure leads to large internal stresses in polycrystalline materials that can cause cracking and extensive defect formation at grain boundaries,[172] especially in thermally cycled material.

The extrinsic grain boundary features described above certainly contribute to the low critical current densities, but recent experiments on individual boundaries in thin films graphically demonstrate that the critical current density (J_c) can be lowered by as much as a factor of 50 by *intrinsic* grain boundaries.[175,176] The ratio of the J_c supported by grain boundaries to the J_c of the grains is plotted versus grain boundary misorientation angle in Fig. 15. The rapid drop in the critical current density ratio with misorientation highlights the fact that the behavior comes from the intrinsic structure of the boundary and is therefore sensitive to the way the dislocation structure in the boundary changes with misorientation.

Characterization of the structures of intrinsic grain boundaries in 123

[175]P. Chaudhari, J. Mannhart, D. Dimos, C. C. Tsuei, J. Chi, M. M. Oprysko, and M. Scheuermann, *Phys. Rev. Lett.* **60,** 1653 (1988).

[176]D. Dimos, P. Chaudhari, J. Mannhart, and F. LeGoues, *Phys. Rev. Lett.* **61,** 219 (1988).

has been limited. Observations of the structure of low-angle tilt boundaries indicate that the misorientation between grains is accommodated by walls of defects with closure failures of 0.39 nm and 1.167 nm.[177] The 0.39 nm closure failure is consistent with dislocations of Burgers vector [010] as observed for perfect lattice dislocations.[178] The defect with the 1.167 nm closure failure indicates a dislocation with an unusually large Burgers vector, corresponding to the c axis of the structure, and it is proposed that the defect is actually a group of three closely spaced $\frac{1}{3}$[001] type partials. Each defect disturbs the continuity of the lattice planes across the boundary for several lattice planes. Given the short coherence length in 123 materials, the disruption of the structure caused by individual dislocations may be sufficient to lower the critical current density that can flow across grain boundaries made of walls of such defects. The misorientation dependence of J_c shown in Fig. 15, however, cannot be completely accounted for by a model in which the dislocations simply act as regions of "bad" material whose spacing decreases with increasing misorientation. Dimos *et al.*[176] therefore propose that the defects could also influence flux pinning in the boundary by providing an easy path for flux penetration.

No direct observations of the structures of intrinsic high-angle grain boundaries have been reported so far. Measurements of misorientations across grain boundaries from electron diffraction patterns[179] and from the external morphologies of clusters of faceted crystals[180] indicate that high-angle grain boundaries with certain preferred misorientations form. The observed misorientations are similar to those observed for special low Σ boundaries in cubic materials. Because most of the observed boundaries are twist type boundaries with the c axis as the misorientation axis, this behavior may simply reflect the similarity of the lengths of the a and b axes.

Two types of grain boundaries also occur in which the adjoining grains are misoriented by exactly 90°.[179,181,182] In one type the c axis in one grain interchanges with the a or b axis in the adjacent grain. In the other type

[177]M. F. Chisholm and D. A. Smith, *Phil. Mag.* (1989).

[178]S. Ikeda, T. Hatano, A. Matsushita, T. Matsumoto, and K. Ogawa, *Jpn. J. Appl. Phys.* **26,** L729 (1987).

[179]L. A. Tietz, B. C. De Cooman, C. B. Carter, D. K. Lathrop, S. E. Russek, and R. A. Buhrman, *J. Electron Microsc. Tech.* **8,** 263 (1988).

[180]D. A. Smith, M. F. Chisholm, and J. Clabes, *Appl. Phys. Lett.* (to appear December 1, 1988).

[181]H. You, J. D. Axe, X. B. Kan, S. C. Moss, J. Z. Liu, and D. J. Lam, *Phys. Rev. B* **37,** 2301 (1988).

[182]H. W. Zandbergen, R. Gronsky, M. Y. Chu, L. C. de Jonghe, G. F. Holland, and A. M. Stacy (1987) (unpublished).

the *a* and *b* axes interchange upon crossing adjacent (001) planes. These boundaries, sometimes referred to as "90° twins," are most commonly seen in partially reacted materials, suggesting that they are growth defects that develop when the 123 structure first forms. Prolonged annealing at 900–950°C greatly reduces the density of these boundaries.

V. Structural Variants

Following the discovery of superconductivity in the Y–Ba–Cu–O system, numerous researchers began to explore the feasibility of substituting different elements into the $Y_1Ba_2Cu_3O_{7-\delta}$ structure. To date, some degree of substitution has been achieved on each site in the structure. Part of the initial enthusiasm for substitutions came from the possibility of further raising the superconducting transition temperature. More recent studies have focussed on the structural, valence, and magnetic effects of cation substitutions in an effort to understand the relevance of various structural features to superconductivity. Several clear issues have emerged from these studies. The aim of this section is to examine the most important of these issues rather than to provide an exhaustive survey of the vast literature that has grown in this area. Several of these topics are still very active areas of research. Thus, it is only possible to present a subjective assessment of the field. After discussion of the various cation substitutions, reports of anion substitutions and investigations of the isotope effect are described.

8. Rare Earth Substitutions

Early studies[183–185] of substitutions concentrated on the replacement of Y by rare earth ions. These surveys found that all but a few of the lanthanide series could be incorporated in the $Y_1Ba_2Cu_3O_{7-\delta}$ structure. Variability in reported results suggested that some lanthanides form the 123 structure more readily than others. Subsequent studies have confirmed that all the lanthanides except Ce and Tb can fully replace Y in

[183]Z. Fisk, J. D. Thompson, E. Zirngiebl, J. L. Smith, and S. W. Cheong, *Solid State Commun.* **62,** 743 (1987).

[184]P. H. Hor, R. L. Meng, Y. Q. Wang, L. Gao, Z. J. Huang, J. Bechtold, K. Forster, and C. W. Chu, *Phys. Rev. Lett.* **58,** 1891 (1987).

[185]E. M. Engler, V. Y. Lee, A. I. Nazzal, R. B. Beyers, G. Lim, P. M. Grant, S. S. P. Parkin, M. L. Ramirez, J. E. Vazquez, and R. J. Savoy, *J. Am. Chem. Soc.* **109,** 2848 (1987).

the $Y_1Ba_2Cu_3O_{7-\delta}$ structure.[186–198] ($Pm_1Ba_2Cu_3O_{7-\delta}$ has not been synthesized due to its rapid radioactive decay, but is suspected to form.) The inability to form Ce and Tb 123 structures is explained by the ease with which Ce^{4+} and Tb^{4+} ions form. Of the structures that have been synthesized only $Pr_1Ba_2Cu_3O_{7-\delta}$ is not superconducting.[199–203] Similarly, this is attributed to the tendency of the +4 ion to form, but experimental evidence for the presence of Pr^{4+} is mixed. Magnetic susceptibility measurements[199,203] detect the presence of an effective moment of $2.9\,\mu_B$ on the Pr ions. By assuming contributions of $3.58\,\mu_B$ and $2.54\,\mu_B$ from the Pr^{+3} and Pr^{+4} ions, respectively, it is estimated that only 10% of the

[186]J. M. Tarascon, W. R. McKinnon, L. H. Greene, G. W. Hull, and E. M. Vogel, *Phys. Rev. B* **36,** 226 (1987).

[187]J. P. Golben, S. Lee, S. Y. Lee, Y. Song, T. W. Noh, X. Chen, and J. R. Gaines, *Phys. Rev. B* **35,** 8705 (1987).

[188]X. T. Xu, J. K. Liang, S. S. Xie, G. C. Che, X. Y. Shao, Z. G. Duan, and C. G. Cui, *Solid State Commun.* **63,** 649 (1987).

[189]Q. R. Zhang, Y. T. Qian, Z. Y. Chen, W. Y. Guan, Y. Zhao, H. Zhang, L. Z. Cao, J. S. Xia, G. Q. Pang, M. J. Zhang, Z. H. He, D. Q. Yu, S. F. Sun, T. Zhang, M. H. Fang, and Z. P. Yang, *Solid State Commun.* **63,** 497 (1987).

[190]K. N. Yang, Y. Dalichaouch, J. Ferreira, B. W. Lee, J. J. Neumeier, M. S. Torikachvili, H. Zhou, and M. B. Maple, *Solid State Commun.* **63,** 515 (1987).

[191]S. Lee, J. P. Golben, Y. Song, S. Y. Lee, T. W. Hoh, X. Chen, J. Testa, and J. R. Gaines, *Appl. Phys. Lett.* **51,** 282 (1987).

[192]S. Tsurumi, M. Hikita, T. Iwata, K. Semba, and S. Kurihara, *Jpn. J. Appl. Phys.* **26,** L856 (1987).

[193]S. Ohshima and T. Wakiyama, *Jpn. J. Appl. Phys.* **26,** L815 (1987).

[194]F. Garcia-Alvarado, E. Moran, M. Vallet, J. M. González-Calbet, M. A. Alario, M. T. Pérez-Frías, J. L. Vicent, S. Ferrer, E. García-Michel, and M. C. Asensio, *Solid State Commun.* **63,** 507 (1987).

[195]R. Escudero, T. Akachi, R. Barrio, L. E. Rendón-Diazmirón, C. Vázquez, L. Baños, G. Gonzáles, and F. Estrada, *Solid State Commun.* **64,** 235 (1987).

[196]E. A. Hayri, K. V. Ramanujachary, S. Li, M. Greenblatt, S. Simizu, and S. A. Friedberg, *Solid State Commun.* **64,** 217 (1987).

[197]J. J. Neumeier, Y. Dalichaouch, J. M. Ferreira, R. R. Hake, B. W. Lee, M. B. Maple, K. N. Torikachvili, K. N. Yang, and H. Zhou, *Appl. Phys. Lett.* **51,** 371 (1987).

[198]R. Liang, Y. Inaguma, Y. Takagi, and T. Nakamura, *Jpn. J. Appl. Phys.* **26,** L1150 (1987).

[199]B. Okai, K. Takahashi, H. Nozaki, M. Saeki, M. Kosuge, and M. Ohta, *Jpn. J. Appl. Phys.* **26,** L1648 (1987).

[200]L. Soderholm, K. Zhang, D. G. Hinks, M. A. Beno, J. D. Jorgensen, C. U. Segre, and I. K. Schuller, *Nature* **328,** 604 (1987).

[201]Y. Dalichaouch, M. S. Torikachvili, E. A. Early, B. W. Lee, C. L. Seaman, K. N. Yang, H. Zhou, and M. B. Maple, *Solid State Commun.* **65,** 1001 (1988).

[202]J. K. Liang, X. T. Xu, S. S. Xie, G. H. Rao, X. Y. Shao, and Z. G. Duan, *Z. Phys. B* **69,** 137 (1987).

[203]A. B. Okai, M. Kosuge, H. Nozaki, K. Takahashi, and M. Ohta, *Jpn. J. Appl. Phys.* **27,** L41 (1988).

Pr ions are in a Pr^{+3} state. This is inconsistent with lattice parameter and bond length measurements made on $Pr_1Ba_2Cu_3O_{7-\delta}$, which follow the trend with ionic radius expected if the Pr ions are predominately in a 3+ state.[204] Partial substitution of Pr for Y in the structure produces a monotonic decrease in the superconducting transition temperature, and substitution of more than half the Y with Pr produces a semiconducting material.[200–203] Again it is found that partial substitution of Pr for Y causes a change in lattice parameters that is consistent with Pr^{3+}, but magnetic susceptibility measurements indicate that Pr is mainly present as Pr^{4+}. Evidence for partial mixing of Pr on the Ba site is also observed,[203] which may contribute to the decrease in T_c. The anomalous behavior of the lattice parameters suggests that there may be structural differences between the Pr 123 structure and the other rare earth 123 structures. One possibility is that Pr^{4+} draws oxygen into the Y layer causing it to expand.[203] For the remaining $R_1Ba_2Cu_3O_{7-\delta}$ structures, transition temperatures on the order of 91–95 K are reported for the fully substituted structures. Remarkably, the presence of magnetic rare earth ions such as Gd and Ho has little effect on the superconducting transition temperature.

Many x-ray and neutron diffraction studies have been made of the rare earth substituted structures.[204–212] A summary of unit cell dimensions and atomic coordinates for the different orthorhombic structures is given in Table V. As expected, the unit cell volume decreases with increasing atomic number, due to the well-known variation of ionic radius with f electron count in the rare earths.[213] Based on data in an early study,[186] it was suggested that T_c for the rare earth compounds increases as the unit cell volume increases.[214] A more comprehensive survey of data from

[204]Y. Le Page, T. Siegrist, S. A. Sunshine, L. F. Schneemeyer, D. W. Murphy, S. M. Zahurak, J. V. Waszczak, W. R. McKinnon, J. M. Tarascon, G. W. Hull, and L. H. Greene, *Phys. Rev. B* **36,** 3617 (1987).

[205]T. Ishigaki, H. Asano, and K. Takita, *Jpn. J. Appl. Phys.* **26,** L987 (1987).

[206]T. Ishigaki, H. Asano, K. Takita, H. Katoh, H. Akinaga, F. Izumi, and N. Watanabe, *Jpn. J. Appl. Phys.* **26,** L1681 (1987).

[207]T. Ishigaki, H. Asano, and T. Takita, *J. Appl. Phys.* **26,** L1226 (1987).

[208]M. Onoda, S. Shamoto, M. Sato, and S. Hosoya, *Jpn. J. Appl. Phys.* **26,** L876 (1987).

[209]K. Takita, H. Akinaga, H. Katoh, T. Ishigaki, and H. Asano, *Jpn. J. Appl. Phys.* **26,** L1023 (1987).

[210]H. Asano, T. Ishigaki, and K. Takita, *Jpn. J. Appl. Phys.* **26,** L714 (1987).

[211]H. Asano, K. Takita, T. Ishigaki, H. Akinaga, H. Katoh, K. Masuda, F. Izumi, and N. Watanabe, *Jpn. J. Appl. Phys.* **26,** L1341 (1987).

[212]H. Asano, K. Takita, H. Katoh, H. Akinaga, T. Ishigaki, M. Nishino, M. Imai, and K. Masuda, *Jpn. J. Appl. Phys.* **26,** L1410 (1987).

[213]R. D. Shannon, *Acta Cryst. A* **32,** 751 (1976).

[214]T. J. Kistenmacher, *Solid State Commun.* **65,** 981 (1988).

TABLE V. UNIT CELL DIMENSIONS, R^{3+} RADII, z COORDINATES, AND O(1) OCCUPANCY FOR $R_1Ba_2Cu_3O_{7-\delta}$, WHERE R = RARE EARTH. THE ESTIMATED STANDARD DEVIATIONS (IN PARENTHESES) REFER TO THE LAST DIGIT PRINTED. (LE PAGE *et al.*[204])

	a(Å)	b(Å)	c(Å)	RADIUS (Å)	
Pr	3.905(2)	3.905(2)	11.660(10)	1.013	
Sm	3.891(1)	3.894(1)	11.660(1)	0.964	
Eu	3.869(2)	3.879(3)	11.693(6)	0.950	
Gd	3.854(2)	3.896(2)	11.701(7)	0.938	
Dy	3.830(3)	3.885(2)	11.709(3)	0.908	
Y	3.827(1)	3.877(1)	11.708(6)	0.905	
Ho	3.846(1)	3.881(1)	11.640(2)	0.894	
Er	3.812(3)	3.851(4)	11.626(2)	0.881	
Tm	3.829(3)	3.860(3)	11.715(2)	0.869	
	z(Ba)	z(Cu(2))	z(O(4))	z(O(2,3))	occ(O(1))
Pr	0.1840(3)	0.3507(8)	0.157(5)	0.371(4)	1.0(2)
Sm	0.1853(2)	0.3554(4)	0.158(3)	0.374(2)	0.6(2)
Eu	0.1847(3)	0.3530(8)	0.159(5)	0.374(4)	0.4(2)
Gd	0.1855(2)	0.3546(4)	0.151(2)	0.377(2)	0.7(2)
Dy	0.1864(2)	0.3564(3)	0.157(2)	0.378(2)	0.7(2)
Y	0.1874(3)	0.3565(4)	0.157(3)	0.379(3)	0.8(2)
Ho	0.1858(2)	0.3577(4)	0.159(3)	0.378(2)	0.6(2)
Er	0.1866(2)	0.3579(4)	0.159(3)	0.381(2)	0.8(2)
Tm	0.1892(1)	0.3593(2)	0.155(2)	0.380(1)	0.5(1)

several sources,[184–186,190,192] however, suggests that the correlation of T_c with unit cell volume is weak if it is present at all. Le Page *et al.*[204] noted that the main effect of rare earth substitution is to change the bond lengths that involve the rare earth ion, as can be seen in their plot of rare earth-Cu(2) bond lengths in Fig. 16. By comparison, the average Ba–Cu distance remains almost constant across the series (Fig. 16 also). These trends, they suggest, indicate that rare earth substitutions have little effect on the substructure formed by the copper-oxygen chains and planes that surround the Ba ions. Subsequent structural studies support this view.[205–212]

Rare earth ions towards the La end of the lanthanide series are large enough to partially substitute on the Ba^{+2} site. The resulting compounds, with the general formula $R_{1+x}Ba_{2-x}Cu_3O_{7\pm\delta}$, exhibit more complex behavior than the other rare earth 123 structures because of their cation solid solution range. Historically, $La_3Ba_3Cu_6O_{14+\delta}$ was identified before $Y_1Ba_2Cu_3O_{7-\delta}$. Based on x-ray diffraction patterns it was suggested that the La structure was an oxygen deficient perovskite in which ordering of

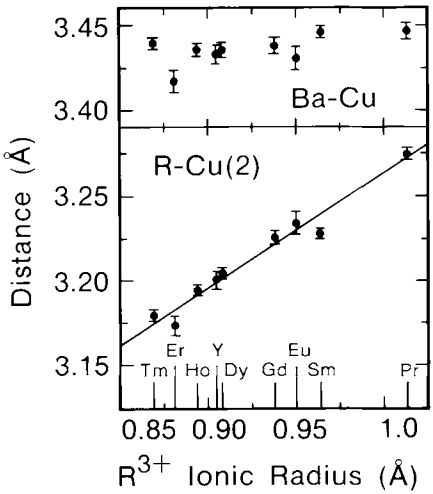

FIG. 16. Averaged Ba–Cu distance and R–Cu(2) distance versus R^{3+} radius, where R = rare earth. The Ba–Cu distance is independent of the R^{3+} radius. The R–Cu(2) distance is composed of an R–O and a Cu(2)–O distance at right angles (the latter distance is independent of the R^{3+} radius) and therefore varies approximately with a slope of $1/\sqrt{2}$. (Le Page *et al.*[204])

the oxygen vacancies tripled one of the cubic perovskite unit cell dimensions.[30] More recent neutron diffraction studies[215–218] found that $La_3Ba_3Cu_6O_{14+\delta}$ is essentially isomorphous with tetragonal $Y_1Ba_2Cu_3O_{7-\delta}$, with La fully replacing Y and the excess La partially replacing Ba in the structure; i.e., the structure is better described as $La_{1.5}Ba_{1.5}Cu_3O_{7+\delta}$. Studies of superconductivity in the La–Ba–Cu–O system have reported transition temperatures that vary widely. Systematic studies of $La_{1+x}Ba_{2-x}Cu_3O_{7+\delta}$, in which x was varied over the range 0 to 0.5, found that T_c decreased with increasing La substitution.[218,219]

[215]W. I. F. David, W. T. A. Harrison, R. M. Ibberson, M. T. Weller, J. R. Grasmeder, and P. Lanchester, *Nature* **328,** 328 (1987).

[216]R. Yoshizaki, H. Sawada, T. Iwazumi, Y. Saito, H. Ikeda, K. Imai, and I. Nakai, *Jpn. J. Appl. Phys.* **26,** L1703 (1987).

[217]F. Izumi, H. Asano, T. Ishigaki, E. Takayama-Muromachi, Y. Matsui, and Y. Uchida, *Jpn. J. Appl. Phys.* **26,** L1153 (1987).

[218]C. U. Segre, B. Dabrowski, D. G. Hinks, K. Zhang, J. D. Jorgensen, M. A. Beno, and I. K. Schuller, *Nature* **329,** 227 (1987).

[219]E. Takayama-Muromachi, Y. Uchida, A. Fujimori, and K. Kato, *Jpn. J. Appl. Phys.* **26,** L1546 (1987).

Single phase materials were obtained only if x was greater than 0.25. Neutron diffraction refinements[218] showed that the more barium-rich compositions are orthorhombic, but the orthorhombicity decreases with increasing La substitution, and the structure becomes tetragonal at $x = 0.5$.

Neutron diffraction was also used to determine the total oxygen content of $La_{1+x}Ba_{2-x}Cu_3O_{7+\delta}$ and the distribution of oxygen in the unit cell.[218] The oxygen content refined to a value greater than seven in all the structures and varied only slightly with the degree of La substitution. In the orthorhombic structures, both oxygen sites in the basal copper plane are partially occupied and show greater disordering of oxygens between the two sites than in orthorhombic $Y_1Ba_2Cu_3O_7$. Increasing La substitution decreased the oxygen order in the basal plane and produced a smooth monotonic decrease in T_c that correlated well with the order parameter. This observation, coupled with the fact that the formal charge on the copper remained constant at a value of about +2.3 across the series, was taken as evidence that ordering of the Cu–O chains was essential for superconductivity.

Studies of partial substitution of La for Ba in $Y_1Ba_{2-x}La_xCu_3O_{7+\delta}$[198,220–224] also found that increasing La substitution induces an orthorhombic-to-tetragonal transition and lowers T_c. The composition at which the $Y_1Ba_{2-x}La_xCu_3O_{7+\delta}$ structure becomes tetragonal is $x \simeq 0.3$–0.4.[198,221] In contrast to the results reported in the $La_{1+x}Ba_{2-x}Cu_3O_{7+\delta}$ system, the orthorhombic-to-tetragonal transition does not appear to be associated with a loss of superconductivity in $Y_1Ba_{2-x}La_xCu_3O_{7+\delta}$. Measurements of the oxygen content by wet iodometric titration indicated that the substitution produces intercalation of oxygen in excess of the O_7 stoichiometry. At low La concentrations ($0 < x < 0.05$), oxygen appears to intercalate as a monomeric species. At high La concentrations, however, the oxygen may intercalate as dimeric O_2^{2-} peroxide ions.[221]

Substitution in the $Nd_{1+x}Ba_{2-x}Cu_3O_{7-\delta}$ system produces similar be-

[220]B. Chevalier, B. Buffat, G. Demazeau, B. Lloret, J. Etourneau, M. Hervieu, C. Michel, B. Raveau, and R. Tournier, *J. de Phys.* **48,** 1619 (1987).

[221]A. Manthiram, X. X. Tang, and J. B. Goodenough, *Phys. Rev. B* **37,** 3734 (1988).

[222]A. Maeda, T. Yabe, K. Uchinokura, M. Izumi, and S. Tanaka, *Jpn. J. Appl. Phys.* **26,** L1550 (1987).

[223]Y. Tokura, J. B. Torrance, T. C. Huang, and A. I. Nazzal, *Phys. Rev. B* **38,** 7156 (1988).

[224]A. Tokiwa, Y. Soyono, M. Kikuchi, R. Suzuki, T. Kajitani, N. Kobayashi, T. Sasaki, O. Nakatsu, and Y. Muto, *Jpn. J. Appl. Phys.* **27,** L1009 (1988).

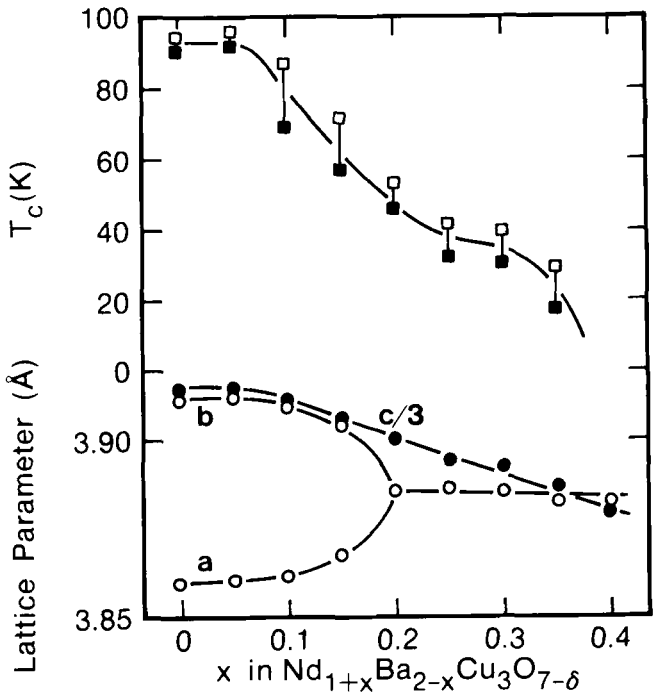

FIG. 17. Dependence of lattice parameters and T_c upon x in $Nd_{1+x}Ba_{2-x}Cu_3O_{7-\delta}$. Open and filled squares represent onset and zero-resistance temperatures, respectively. (Takita *et al.*[229])

havior to that in the La 123 compounds,[225–232] with a substitution-induced orthorhombic-to-tetragonal transition occurring at $x = 0.2$.[227,229] As in $Y_1Ba_{2-x}La_xCu_3O_{7+\delta}$, the orthorhombic-to-tetragonal transition has no influence on the decrease in T_c that occurs with increasing Nd substitution, and tetragonal material can be superconducting. Typical data for the variation of T_c and unit cell dimensions in $Nd_{1+x}Ba_{2-x}Cu_3O_{7-\delta}$ as a function of x are shown in Fig. 17. At higher substitution levels

[225]F. Izumi, S. Takekawa, Y. Matsui, N. Iyi, H. Asano, T. Ishigaki, and N. Watanabe, *Jpn. J. Appl. Phys.* **26,** L1616 (1987).

[226]R. J. De Angelis, J. W. Brill, M. Chung, W. D. Arnett, X. D. Xiang, G. Minton, L. A. Rice, and C. E. Hamrin, Jr., *Solid State Commun.* **64,** 1353 (1987).

[227]S. Takekawa, H. Nozaki, Y. Ishizawa, and N. Iyi, *Jpn. J. Appl. Phys.* **26,** L2076 (1987).

[228]H. Nozaki, S. Takekawa, and Y. Ishizawa, *Jpn. J. Appl. Phys.* **27,** L31 (1988).

[229]K. Takita, H. Katoh, H. Akinaga, M. Nishino, T. Ishigaki, and H. Asano, *Jpn. J. Appl. Phys.* **27,** L57 (1987).

[230]S. Tsurumi, T. Iwata, Y. Tajima, and M. Hikita, *Jpn. J. Appl. Phys.* **27,** L80 (1988).

[231]K. Takita, H. Akinaga, H. Katoh, H. Asano, and K. Masuda, *Jpn. J. Appl. Phys.* **27,** L67 (1988).

[232]K. Takita, H. Akinaga, H. Katoh, and K. Masuda, *Jpn. J. Appl. Phys.* **27,** L607 (1988).

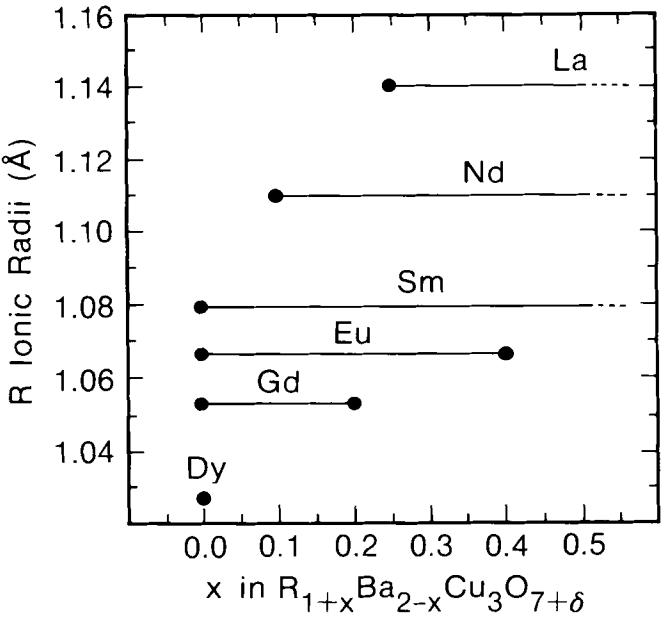

FIG. 18. Solid solution ranges for the systems $R_{1+x}Ba_{2-x}Cu_3O_{7+\delta}$ with R = La, Nd, Sm, Eu, Gd, and Dy. The full lines indicate the region in which a single phase is observed, while the broken lines indicate the possible extension of the single phase into regions not studied. (Zhang *et al.*[234])

($x = 0.25$—0.4) the Nd-substituted material is reportedly semiconducting,[228] but treatments in high-pressure oxygen at 450°C have restored superconductivity in materials with x as high as 0.5.[230] Neutron diffraction refinements[225] and hydrogen reduction[227] of the tetragonal superconducting materials indicate that the oxygen content is nearly 7 and the two basal plane oxygen sites are approximately 50% occupied, as in the La system. At higher Nd concentrations ($x = 0.8$) the presence of a superlattice that doubles the a and c axes of the structure has been detected by electron diffraction.[233]

Solid solution ranges for several other large rare earth ions have now been explored.[234–236] A graph summarizing the data from a study by Zhang *et al.*[234] is shown in Fig. 18. Although the solubility ranges differ

[233]Y. Matsui, S. Takekawa, and N. Iyi, *Jpn. J. Appl. Phys.* **26,** L1693 (1987).
[234]K. Zhang, B. Dabrowski, C. U. Segre, D. G. Hinks, I. K. Schuller, J. D. Jorgensen, and M. Slaski, *J. Phys. C* **20,** L935 (1987).
[235]H. Akinaga, H. Katoh, K. Takita, H. Asano, and K. Masuda, *Jpn. J. Appl. Phys.* **27,** L610 (1988).
[236]T. Iwata, M. Hikita, Y. Tajima, and S. Tsurumi, *Jpn. J. Appl. Phys.* **26,** L2049 (1987).

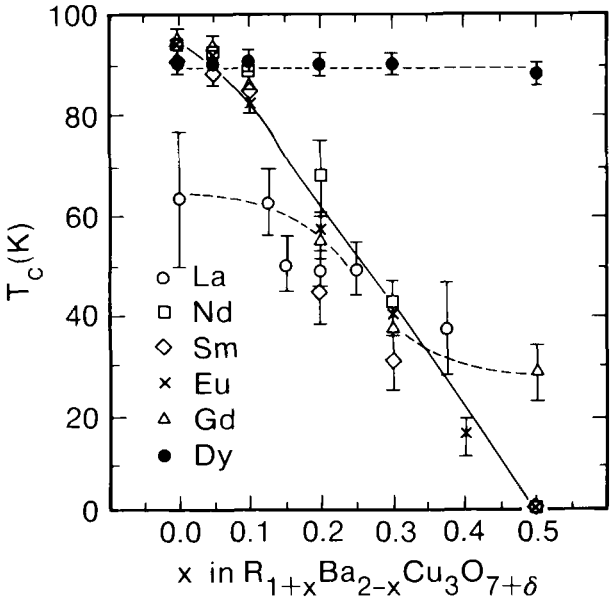

FIG. 19. Superconducting transition temperatures as a function of x for the systems $R_{1+x}Ba_{2-x}Cu_3O_{7+\delta}$ with R = La, Nd, Sm, Eu, Gd, and Dy. The error bars indicate the 90% and 10% points of the resistivity transition. Note the deviations from universal behavior for La, Gd, and Dy, indicating the ends of their solubility ranges. (Zhang *et al.*[234])

somewhat from studies that used different preparative conditions, overall solubility trends with ionic radius are evident. Figure 18 suggests that there may be a lower solubility limit for the larger rare earth ions determined by whether or not the ion is small enough to fit in the yttrium site. An upper solubility limit is determined by the size match to the larger barium site. Intermediate-sized ions such as samarium thus have extensive solubility. Zhang *et al.*[234] also suggest that the difficulty in forming the ytterbium and lutetium structures could be caused by their being too small to fit in even the yttrium site. The plot of T_c versus x shown in Fig. 19 indicates that over the composition ranges where solid solutions form, T_c decreases as a more or less universal function of x for each of the rare earths. As a result, dysprosium, which has almost no solid solution range, produces only a small variation in T_c, whereas samarium, which has extensive solubility, varies T_c over a wide composition range. Iqbal *et al.*[237] report that the solid solution

[237]Z. Iqbal, F. Reindinger, A. Bose, N. Cipollini, T. J. Taylor, H. Eckhardt, B. L. Ramakrishna, and E. W. Ong, *Nature* **331,** 326 (1988).

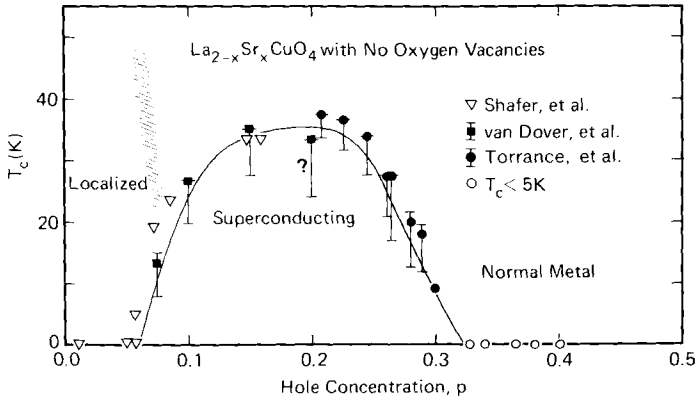

FIG. 20. The dependence of T_c on hole concentration in $La_{2-x}Sr_xCuO_4$ with no oxygen vacancies. The question mark refers to the possibility that this sample may have some oxyen vacancies. (Torrance *et al.*[238])

$Y_{1+x}Ba_{2-x}Cu_3O_{7-\delta}$, with $x = 0.5$ and $x = 0.375$, can form as a metastable phase. The yttrium ion, however, is smaller than Dy^{+3}, and therefore a stable Y–Ba solid solution is unlikely under normal preparative conditions. The fact that a wide range of compositions in the Y–Ba–Cu–O system have almost identical superconducting transition temperatures supports this conclusion.

Considerable speculation has arisen about the cause of the variations in T_c across the rare earth solid solution ranges. Initial attempts to correlate the decrease in T_c with the disruption of chains and the degree of order in the basal plane of the structure[218] appear to be incorrect, since T_c varies even in composition ranges where the tetragonal phase forms and hence the degree of order is constant. Hole concentration measurements (made using a wet chemical method) in the simpler $La_{2-x}Sr_xCuO_{4-\delta}$ ($x = 0$–0.4) system indicate that T_c is strongly correlated to the concentration of holes in the structure,[238] as can be seen from the data in Fig. 20. A similar correlation can be made for the 123 rare earth solid solutions if the hole concentration is estimated using a simple model in which it is directly controlled by the substitution of trivalent rare earth ions for the divalent Ba ions.[231] The model is based on the assumption that the oxygen concentration remains constant on substitution. Meas-

[238]M. W. Shafer, T. Penney, and B. Olsen, *Phys. Rev. B* **36,** 4047 (1987); J. B. Torrance, Y. Tokura, A. I. Nazzal, A. Bezinge, T. C. Huang, and S. S. P. Parkin, *Phys. Rev. Lett.* **61,** 1127 (1988); and R. B. van Dover, R. J. Cava, B. Batlogg, and E. A. Rietman, *Phys. Rev. B* **35,** 5337 (1987).

urements on $Y_1Ba_{2-x}La_xCu_3O_{7+\delta}$, however, indicate that the oxygen content of the structure increases with increasing substitution[221] and compensates for the introduction of the La^{3+} ion if the oxygen is introduced as O^{-2} ions. This observation led to the suggestion that oxygen may intercalate as O_2^{-2} peroxide ions, which would then require partial compensation for the charge on the substituted ions by a reduction in the number of holes.[221] Indirect evidence for peroxide formation in the

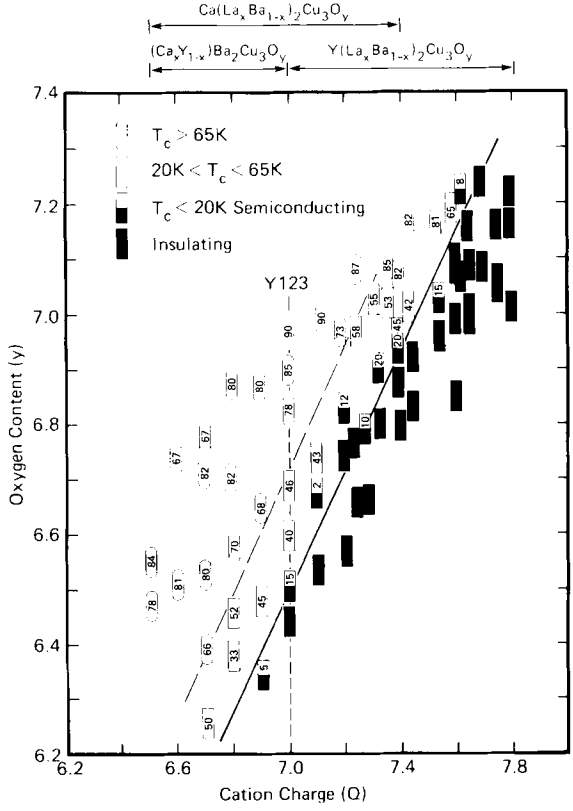

FIG. 21. (a) The oxygen content (±0.03) measured for a series of isostructural samples made with different total charge, Q, on the non-copper metals. The short dashed line labelled Y123 is for $Y_1Ba_2Cu_3O_y$. The solid line is drawn to separate insulating and superconducting samples, while the long dashed line is drawn to separate the high T_c samples from those with $20\,K < T_c < 65\,K$, where T_c is the zero resistance temperature. In (b) the data are replotted using the relation $Q + 3(2 + p) = 2y$ to calculate the average $[Cu\text{–}O]^{+p}$ charge. (Tokura *et al.*[223])

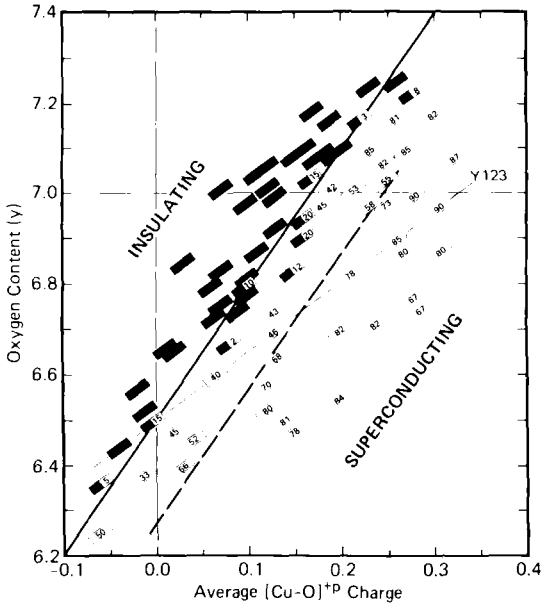

FIG. 21. (b)

$Y_1Ba_2Cu_3O_{7-\delta}$ structure has been obtained by Shafer *et al.*[239] by dissolving isotope-tagged materials. In spite of this possible difficulty with the simple compensation model of Takita *et al.*,[231] measurements of hole concentrations made using the Hall effect correlate with the trend predicted by the model for Nd-doped materials.[232] Further experiments, including measurements of charge on the copper ions and hole concentrations from Hall measurements, are needed to confirm these results and determine if the same type of behavior occurs for the other rare earth solid solutions.

Tokura *et al.*[223] looked at 123 materials in which La substitution on the Ba site, Ca substitution on the Y site, and annealing in different pressures of oxygen were used to vary independently the effective copper valence $(2+p)$ and the oxygen content (y) over a wide range (see Fig. 21). They found that a high effective copper valence in the structure alone was not sufficient to produce superconductivity and suggested that the hole concentrations in the planes must be high for superconductivity. Nonsuperconducting behavior observed in materials with a high average

[239]M. W. Shafer, R. A. de Groot, M. M. Plechaty, and G. J. Scilla, *Physica C* **153–155,** 836 (1988).

hole concentration was then explained by the possibility that holes preferentially form on the chains rather than on the planes. By postulating a threshold concentration for hole formation in the planes that depends on the oxygen content of the chains, Tokura *et al.*[223] rationalized much of their experimental data and obtained a correlation between T_c and the hole concentration within the planes. Direct verification of these ideas, however, will be difficult, because it requires localized measurements of hole concentrations in the planes and in the chains.

9. Transition Element Substitutions

Most of the work on copper substitution has focussed on elements in the series from Fe to Ga. Preliminary studies showed that each element strongly suppresses T_c, but differed as to which element has the largest effect.[240–242] From investigations of the variation in T_c with the degree of substitution,[241,243,244] it is now generally agreed that T_c is most strongly suppressed by zinc. Iron and cobalt, which act similarly, have a lesser effect. Nickel reportedly[241–243] has the least effect on T_c, but was found to suppress T_c as strongly as zinc in one study.[244] With nickel or zinc additions, the fully oxygenated phase remains orthorhombic.[242] In contrast, transition to a tetragonal structure occurs with small additions of iron, cobalt, or gallium. The retention of an orthorhombic structure in the Ni- and Zn-substituted materials has been rationalized on the basis that Ni and Zn substitute as 2+ ions whereas Ga, Co, and Fe substitute with higher valence states (+3 or +4). The higher valence ions could then draw excess oxygen into the structure in order to increase their oxygen coordination, causing disordering of the oxygens in the basal copper plane. This argument is based on the assumption that the higher valence ions substitute into the Cu(1) chain sites. As shown in Fig. 22, the variation in T_c that occurs on substitution is not influenced by the orthorhombic-to-tetragonal transition.

[240]G. Xiao, F. H. Streitz, A. Gavrin, Y. W. Du, and C. L. Chien, *Phys. Rev. B* **35,** 8782 (1987).

[241]S. B. Oseroff, D. C. Vier, J. F. Smyth, C. T. Salling, S. Schultz, Y. Dalichaouch, B. W. Lee, M. B. Maple, Z. Fisk, J. D. Thompson, J. L. Smith, and E. Zirngiebl, *Solid State Commun.* **64,** 241 (1987).

[242]Y. Maeno, T. Tomita, M. Kyogoku, S. Awaji, Y. Aoki, K. Hoshino, A. Minami, and T. Fujita, *Nature* **328,** 512 (1987).

[243]E. Takayama-Muromachi, Y. Uchida, and K. Kato, *Jpn. J. Appl. Phys.* **26,** L2087 (1987).

[244]J. M. Tarascon, P. Barboux, P. F. Miceli, L. H. Greene, G. W. Hull, M. Eibschutz, and S. A. Sunshine, *Phys. Rev. B* **37,** 7458 (1988).

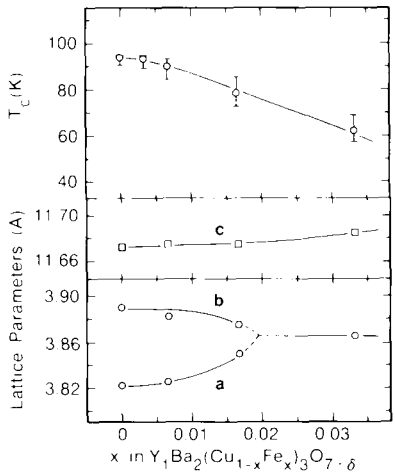

FIG. 22. Dependence of lattice parameters and T_c upon x in $Y_1Ba_2(Cu_{1-x}Fe_x)_3O_{7\pm\delta}$. Doping with Fe induces an orthorhombic-to-tetragonal phase transition at $\cong 0.02$ but the variation in T_c with x is smooth and insensitive to the structural transition. (Maeno *et al.*[242])

Analysis of substitutions for copper is complicated by the fact that two distinct copper sites exist in the $Y_1Ba_2Cu_3O_{7-\delta}$ structure. Much effort has therefore been directed towards identifying the way in which the substituents are distributed between the two sites. Conflicting conclusions have been reached in many cases. For example, neutron diffraction data from a $Y_1Ba_2Cu_{2.7}Zn_{0.3}O_{6.75}$ sample located 75% of the Zn^{+2} ions in the Cu(2) site,[245] but a second study on a sample with less zinc, $Y_1Ba_2Cu_{2.8}Zn_{0.2}O_{6.8}$, reached the opposite conclusion and placed all of the zinc in the Cu(1) site.[246] Results also disagree for the nickel substituted materials. Here, neutron diffraction indicates that the Ni ions are located entirely on the Cu(2) site in the CuO_2 planes,[245] but Raman scattering suggests that Ni^{+2} substitutes into the Cu(1) site in the chains.[247] For cobalt it is agreed[245,248–250] that substitution occurs prima-

[245]T. Kajitani, K. Kusaba, M. Kikuchi, Y. Syono, and M. Hirabayashi, *Jpn. J. Appl. Phys.* **27,** L354 (1988).

[246]G. Xiao, M. Z. Cieplak, D. Musser, A. Gavrin, F. H. Streitz, C. L. Chien, J. J. Rhyne, and J. A. Gotaas, *Nature* **332,** 238 (1988).

[247]Z. Iqbal, S. W. Steinhauser, A. Bose, N. Cipollini, and H. Echhardt, *Phys. Rev. B* **36,** 2283 (1987).

[248]T. Kajitani, K. Kusaba, M. Kikuchi, Y. Syono, and M. Hirabayashi, *Jpn. J. Appl. Phys.* **26,** L1727 (1987).

[249]P. F. Miceli, J. M. Tarascon, L. H. Greene, P. Barboux, F. J. Rotella, and J. D. Jorgensen, *Phys. Rev. B* **37,** 5932 (1988).

[250]Y. K. Tao, J. S. Swinnea, A. Manthiram, J. S. Kim, J. B. Goodenough, and H. Stienfink, *J. Mater. Res.* **3,** 248 (1988).

rily on the Cu(1) site. It is difficult to locate gallium by x-ray or neutron diffraction because the scattering amplitudes for gallium and copper are similar. We found no reports with direct evidence for the location of gallium in gallium-substituted 123.

The most comprehensive studies of the location of a substituted ion have been made for iron because its local state can be probed using Mossbauer spectroscopy. Unfortunately, considerable disagreement has arisen about the site assignment of the observed quadrupole doublets.[251–260] Two prominent quadrupole doublets are seen at room temperature,[251–254] one with a splitting of 1.05 mm/s and the other with a larger splitting of 1.97 mm/s. Both doublets have a small isomer shift of about −0.1 to −0.2 mm/s. Some researchers suggest that the spectra consist of two doublets with nearly the same splitting but different isomer shifts.[254,257] This assignment seems unlikely because changes in iron or oxygen content then do not affect the intensity of the doublets symmetrically. Rough estimates of the field gradients in the Cu(1) and Cu(2) sites led Tang *et al.*[251] to assign the larger splitting (1.97 mm/s) to Fe^{3+} ions located in the Cu(1) site and the smaller splitting to the Cu(2) site, whereas Coey *et al.*[252] reached the opposite conclusion. Assignment on the assumption that the iron is uniformly distributed between sites led Zhou *et al.*[255] to conclude that the more intense doublet with the smaller splitting came from Fe^{+3} on the more abundant Cu(2) site.

Variations in the Mossbauer spectra with composition have also been studied. For example, Bauminger *et al.*[256] compared spectra from oxygenated and quenched samples and found changes in the intensities of both doublets. Because it seems unlikely that the distribution of iron in the two sites changes on cooling, and because the oxygen environment

[251]H. Tang, Z. Q. Qiu, Y. Du, G. Xiao, C. L. Chien, and J. C. Walker, *Phys. Rev. B* **36,** 4018 (1987).

[252]J. M. D. Coey and K. Donnelly, *Z. Phys. B* **67,** 513 (1987).

[253]Z. Q. Qiu, Y. W. Du, H. Tang, J. C. Walker, W. A. Bryden, and K. Moorjani, *J. Magnetism and Magnetic Mater.* **69,** L221 (1987).

[254]R. Gómez, S. Aburto, M. L. Marquina, M. Jiménez, V. Marquina, C. Quintanar, T. Akachi, R. Escudero, R. A. Barrio, and D. Rios-Jara, *Phys. Rev. B* **36,** 7226 (1987).

[255]X. Z. Zhou, M. Raudsepp, Q. A. Pankhurst, A. H. Morrish, Y. L. Luo, and I. Maartense, *Phys. Rev. B* **36,** 7230 (1987).

[256]E. R. Bauminger, M. Kowitt, I. Felner, and I. Nowik, *Solid State Commun.* **65,** 123 (1988).

[257]C. W. Kimball, J. L. Matykiewicz, J. Giapintzakis, A. E. Dwight, M. B. Brodsky, M. Slaski, B. D. Dunlap, and F. Y. Fradin, *Physica B* **148,** 309 (1987).

[258]T. Tamaki, T. Komai, A. Ito, Y. Maeno, and T. Fujita, *Solid State Commun.* **65,** 43 (1988).

[259]M. Takano and Y. Takeda, *Jpn. J. Appl. Phys.* **26,** L1862 (1987).

[260]M. W. Dirken, R. C. Thiel, H. H. A. Smit, and H. W. Zandbergen, *Physica C* **156,** 303 (1988).

around the Cu(2) site is unchanged by oxygenation, they proposed that both doublets must come from Fe^{+3} in the Cu(1) site. Furthermore, they suggested that the doublets came from ions in the chain sites coordinated with different numbers of oxygens. A more detailed study of the effect of oxygen content on the spectra, in which the iron content was kept constant and the oxygen content varied,[259] found that the doublet with the largest splitting remained constant for oxygen contents from 6.0 to 6.9, while the second doublet grew with increasing oxygen content. This behavior suggests that the doublet that remains constant comes from iron in the unchanging Cu(2) site and that the change in the second doublet comes from changes in the environment of Fe^{+3} ions on the Cu(1) site. At oxygen contents higher than 6.8, changes in both doublets were observed that were attributed to Fe ions transferring from the Cu(2) site to the Cu(1) site.

In some studies, an additional doublet with a splitting of 0.58 mm/s and an isomer shift of 0.36 mm/s was observed. This doublet has been attributed to Fe^{3+} in Cu(1) sites coordinated with different numbers of oxygens,[252,255–260] Fe^{+3} in octahedrally coordinated sites in the Cu(2) layer,[259] and increased Fe^{+3} coordination at sites in grain boundaries or twins.[252] The assignment of a +3 oxidation state to Fe has also been questioned and the suggestion made that some peaks may be caused by impurity phases.[261]

Diffraction studies of iron-doped materials provide more direct information about the location of iron in the structure. These studies find that the iron substitutes primarily on the Cu(1) site,[250,261,262] thus favoring the assignment of Mossbauer peaks proposed by Bauminger *et al.*[256] The combination of the Mossbauer and x-ray diffraction data strongly supports the suggestion that iron has several different oxygen coordinations in the chains.[261,262] The observation that Co ions substitute onto the chain sites is also consistent with this idea. The proposal that the higher valence ions change the distribution of oxygen in the basal plane of the structure in order to increase their oxygen coordination therefore seems reasonable.

The coordination of iron in the chains with additional oxygen provides an energetically favorable means for the chains to branch or intersect with each other. Increased iron content should thus cause more branches, loops, and zig-zags (twins) in the chains.[243,263] On average such a

[261]G. Roth, G. Heger, B. Renker, J. Pannetier, V. Caignaert, M. Hervieu, and B. Raveau, *Z. Phys. B* **71,** 43 (1988).

[262]P. Bordet, J. L. Hodeau, P. Strobel, M. Marezio, and A. Santoro, *Solid State Commun.* **66,** 435 (1988).

[263]Y. Oda, H. Fujita, H. Toyoda, T. Kaneko, T. Kohara, I. Nakada, K. Asayama, *Jpn. J. Appl. Phys.* **26,** L1660 (1987).

structure has tetragonal symmetry, but microdomains of the orthorhombic structure are preserved. TEM studies have provided direct evidence for this microdomain formation.[261,262,264] Evidence has also been found for the clustering of iron along {110} planes in the crystal, as expected if iron atoms try to maximize their oxygen coordination.[262] The observed microdomain structure varies with iron concentration.[264] Below the critical concentration needed to form the tetragonal phase (as determined by x-ray diffraction), the structure is orthorhombic and the normal twinning behavior is observed, although the twin spacing is finer than that observed in iron-free 123. Above the critical concentration, the microdomain structure forms and becomes finer with increasing iron content. Similar behavior should be observed in cobalt- and gallium-substituted 123 if the explanation for the impurity-induced orthorhombic-to-tetragonal transition in these systems is the same, but so far microstructural studies of these materials have not been reported.

In iron- and cobalt-substituted 123, the *a* and *b* lattice parameters converge when only 1–3% of the copper is replaced.[242,244,250,265,266] In gallium-substituted 123, the lattice parameters converge more slowly and the tetragonal phase forms after 10% substitution.[247,267] The *a* and *b* lattice parameters also converge with nickel additions, but a multiphase region is reached before the tetragonal phase forms.[244] With zinc additions, the *a* and *b* lattice parameters first converge slightly and then the difference between them remains almost constant.[244,246]

The observation of microdomains in iron-doped 123 implies that the material remains orthorhombic beyond the concentration needed to form the tetragonal phase on a macroscopic scale. The question then remains as to how disordered the oxygen is in the orthorhombic microdomains. The macroscopic lattice parameters are deceptive since they reflect the influence of both the oxygen disorder and the strains that arise to accommodate microdomain formation. Indeed it is unclear whether or not there is a true phase transformation from an orthorhombic to a tetragonal structure. If there is an order-disorder transformation, it occurs at a higher iron concentration than that deduced from x-ray measurements of lattice constants. At the higher iron concentrations, where the microdomain size approaches unit cell dimensions, the microdomain model is no longer meaningful and the structure must

[264]Z. Hiroi, M. Takano, Y. Takeda, R. Kanno, and Y. Bando, *Jpn. J. Appl. Phys.* **27,** L580 (1988).

[265]J. Langen, M. Veit, M. Galffy, H. D. Jostarndt, A. Erle, S. Blumenröder, H. Schmidt, and E. Zirngiebl, *Solid State Commun.* **65,** 973 (1988).

[266]H. Obara, H. Oyanagi, K. Murata, H. Yamasaki, H. Ihara, M. Tokumoto, Y. Nishihara, and Y. Kimura, *Jpn. J. Appl. Phys.* **27,** L603 (1988).

[267]M. Hiratani, Y. Ito, K. Miyauchi, and T. Kudo, *Jpn. J. Appl. Phys.* **26,** L1997 (1987).

become truly tetragonal. The concentration at which this occurs is not known, but should depend on how the iron is distributed between the chain and plane sites and the degree to which the iron tends to cluster.

In addition to substitutions affecting oxygen ordering, the oxygen content of the unit cell may increase with increasing gallium, cobalt, or iron substitution to compensate for the higher oxidation state of the ions. Iodometric titration and neutron diffraction measurements of the oxygen content of cobalt- and iron-doped 123 confirm this trend, as seen in the plot of oxygen content versus degree of substitution given in Fig. 23.[244,250] It is possible that oxygen intercalates in the form of peroxide ions as proposed in rare-earth-substituted 123,[250] but at present there is no direct evidence for this.

The reason for the suppression of T_c in transition-element-doped 123 remains obscure. The substitution-induced orthorhombic-to-tetragonal transition suggests strong similarity to the behavior in the rare earth solid solution materials. There is no evidence, however, that the symmetry change itself is linked to the depression of T_c. Indeed, the material remains orthorhombic with zinc substitution, yet zinc shows the strongest effect on T_c. This behavior may reflect the tendency of zinc to substitute into the copper oxygen planes and so directly disrupt the superconductivity. In this respect it is particularly important to reconcile the conflicting data about the location of zinc in the structure.[245,246] Nickel substitution may have the same direct influence on superconductivity, since the existing diffraction data indicate that nickel substitution occurs

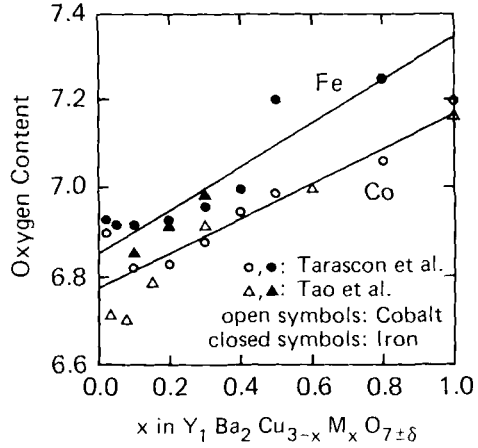

FIG. 23. Total oxygen content of $Y_1Ba_2Cu_{3-x}M_xO_{7\pm\delta}$ as a function of x for M = Co, Fe. Increasing substitution induces intercalation of oxygen into the structure. (Compilation of data from Tarascon *et al.*[244] and Tao *et al.*[250])

in the planes.[245] A possible effect of the trivalent iron, cobalt, and gallium ions on T_c is to alter the hole concentration in the material, as has been suggested for $La_{2-x}Sr_xCuO_{4-y}$[238] and the rare earth solid solution materials.[231] Measurements of hole concentrations in the different materials are needed to test this idea.

10. Substitutions of Other Cations

Sc, Ca, and Na can partially replace yttrium. For scandium, T_c drops only slightly with up to 75% replacement of yttrium.[268] Larger Sc concentrations then cause a rapid drop in T_c, and the material becomes nonsuperconducting if more than 81% of the yttrium is replaced. Data for Na substitution indicate that replacement of up to 60% of the yttrium is possible, but that T_c continuously drops with increasing substitution.[201,269] To explore further the relationship between hole concentration and T_c, attempts have been made deliberately to dope holes into the $Y_1Ba_2Cu_3O_{7-\delta}$ structure by substituting Ca into the Y site.[223,224,270] Doping with Ca alone depresses T_c, but since the oxygen content decreases with Ca doping, the total hole concentration is also reduced. A more extensive solid solution range for calcium is observed in the $La_{1-x}Ca_xBa_2Cu_3O_{7-\delta}$ and $Nd_{1-x}Ca_xBa_2Cu_3O_{7-\delta}$ systems, and again T_c is depressed on substitution.[223,270]

A wide variety of elements, including Ag,[271–273] Al,[244,274,275] Cr,[240,241,271] Li,[271] Mn,[241,271] Pt,[271] Ti,[240] and V[276] can substitute into the copper sites in $Y_1Ba_2Cu_3O_{7-\delta}$. In each case T_c is suppressed, and, to date, complete replacement of copper without the destruction of superconductivity has not been achieved. Silver and vanadium appear to have the least deleterious effect on superconductivity, but it is unclear whether

[268]B. R. Zhao, Y. H. Shi, Y. Lu, H. S. Wang, Y. Y. Zhao, and L. Li, *Solid State Commun.* **63,** 409 (1987).

[269]A. Fartash and H. Oesterreicher, *Solid State Commun.* **66,** 39 (1988).

[270]H. Uwe, T. Sakuda, H. Asano, T. S. Han, K. Yagi, R. Harada, M. Iha, and Y. Yokoyama, *Jpn. J. Appl. Phys.* **27,** L577 (1988).

[271]P. Strobel, C. Paulsen, and J. L. Tholence, *Solid State Commun.* **65,** 585 (1988).

[272]C. V. Tomy, A. M. Umarji, D. T. Adroja, S. K. Malik, R. Prasad, N. C. Soni, A. Mohan, and C. K. Gupta, *Solid State Commun.* **64,** 889 (1987).

[273]Y. Saito, T. Noji, A. Endo, N. Higuchi, K. Fujimoto, T. Oikawa, A. Hattori, and K. Furuse, *Jpn. J. Appl. Phys.* **26,** L832 (1987).

[274]J. P. Franck, J. Jung, and M. A. K. Mohamed, *Phys. Rev. B* **36,** 2308 (1987).

[275]T. Siegrist, L. F. Schneemeyer, J. V. Waszczak, N. P. Singh, R. L. Opila, B. Batlogg, L. W. Rupp, and D. W. Murphy, *Phys. Rev. B* **36,** 8365 (1987).

[276]S. X. Dou, A. J. Bourdillon, X. Y. Sun, J. P. Zhou, H. K. Liu, N. Savvides, D. Haneman, C. C. Sorrell, and K. E. Easterling, *J. Phys. C* **21,** L127 (1988).

or not these elements have an appreciable solubility in the structure, as both form multiphase materials.[271–273,276] Substitution of 1–2% aluminum causes the structure to become tetragonal.[244,275] X-ray diffraction studies of Al-doped single crystals found that Al substitutes for Cu in the Cu(1) chain sites.[275] Thus Al behaves in a similar manner to the trivalent and tetravalent transition metal ions.

There are few reports of substitution in the barium site other than the substitution of the larger lanthanide ions that have already been discussed. Most of the work has concentrated on the substitution of strontium for barium.[277–281] Up to 50% of the barium can be replaced by strontium, but the substitution is accompanied by a linear decrease in T_c with concentration.[277,278,280] Attempts to correlate T_c with oxygen content have been unsuccessful.[280] Some argue that the slightly smaller size of strontium perturbs the structure, causing a slight collapse in the copper-oxygen structure around the barium site, which lowers T_c.[278] Potassium had little effect on T_c when up to 10% of the barium was replaced.[282]

11. Oxygen Substitution

There have been several reports of oxygen substitutions causing dramatic increases in T_c. In particular, it was claimed that fluorine substitution produced a material with zero resistance at temperatures as high as 155 K.[283,284] Attempts to reproduce these results, however, have not been successful.[285–287] Solid-state reaction routes resulted in little

[277]T. Wada, S. Adachi, T. Mihara, and R. Inaba, *Jpn. J. Appl. Phys.* **26,** L706 (1987).

[278]B. W. Veal, W. K. Kwok, A. Umezawa, G. W. Crabtree, J. D. Jorgensen, J. W. Downey, L. J. Nowicki, A. W. Mitchell, A. P. Paulikas, and C. H. Sowers, *Appl. Phys. Lett.* **51,** 279 (1987).

[279]T. Wada, S. Adachi, O. Inoue, S. Kawashima, and T. Mihara, *Jpn. J. Appl. Phys.* **26,** L1475 (1987).

[280]A. Ono, T. Tanaka, H. Nozaki, and Y. Ishizawa, *Jpn. J. Appl. Phys.* **26,** L1687 (1987).

[281]Q. R. Zhang, L. Cao, Y. Qian, Z. Chen, Y. Zhao, G. Pang, H. Zhang, J. Xia, M. Zhang, D. Yu, Z. He, S. Sun, M. Fang, and T. Zhang, *Solid State Commun.* **63,** 535 (1987).

[282]I. Felner and B. Barbara, *Solid State Commun.* **66,** 205 (1988).

[283]S. R. Ovshinsky, R. T. Young, D. D. Allred, G. DeMaggio, and G. A. Van der Leeden, *Phys. Rev. Lett.* **58,** 2579 (1987).

[284]X. R. Meng, Y. R. Ren, M. Z. Lin, Q. Y. Tu, Z. J. Lin, L. H. Sang, W. Q. Ding, M. H. Fu, Q. Y. Meng, C. J. Li, X. H. Li, G. L. Qiu, and M. Y. Chen, *Solid State Commun.* **64,** 325 (1987).

[285]R. N. Bhargava, S. P. Herko, and W. N. Osborne, *Phys. Rev. Lett.* **59,** 1468 (1987).

[286]A. K. Tyagi, S. J. Patwe, U. R. K. Rao, and R. M. Iyer, *Solid State Commun.* **65,** 1149 (1988).

[287]P. K. Davies, J. A. Stuart, D. White, C. Lee, P. M. Chaikin, M. J. Naughton, R. C. Yu, and R. L. Ehrenkaufer, *Solid State Commun.* **64,** 1441 (1987).

or no fluorine substitution. When partial substitution was achieved, T_c remained the same or was slightly depressed. Sulphur[288] and nitrogen[289–291] substitution have also been reported to raise T_c, but again the results have not been confirmed and the effects are short lived. Another report indicates that some sulphur substitution can take place but that the substitution has no effect on T_c.[292]

In addition to studies of oxygen substitution by different atomic species, several studies were made of ^{18}O substitution to determine if the isotope shift in T_c expected for phonon-mediated superconductivity occurs in these materials. By a process of reduction followed by reannealing in ^{18}O gas, as much as 90% of the ^{16}O can be exchanged in the $Y_1Ba_2Cu_3O_{7-\delta}$ structure.[293–299] In studies where 75 to 90% of the ^{16}O was exchanged, decreases in T_c too small to be significant were observed.[293,294] In a third study, a significant decrease in T_c of 0.3—0.4 K on 90% exchange was detected, indicating that phonons may play an important role in the pairing mechanism.[295] It was suggested that the absence of an effect in earlier studies was caused by preferential substitution of the isotope into sites that did not influence the superconducting behavior.[296] Replies to this comment noted that this was unlikely in view of the large fraction of ^{16}O that was exchanged[297] and the evidence from Raman spectroscopy that a substantial fraction of the substituted ^{18}O occupies sites in the copper-oxygen planes.[298] Later results confirmed the presence of a small shift but again disagreed as to

[288]K. N. R. Taylor, D. N. Matthews, and G. J. Russell, *J. Cryst. Growth* **85,** 628 (1987).

[289]D. N. Matthews, A. Bailey, R. A. Vaile, G. J. Russell, and K. N. R. Taylor, *Nature* **328,** 786 (1987).

[290]D. D. Sarma, C. T. Simmons, and G. Kaindl, *Nature* **330,** 213 (1987).

[291]K. N. R. Taylor, G. J. Russell, D. N. Matthews, A. Bailey, and R. A. Vaile, *Nature,* **330,** 214 (1987).

[292]I. Felner, I. Nowik, and Y. Yeshurun, *Phys. Rev. B* **36,** 3923 (1987).

[293]B. Batlogg, R. J. Cava, A. Jayaraman, R. B. van Dover, G. A. Kourouklis, S. Sunshine, D. W. Murphy, L. W. Rupp, H. S. Chen, A. White, K. T. Short, A. M. Mujsce, and E. A. Rietman, *Phys. Rev. Lett.* **58,** 2333 (1987).

[294]L. C. Bourne, M. F. Crommie, A. Zettl, H. C. Loye, S. W. Keller, K. L. Leary, A. M. Stacy, K. J. Chang, M. L. Cohen, and D. E. Morris, *Phys. Rev. Lett.* **58,** 2337 (1987).

[295]K. J. Leary, H. C. Loye, S. W. Keller, T. A. Faltens, W. K. Ham, J. N. Michaels, and A. M. Stacy, *Phys. Rev. Lett.* **59,** 1236 (1987).

[296]M. Grimsditch, T. O. Brun, R. Bhadra, B. Dabrowski, D. G. Hinks, J. D. Jorgensen, M. A. Beno, J. Z. Liu, H. B. Schüttler, C. U. Segre, L. Soderholm, B. W. Veal, and I. K. Schuller, *Phys. Rev. Lett.* **60,** 752 (1988).

[297]A. Zettl and J. Kinney, *Phys. Rev. Lett.* **60,** 753 (1988).

[298]B. Batlogg, R. J. Cava, and M. Stavola, *Phys. Rev. Lett.* **60,** 754 (1988).

[299]H. Katayama-Yoshida, T. Hirooka, A. J. Mascarenhas, Y. Okabe, T. Takahashi, T. Sasaki, A. Ochiai, T. Suzuki, J. I. Pankove, T. Ciszek, and S. K. Deb, *Jpn. J. Appl. Phys.* **26,** L2085 (1987).

the magnitude of the shift.[299-301] Preparation of materials enriched in ^{135}Ba, ^{136}Ba, ^{63}Cu, or ^{65}Cu failed to detect any isotope shift associated with the cation lattice.[299,302-304] Although the detection of an isotope shift on oxygen substitution implies that phonons are involved in the pairing mechanism, the small magnitude of the shift suggests that additional interactions are also involved.

VI. Related Structures

The main reasons for studying related superconducting structures are largely the same as those for studying structural variants of 123, namely to determine which structural features play an important role in superconductivity and to look for materials with better superconducting properties. In this section, we describe the basic structures of three related families of copper-oxide-based superconductors: $La_{2-x}M_xCuO_{4-y}$ (M = Ba, Sr, or Ca), $Bi_2Ca_{n-1}Sr_2Cu_nO_{2n+4}$ ($n = 1$, 2, or 3), and $Tl_mCa_{n-1}Ba_2Cu_nO_{2(n+1)+m}$ ($m = 1$ or 2, $n = 1$, 2, or 3).

12. Lanthanum Copper Oxides

Bednorz and Müller[1,2] first discovered high-temperature superconductivity in barium-doped lanthanum copper oxide, $La_{2-x}Ba_xCuO_{4-y}$, a material that was studied previously by Michel and Raveau[305] for electrocatalytic applications. The room temperature structure of this phase is isomorphic to K_2NiF_4, body-centered tetragonal with space group *I4/mmm*. The structure is made by stacking alternate layers of perovskite, $LaCuO_3$, and rock salt, LaO, along the c axis such that the copper sites in one perovskite layer are aligned with the lanthanum sites in the next perovskite layer (Fig. 24).

A tetragonal-to-orthorhombic phase transition occurs in $La_{2-x}M_xCuO_{4-y}$ at low temperatures and/or low dopant

[300]H. C. Loye, K. J. Leary, S. W. Keller, W. K. Ham, T. A. Faltens, J. N. Michaels, and A. M. Stacy, *Science* **238,** 1558 (1987).

[301]D. E. Morris, R. M. Kuroda, A. G. Markelz, J. H. Nickel, and J. Y. T. Wei, *Phys. Rev. B* **37,** 5936 (1988).

[302]L. C. Bourne, A. Zettl, T. W. Barbee III, and M. L. Cohen, *Phys. Rev. B.* **36,** 3990 (1987).

[303]T. Hidaka, T. Matsui, and Y. Nakagawa, *Jpn. J. Appl. Phys.* **27,** L553 (1988).

[304]Q. Lin, Y. N. Wei, Q. W. Yan, G. H. Chen, P. L. Zhang, Z. G. Shen, Y. M. Ni, Q. S. Yang, C. X. Liu, T. S. Ning, J. K. Zhao, Y. Y. Shao, S. H. Han, and J. Y. Li, *Solid State Commun.* **65,** 869 (1988).

[305]C. Michel and B. Raveau, *Rev. Chim. Miner.* **21,** 407 (1984).

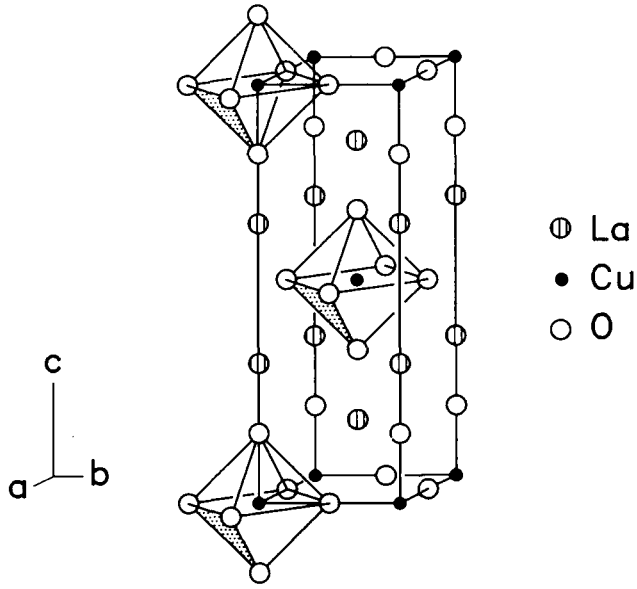

FIG. 24. The tetragonal La_2CuO_4 structure.

concentrations.[306–309] At the transition, adjacent CuO_6 octahedra tilt about the [110] direction in opposite directions, thereby buckling the CuO_2 planes and doubling the unit cell size. The orthorhombic unit cell, $\sim\sqrt{2}\,a_p \times \sim\sqrt{2}\,a_p \times c$, is related to the tetragonal cell, $a_p \times a_p \times c$, by a 45° rotation about the tetragonal c axis. By convention, for the orthorhombic space group *Cmca*, the long axis of the unit cell is the b axis (whereas it is the c axis in the tetragonal unit cell). The tetragonal-to-orthorhombic transition temperature changes dramatically with doping. For example, it varies from 533 K in undoped La_2CuO_{4-y}[306] to 12 K in $La_{1.8}Sr_{0.2}CuO_{4-y}$.[309] Fleming *et al.*[309] found that the structure is orthorhombic in the superconducting state and that the largest volume fraction of ideal diamagnetism occurs for compositions in which the tetragonal-to-orthorhombic transition temperature coincides with the

[306]J. M. Longo and P. M. Raccah, *J. Solid State Chem.* **6,** 526 (1973).

[307]V. B. Grande, Hk. Müller-Buschbaum, and M. Schweizer, *Z. Anorg. Allg. Chem.* **428,** 120 (1977).

[308]J. D. Jorgensen, H. B. Schüttler, D. G. Hinks, D. W. Capone II, K. Zhang, M. B. Brodsky, and D. J. Scalapino, *Phys. Rev. Lett.* **58,** 1024 (1987).

[309]R. M. Fleming, B. Batlogg, R. J. Cava, and E. A. Rietman, *Phys. Rev. B* **35,** 7191 (1987).

superconducting transition temperature. Fleming *et al.*[309] and others[310,311] concluded that the latter result is fortuitous; there does not appear to be a direct connection between this lattice instability and superconductivity. For clarity, it should be noted that the tetragonal-to-orthorhombic transition in $La_{2-x}M_xCuO_{4-y}$ caused by tilting of the CuO_6 octahedra is not related in any way to the orthorhombic-to-tetragonal transition in 123 caused by oxygen disordering on the basal copper planes.

At least one additional structural transition occurs in $La_{2-x}M_xCuO_{4-y}$ at very low temperatures. Early experimental and theoretical studies[312–314] found evidence for structural instability, possibly due to a monoclinic distortion. A more recent study[315] proposed that there is a transformation to a new tetragonal structure with space group $P4_2/ncm$. The role of these proposed transitions in superconductivity has yet to be established.

Like 123, the precise structure and resulting properties of $La_{2-x}M_xCuO_{4-y}$ depend sensitively on processing.[1,2,316–320] Many of the early studies examined the effects of changing the alkaline earth dopant and its concentration. Superconducting transition temperatures of 37, 32, and 17 K were found for Sr, Ba, and Ca, respectively, for $x \sim 0.15$.[320] It rapidly became evident, however, that oxygen and lanthanum deficiencies also affect superconducting properties. This point was brought out in studies of undoped $La_{2-\Delta}CuO_{4-y}$, which can be either a 40 K superconductor[321–323] or an antiferromagnetic insulator,[324–329] depending

[310]W. Weber, *Phys. Rev. Lett.* **58,** 1371 (1987).

[311]P. Böni, J. D. Axe, G. Shirane, R. J. Birgeneau, D. R. Gabbe, H. P. Jenssen, M. A. Kastner, C. J. Peters, P. J. Picone, and T. R. Thurston, *Phys. Rev. B* **38,** 185 (1988).

[312]S. C. Moss, K. Forster, J. D. Axe, H. You, D. Hohlwein, D. E. Cox, P. H. Hor, R. L. Meng, and C. W. Chu, *Phys. Rev. B* **35,** 7195 (1987).

[313]R. V. Kasowski, W. Y. Hsu, and F. Herman, *Solid State Commun.* **63,** 1077 (1987).

[314]D. McK. Paul, G. Balakrishnan, N. R. Bernhoeft, W. I. F. David, and W. T. A. Harrison, *Phys. Rev. Lett.* **58,** 1976 (1987).

[315]J. D. Axe, D. E. Cox, K. Mohanty, H. Moudden, A. R. Moodenbaugh, Y. Xu, and T. R. Thurston, *IBM J. Res. Develop.* (1989) (in press).

[316]S. Uchida, H. Takagi, K. Kitazawa, and S. Tanaka, *Jpn. J. Appl. Phys.* **26,** L1 (1987).

[317]H. Takagi, S. Uchida, K. Kitazawa, and S. Tanaka, *Jpn. J. Appl. Phys.* **26,** L123 (1987).

[318]C. W. Chu, P. H. Hor, R. L. Meng, L. Gao, Z. J. Huang, and Y. Q. Wang, *Phys. Rev. Lett.* **58,** 405 (1987).

[319]R. J. Cava, R. B. van Dover, B. Batlogg, and E. A. Rietman, *Phys. Rev. Lett.* **58,** 408 (1987).

[320]J. G. Bednorz, K. A. Müller, and M. Takashige, *Science* **236,** 73 (1987).

[321]J. Beille, R. Cabanel, C. Chaillout, B. Chevallier, G. Demazeau, F. Deslandes, J. Etourneau, P. Lejay, C. Michel, J. Provost, B. Raveau, A. Sulpice, J. L. Tholence, and R. Tournier, *C.R. Acad. Sci. Ser. 2* **304,** 1097 (1987).

[322]K. Sekizawa, Y. Takano, H. Takigami, S. Tasaki, and T. Inaba, *Jpn. J. Appl. Phys.* **26,** L840 (1987).

on the lanthanum and oxygen concentrations. Thus, the preparation of thermodynamically well-defined samples of these doped ternary oxides is just as difficult as the preparation of well-defined quaternary 123 samples, if not more so. The discovery of the 123 materials preempted many more quantitative studies of processing-structure-property relationships in the lanthanum copper oxides.

13. Bismuth-Containing Superconductors

In May 1987, Michel *et al.*[330] reported the discovery of superconductivity between 7 and 22 K in the Bi–Sr–Cu–O system. Because of the intense interest in the 90 K materials at that time, their report did not attract widespread interest. However, attention quickly focussed on the bismuth-containing superconductors in January 1988 when Maeda *et al.*[4] and Chu *et al.*[331] reported that adding Ca to the Bi–Sr–Cu–O system produced material that was superconducting above liquid nitrogen temperature. Three superconducting oxides were subsequently identified in the Bi–Ca–Sr–Cu–O system:[332–347] $Bi_2Sr_2Cu_1O_{6+x}$ ($T_c = 7 - 22$ K), $Bi_2Ca_1Sr_2Cu_2O_{8+x}$ ($T_c \sim 85$ K), and $Bi_2Ca_2Sr_2Cu_3O_{10+x}$ ($T_c \sim 110$ K). For brevity, these phases will be referred to as Bi2021, Bi2122, and Bi2223, respectively. The structures consist of perovskite-like units containing one, two, or three CuO_2 planes sandwiched between Bi–O bilayers (Fig. 25(d), (e), and (f)). Bi2021, the phase responsible for the results reported by Michel *et al.*[330] remains the least studied of the three because of its low transition temperature.[344,345]

[323]P. M. Grant, S. S. P. Parkin, V. Y. Lee, E. M. Engler, M. L. Ramirez, J. E. Vazquez, G. Lim, R. D. Jacowitz, and R. L. Greene, *Phys. Rev. Lett.* **58,** 2482 (1987).

[324]Y. Yamaguchi, H. Yamauchi, M. Ohashi, H. Yamamoto, N. Shimoda, M. Kikuchi, and Y. Syono, *Jpn. J. Appl. Phys.* **26,** L447 (1987).

[325]R. L. Greene, H. Maletta, T. S. Plaskett, J. G. Bednorz, and K. A. Müller, *Solid State Commun.* **63,** 379 (1987).

[326]D. Vaknin, S. K. Sinha, D. E. Moncton, D. C. Johnston, J. Newsam, C. R. Safinya, and H. E. King, Jr., *Phys. Rev. Lett.* **58,** 2802 (1987).

[327]S. Mitsuda, G. Shirane, S. K. Sinha, D. C. Johnston, M. S. Alvarez, D. Vaknin, and D. E. Moncton, *Phys. Rev. B* **36,** 822 (1987).

[328]T. Freltoft, J. P. Remeika, D. E. Moncton, A. S. Cooper, J. E. Fischer, D. Harshman, G. Shirane, S. K. Sinha, and D. Vaknin, *Phys. Rev. B* **36,** 826 (1987).

[329]D. C. Johnston, J. P. Stokes, D. P. Goshorn, and J. T. Lewandowski, *Phys. Rev. B* **36,** 4007 (1987).

[330]C. Michel, M. Hervieu, M. M. Borel, A. Grandin, F. Deslandes, J. Provost, and B. Raveau, *Z. Phys. B* **68,** 421 (1987).

[331]C. W. Chu, J. Bechtold, L. Gao, P. H. Hor, Z. J. Huang, R. L. Meng, Y. Y. Sun, Y. Q. Wang, and Y. Y. Xue, *Phys. Rev. Lett.* **60,** 941 (1988).

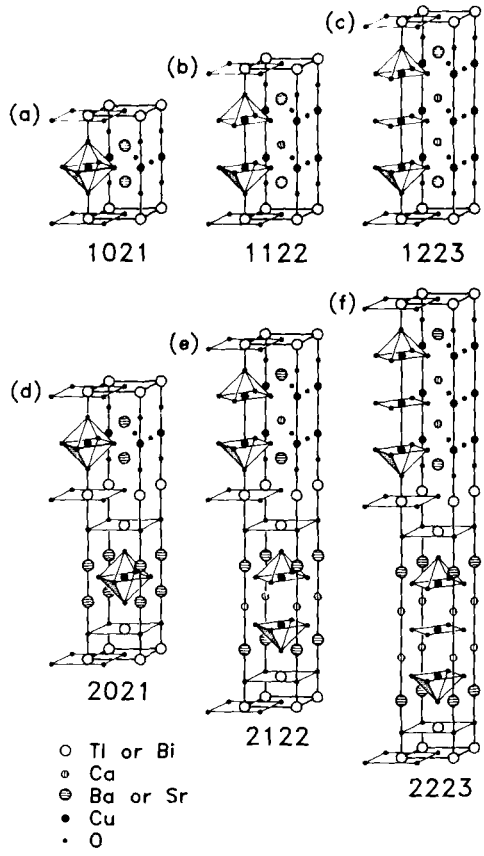

FIG. 25. Nominal unit cells for the bismuth- and thallium-containing superconductors: (a) $Tl_1Ba_2Cu_1O_5$, (b) $Tl_1Ca_1Ba_2Cu_2O_7$, (c) $Tl_1Ca_2Ba_2Cu_3O_9$, (d) $Tl_2Ba_2Cu_1O_6$, (e) $Tl_2Ca_1Ba_2Cu_2O_8$, and (f) $Tl_2Ca_2Ba_2Cu_3O_{10}$. Only the 2021, 2122, and 2223 structures form in the Bi–Ca–Sr–Cu–O system, whereas all six structures form in the Tl–Ca–Ba–Cu–O system. (Beyers *et al.*[366])

[332]R. M. Hazen, C. T. Prewitt, R. J. Angel, N. L. Ross, L. W. Finger, C. G. Hadidiacos, D. R. Veblen, P. J. Heaney, P. H. Hor, R. L. Meng, Y. Y. Sun, T. Q. Wang, Y. Y. Xue, Z. J. Huang, L. Gao, J. Bechtold, and C. W. Chu, *Phys. Rev. Lett.* **60,** 1174 (1988).

[333]Y. Bando, T. Kijima, T. Kitami, J. Tanaka, F. Izumi, and M. Yokoyama, *Jpn. J. Appl. Phys.* **27,** L358 (1988).

[334]Y. Matsui, H. Maeda, Y. Tanaka, and S. Horiuchi, *Jpn. J. Appl. Phys.* **27,** L361 (1988).

[335]E. Takayama-Muromachi, Y. Uchida, A. Ono, F. Izumi, M. Onoda, Y. Matsui, K. Kosuda, S. Takekawa, and K. Kato, *Jpn. J. Appl. Phys.* **27,** L365 (1988).

[336]M. A. Subramanian, C. C. Torardi, J. C. Calabrese, J. Gopalakrishnan, K. J. Morrissey, T. R. Askew, R. B. Flippen, U. Chowdhry, and A. W. Sleight, *Science* **239,** 1015 (1988).

Bi2122 has been the most extensively studied bismuth-containing superconductor.[332–344,347–358] The perovskite-like unit in Bi2122 is remarkably similar to that in 123; the Ca and Sr cations in Bi2122 play the same roles as the Y and Ba cations in 123. The linear chains in the 123 structure are replaced by the Bi–O bilayers, proving that linear chains are not essential for high-temperature superconductivity. Early on there was speculation that the atomic arrangements in Bi2122, especially in the

[337]D. R. Veblen, P. J. Heaney, R. J. Angel, L. W. Finger, R. M. Hazen, C. T. Prewitt, N. L. Ross, C. W. Chu, P. H. Hor, and R. L. Meng, *Nature* **332,** 334 (1988).

[338]J. M. Tarascon, Y. Le Page, P. Barboux, B. G. Bagley, L. H. Greene, W. R. McKinnon, G. W. Hull, M. Giroud, and D. M. Hwang, *Phys. Rev. B* **37,** 9382 (1988).

[339]T. M. Shaw, S. A. Shivashankar, S. J. La Placa, J. J. Cuomo, T. R. McGuire, R. A. Roy, K. H. Kelleher, and D. S. Yee, *Phys. Rev. B* **37,** 9856 (1988).

[340]S. A. Sunshine, T. Siegrist, L. F. Schneemeyer, D. W. Murphy, R. J. Cava, B. Batlogg, R. B. van Dover, R. M. Fleming, S. H. Glarum, S. Nakahara, R. Farrow, J. J. Krajewski, S. M. Zahurak, J. V. Waszczak, J. H. Marshall, P. Marsh, L. W. Rupp, Jr., and W. F. Peck, *Phys. Rev. B* **38,** 893 (1988).

[341]T. Kijima, J. Tanaka, Y. Bando, M. Onoda, and F. Izumi, *Jpn. J. Appl. Phys.* **27,** L369 (1988).

[342]P. Bordet, J. J. Capponi, C. Chaillout, J. Chenavas, A. W. Hewat, E. A. Hewat, J. L. Hodeau, M. Marezio, J. L. Tholence, and D. Tranqui, *Physica C* **153–155,** 623 (1988).

[343]P. Bordet, J. J. Capponi, C. Chaillout, J. Chenavas, A. W. Hewat, E. A. Hewat, J. L. Hodeau, M. Marezio, J. L. Tholence, and D. Tranqui, *Physica C* **156,** 189 (1988).

[344]J. B. Torrance, Y. Tokura, S. J. La Placa, T. C. Huang, R. J. Savoy, and A. I. Nazzal, *Solid State Commun.* **66,** 703 (1988).

[345]G. Van Tendeloo, H. W. Zandbergen, and S. Amelinckx, *Solid State Commun.* **66,** 927 (1988).

[346]H. W. Zandbergen, Y. K. Huang, M. J. V. Menken, J. N. Li, K. Kadowaki, A. A. Menovsky, G. Van Tendeloo, and S. Amelinckx, *Nature* **332,** 620 (1988).

[347]H. W. Zandbergen, P. Groen, G. Van Tendeloo, J. Van Landuyt, and S. Amelinckx, *Solid State Commun.* **66,** 397 (1988).

[348]Y. Matsui, H. Maeda, Y. Tanaka, and S. Horiuchi, *Jpn. J. Appl. Phys.* **27,** L372 (1988).

[349]E. A. Hewat, M. Dupuy, P. Bordet, J. J. Capponi, C. Chaillout, J. L. Hodeau, and M. Marezio, *Nature* **333,** 53 (1988).

[350]R. L. Withers, J. S. Anderson, B. G. Hyde, J. G. Thompson, L. R. Wallenberg, J. D. Fitzgerald, and A. M. Stewart, *J. Phys. C* **21,** L417 (1988).

[351]M. Onoda, A. Yamamoto, E. Takayama-Muromachi, and S. Takekawa, *Jpn. J. Appl. Phys.* **27,** L833 (1988).

[352]P. L. Gai and P. Day, *Physica C* **152,** 335 (1988).

[353]H. W. Zandbergen, W. A. Groen, F. C. Mijlhoff, G. Van Tendeloo, and S. Amelinckx, *Physica C* **156,** 325 (1988).

[354]S. Ikeda, H. Ichinose, T. Kimura, T. Matsumoto, H. Maeda, Y. Ishida, and K. Ogawa, *Jpn. J. Appl. Phys.* **27,** L999 (1988).

[355]G. Van Tendeloo, H. W. Zandbergen, J. Van Landuyt, and S. Amelinckx, *Appl. Phys. A* **46,** 153 (1988).

[356]G. S. Grader, E. M. Gyorgy, P. K. Gallagher, H. M. O'Bryan, D. W. Johnson, Jr., S. Sunshine, S. M. Zahurak, S. Jin, and R. C. Sherwood, *Phys. Rev. B* **38,** 757 (1988).

[357]H. Niu, N. Fukushima, and K. Ando, *Jpn. J. Appl. Phys.* **27,** L1442 (1988).

[358]A. K. Cheetham, A. M. Chippindale, and S. J. Hibble, *Nature* **333,** 21 (1988).

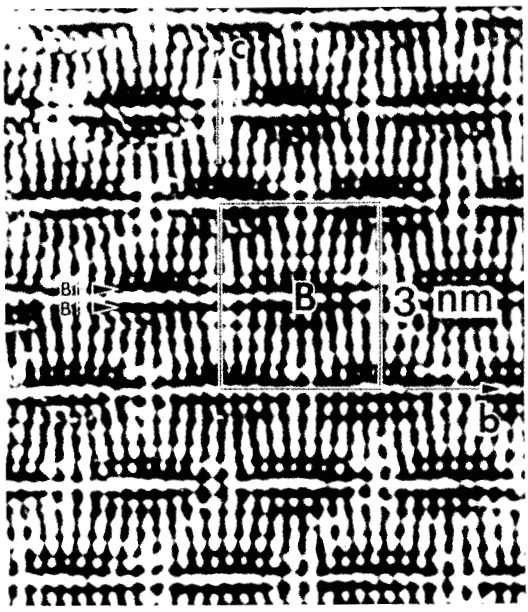

FIG. 26. High-resolution TEM image along the [100] directions in Bi2122 showing the incommensurate modulation. Lattice distortions and so-called "Bi-concentrated bands" (marked B) are easily seen. (Matsui *et al.*[348])

Bi–O bilayers, were the same as those in Aurivillius[359] phases, but this was shown later to be incorrect. Weak bonding between the Bi–O bilayers results in easy cleavage between these planes. The precise atomic arrangements in Bi2122 are more complicated than those indicated by the tetragonal subcell ($a_p \times a_p \times c$) in Fig. 25(d). TEM studies[332–334,336–339] found that the structure has an orthorhombic subcell ($\sim\sqrt{2}a_p \times \sim\sqrt{2}a_p \times c$) with a 25.8 Å ($\sim 5\sqrt{2}a_p$) incommensurate superlattice modulation present along the b axis (Fig. 26). Numerous studies[348–353] have tried to identify the source of the incommensurate structure, but the precise atomic arrangements giving rise to the modulation have yet to be unambiguously determined. Proposed sources include displacement of the Bi cations from their ideal sites to accommodate the mismatch between the perovskite-like units and the Bi–O bilayers,[347] incorporation of extra oxygen in the Bi–O bilayers,[349,353] periodic substitution of Bi by Sr, Ca, or vacancies,[339,348] and puckering of the CuO_2 planes that results in rotation of the individual CuO_5 polyhedra.[352] Two additional factors

[359]B. Aurivillius, *Arkiv. Kemi.* **1**, 463 (1949); **1**, 499 (1949); **2**, 519 (1950); and **5**, 39 (1952).

will complicate a complete determination of this crystal structure. First, high densities of intergrowths of perovskite-like units containing either one, three, or four CuO_2 planes are commonly found in Bi2122.[332,333,337,354,355] Second, there is a solid solubility range between Ca and Sr that may not extend to the ideal $Bi_2Ca_1Sr_2Cu_2O_8$ composition.[338,356,357] For the idealized $Bi_2Ca_1Sr_2Cu_2O_8$ structure, the average copper valence is +2 and the material is expected to be a Mott-Hubbard insulator. Several mechanisms to increase the copper valence have been proposed, including excess oxygen in the Bi–O bilayers[349,353] and Sr deficiency,[358] but this question cannot be resolved without better structure data.

The processing conditions required to form single phase or single crystal Bi2223 have yet to be determined.[360–362] Consequently, the structure and properties of this phase have not been studied extensively. The first Bi–Ca–Sr–Cu–O samples displayed sharp drops in resistance at ~110 K, but did not reach zero resistance above 100 K.[4,331] Susceptibility measurements indicated that two superconducting transitions were present in most samples, one at 85 K and the other at 110 K. Subsequent studies identified Bi2122 as the 85 K phase and linked the 110 K transition to the presence of the Bi2223 phase.[346,347] The connectivity between Bi2223 grains appears to be quite poor, because it is difficult to reach zero resistance at 110 K even in samples in which Bi2223 is the predominant phase. Unless the difficulties in preparing Bi2223 can be overcome, there is little chance for scientific or technical progress in studies of this phase.

14. Thallium-Containing Superconductors

Sheng and Hermann's[5] discovery of superconductivity above liquid nitrogen temperature in the Tl–Ba–Cu–O system in January 1988 was initially overshadowed by the breakthroughs in the Bi–Ca–Sr–Cu–O system. While numerous researchers struggled to achieve zero resistivity above 100 K in the bismuth system, Sheng and Hermann added Ca to their system and produced a Tl–Ca–Ba–Cu–O mixture that reached zero resistance at 107 K.[6] This result sparked numerous investigations of the

[360]J. M. Tarascon, Y. Le Page, L. H. Greene, B. G. Bagley, P. Barboux, D. M. Hwang, G. W. Hull, W. R. McKinnon, and M. Giroud, *Phys. Rev. B* **38,** 2504 (1988).

[361]H. Nobumasa, K. Shimizu, Y. Kitano, and T. Kawai, *Jpn. J. Appl. Phys.* **27,** L846 (1988).

[362]J. L. Tallon, R. G. Buckley, P. W. Gilberd, M. R. Presland, I. W. M. Brown, M. E. Bowden, L. A. Christian, and R. Goguel, *Nature* **333,** 153 (1988).

phases present in the Tl–Ca–Ba–Cu–O system.[363–384] Two superconducting phases were identified in Sheng and Hermann's[6] samples by Hazen *et al.*,[363] $Tl_2Ca_1Ba_2Cu_2O_{8+x}$ and $Tl_2Ca_2Ba_2Cu_3O_{10+x}$. Then Parkin *et al.*[364] changed the processing conditions to greatly increase the amount of the $Tl_2Ca_2Ba_2Cu_3O_{10+x}$ phase and produced a material with bulk supercon-

[363]R. M. Hazen, L. W. Finger, R. J. Angel, C. T. Prewitt, N. L. Ross, C. G. Hadidiacos, P. J. Heaney, D. R. Veblen, Z. Z. Sheng, A. El Ali, and A. M. Hermann, *Phys. Rev. Lett.* **60,** 1657 (1988).

[364]S. S. P. Parkin, V. Y. Lee, E. M. Engler, A. I. Nazzal, T. C. Huang, G. Gorman, R. Savoy, and R. Beyers, *Phys. Rev. Lett.* **60,** 2539 (1988).

[365]S. S. P. Parkin, V. Y. Lee, A. I. Nazzal, R. Savoy, R. Beyers, and S. J. La Placa, *Phys. Rev. Lett.* **61,** 750 (1988).

[366]R. Beyers, S. S. P. Parkin, V. Y. Lee, A. I. Nazzal, R. Savoy, G. Gorman, T. C. Huang, and S. La Placa, *Appl. Phys. Lett.* **53,** 432 (1988).

[367]S. S. P. Parkin, V. Y. Lee, A. I. Nazzal, R. Savoy, T. C. Huang, G. Gorman, and R. Beyers, *Phys. Rev. B* **38,** 6531 (1988).

[368]M. A. Subramanian, J. C. Calabrese, C. C. Torardi, J. Gopalakrishnan, T. R. Askew, R. B. Flippen, K. J. Morrissey, U. Chowdhry, and A. W. Sleight, *Nature* **332,** 420 (1988).

[369]C. C. Torardi, M. A. Subramanian, J. C. Calabrese, J. Gopalakrishnan, E. M. McCarron, K. J. Morrissey, T. R. Askew, R. B. Flippen, U. Chowdhry, and A. W. Sleight, *Phys. Rev. B* **38,** 225 (1988).

[370]C. C. Torardi, M. A. Subramanian, J. C. Calabrese, J. Gopalakrishnan, K. J. Morrissey, T. R. Askew, R. B. Flippen, U. Chowdhry, and A. W. Sleight, *Science* **240,** 631 (1988).

[371]S. Iijima, T. Ichihashi, and Y. Kubo, *Jpn. J. Appl. Phys.* **27,** L817 (1988).

[372]S. Iijima, T. Ichihashi, Y. Shimakawa, T. Manako, and Y. Kubo, *Jpn. J. Appl. Phys.* **27,** L837 (1988).

[373]S. Iijima, T. Ichihashi, Y. Shimakawa, T. Manako, and Y. Kubo, *Jpn. J. Appl. Phys.* **27,** L1054 (1988).

[374]S. Iijima, T. Ichihashi, Y. Shimakawa, T. Manako, and Y. Kubo, *Jpn. J. Appl. Phys.* **27,** L1061 (1988).

[375]D. S. Ginley, E. L. Venturini, J. F. Kwak, R. J. Baughman, M. J. Carr, P. F. Hlava, J. E. Schirber, and B. Morosin, *Physica C* **152,** 217 (1988).

[376]B. Morosin, D. S. Ginley, E. L. Venturini, P. F. Hlava, R. J. Baughman, J. F. Kwak, and J. E. Schirber, *Physica C* **152,** 223 (1988).

[377]B. Morosin, D. S. Ginley, P. F. Hlava, M. J. Carr, R. J. Baughman, J. E. Schirber, E. L. Venturini, and J. F. Kwak, *Physica C* **152,** 413 (1988).

[378]J. D. Fitz Gerald, R. L. Whithers, J. G. Thompson, L. R. Wallenberg, J. S. Anderson, and B. G. Hyde, *Phys. Rev. Lett.* **60,** 2797 (1988).

[379]P. Haldar, A. Roig-Janicki, S. Sridhar, and B. C. Giessen, *Mater. Lett.* (1988) (in press).

[380]H. W. Zandbergen, G. Van Tendeloo, J. Van Landuyt, and S. Amelinckx, *Appl. Phys. A* **46,** 233 (1988).

[381]Y. Shimakawa, Y. Kubo, T. Manako, Y. Nakabayashi, and H. Igarashi, *Physica C* **156,** 97 (1988).

[382]A. W. Hewat, E. A. Hewat, J. Brynestad, H. A. Mook, and E. D. Specht, *Physica C* **152,** 438 (1988).

[383]A. W. Hewat, P. Bordet, J. J. Capponi, C. Chaillout, J. Chenavas, M. Godinho, E. A. Hewat, J. L. Hodeau, and M. Marezio, *Physica C* **156,** 369 (1988).

[384]E. A. Hewat, P. Bordet, J. J. Capponi, C. Chaillout, J. Chenavas, M. Godinho, A. W. Hewat, J. L. Hodeau, and M. Marezio, *Physica C* **156,** 375 (1988).

ductivity at 125 K, the highest superconducting transition temperature yet found.

Six perovskite-related oxides have been identified in the Tl–Ca–Ba–Cu–O system thus far: $Tl_1Ba_2Cu_1O_5$, $Tl_1Ca_1Ba_2Cu_2O_7$, $Tl_1Ca_2Ba_2Cu_3O_9$, $Tl_2Ba_2Cu_1O_6$, $Tl_2Ca_1Ba_2Cu_2O_8$, and $Tl_2Ca_2Ba_2Cu_3O_{10}$ (Fig. 25). For brevity, these phases will be referred to as Tl1021, Tl1122, Tl1223, Tl2021, Tl2122, and Tl2223. Both the size and the separation of the Cu perovskite-like units can be independently varied in the thallium-containing superconductors. Tl2021, Tl2122, and Tl2223 are made up of Cu perovskite-like units containing one, two, and three CuO_2 planes separated by Tl–O *bilayers*, respectively, and are thallium analogs to the nominal Bi2021, Bi2122, and Bi2223 structures. Conversely, Tl1021, Tl1122, and Tl1223 are made up of Cu perovskite-like units containing one, two, and three CuO_2 planes separated by Tl–O *monolayers*, respectively, and have no bismuth analogs. All of the oxides have a tetragonal structure at room temperature. The oxides with Tl–O monolayers have primitive tetragonal cells, whereas the oxides with Tl–O bilayers have body-centered tetragonal cells. Tl2021 has two polymorphs, one face-centered orthorhombic and the other body-centered tetragonal. The nominal compositions and structures of these oxides are summarized in Table VI.[366]

Superlattice modulations have been observed in all of the structures except Tl1021. For Tl1122 and Tl1223 the wave vectors are $\langle 0.29, 0, 0.5\rangle$ type,[365–367] while for Tl2122 and Tl2223 the wave vectors are $\langle 0.17, 0, 1\rangle$ type.[366,367,378,380,382] The symmetry of these crystals remains tetragonal if the modulations are two-dimensional, but is lowered to orthorhombic if the modulations are one-dimensional. Both Tl2021 polymorphs contain superlattice modulations with an approximate wave vector $\langle \overline{0.16}, 0.08, 1\rangle$ in the tetragonal $a_p \times a_p$ setting [and $\langle \overline{0.08}, 0.24, 1\rangle$ in the orthorhombic $\sqrt{2}a_p \times \sqrt{2}a_p$ setting].[366,367,384] Taking the superlattice into account lowers the symmetry of these two structures to monoclinic, with the c axis being the unique axis. The superlattice modulations in the thallium-containing superconductors are distinct from those found in the related bismuth-containing superconductors and are much weaker in intensity. As for the bismuth-containing superconductors, the source of these modulations is still being investigated. Local distortions in the Tl–O layers are believed to be the most probable cause of the modulations in the materials with bilayer and trilayer Cu perovskite-like units. Recent neutron diffraction and high-resolution TEM studies[383,384] suggest that the modulations in both Tl2021 polymorphs arise from ordered vacancies on one-eighth of the Tl and O sites in the Tl–O layers.

The predominant defects in crystals with bilayer or trilayer Cu perovskite-like units are intergrowths.[364,366,367,371–373,380] High-resolution

TABLE VI. MEASURED PROPERTIES OF Tl–Ca–Ba–Cu OXIDES. (BEYERS *et al.*[366])

NAME	COMPOSITION	CRYSTAL STRUCTURE	LATTICE PARAMETERS (Å)	SUPERLATTICE WAVE VECTOR	T_c(K)
1021	$Tl_{1.2}Ba_2Cu_{0.7}O_{4.8}$	prim. tetragonal	$a = 3.869(2)$ $c = 9.694(9)$	[1]	[2]
1122	$Tl_{1.1}Ca_{0.9}Ba_2Cu_{2.1}O_{7.1}$	prim. tetragonal	$a = 3.8505(7)$ $c = 12.728(2)$	$\langle 0.29, 0, 0.5 \rangle$	80
1223	$Tl_{1.1}Ca_{1.8}Ba_2Cu_{3.0}O_{9.7}$	prim. tetragonal	$a = 3.8429(6)$ $c = 15.871(3)$	$\langle 0.29, 0, 0.5 \rangle$	110
2021	$Tl_{1.9}Ba_2Cu_{1.1}O_{6.4}$	f.c. orthorhombic	$a = 5.445(2)$ $b = 5.492(1)$ $c = 23.172(6)$	$\langle \overline{0.08}, 0.24, 1 \rangle$	[2]
	$Tl_{1.8}Ca_{0.02}Ba_2Cu_{1.1}O_{6.3}$	b.c. tetragonal[3]	$a = 3.8587(4)$ $c = 23.152(2)$	$\langle \overline{0.16}, 0.08, 1 \rangle$	20[4]
2122	$Tl_{1.7}Ca_{0.9}Ba_2Cu_{2.3}O_{8.1}$	b.c. tetragonal	$a = 3.857(1)$ $c = 29.39(1)$	$\langle 0.17, 0, 1 \rangle$	108
2223	$Tl_{1.6}Ca_{1.8}Ba_2Cu_{3.1}O_{10.1}$	b.c. tetragonal	$a = 3.822(4)$ $c = 36.26(3)$	$\langle 0.17, 0, 1 \rangle$	125

[1]No superlattice modulations have been observed in these crystals thus far.
[2]Non-metallic or weakly metallic samples with no superconducting transition observed down to 4.2 K.
[3]Taking the superlattice into account lowers the symmetry of this structure to monoclinic with the c axis being the unique axis.
[4]Refs. 363 and 369 report $T_c = 80$ K for tetragonal 2021.

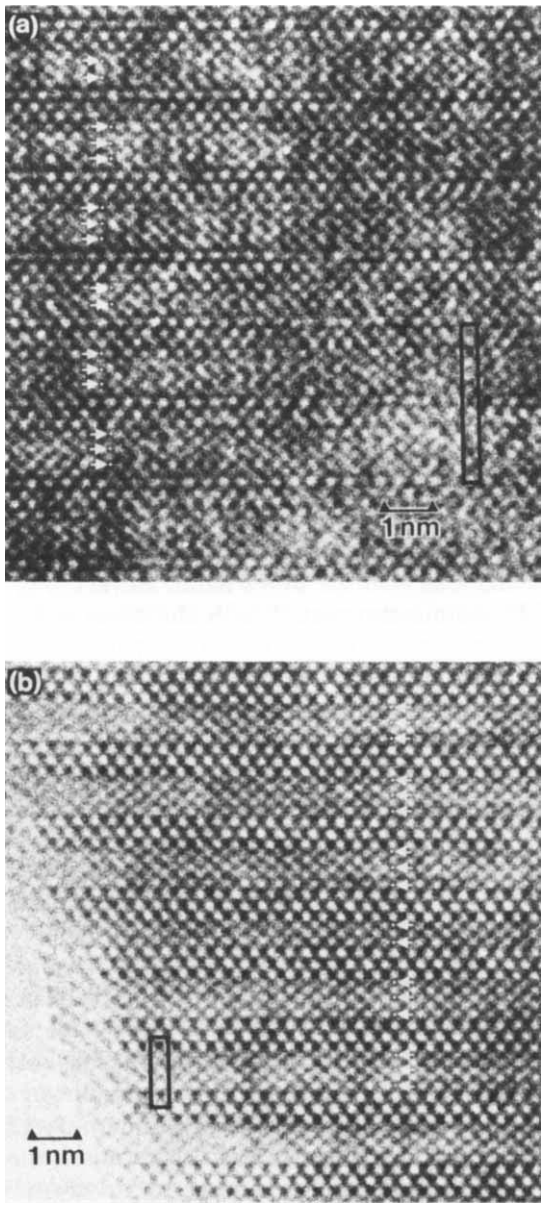

FIG. 27. High-resolution TEM images along the [100] direction in (a) Tl2223 and (b) Tl1223, showing bilayer Cu perovskite intergrowths. The black rectangles outline the unit cells and the white arrows point out the copper columns. (Beyers *et al.*[366])

TEM studies found a wide variety of intergrowths, each corresponding to the addition or deletion of a perovskite-like unit or a Tl–O layer from the ideal structure. The superconducting transition temperatures in these crystals vary with the density of stacking defects. For example, Parkin *et al.*[364] found that defect-free Tl2223 crystals have a T_c of 125 K, whereas Tl2223 crystals containing a high density of randomly distributed bilayer Cu perovskite intergrowths have a T_c of only 118 K [Fig. 27(a)]. Similarly, Beyers *et al.*[366] reported that randomly distributed Tl1122 intergrowths reduce the T_c of Tl1223 crystals from 110 K to 100 K [Fig. 27(b)] and the T_c of Tl2122 crystals from 108 K to 95 K. It is difficult to say whether it is the local change in structure or the change in composition produced by the intergrowths that affects the superconducting transition temperature because these are concurrent changes.

From a scientific viewpoint, the most interesting thallium-containing superconductors may turn out to be those containing single CuO_2 layers, Tl2021 and Tl1021. Hazen *et al.*[363] identified Tl2021 as the 80 K superconductor in Sheng and Hermann's[5] Tl–Ba–Cu–O samples. Torardi *et al.*[369] verified this result and found Tl2021 to be tetragonal with no superlattice modulations. On the other hand, Beyers *et al.*[366] found that tetragonal Tl2021 contained superlattice modulations and was only a 20 K superconductor, whereas orthorhombic Tl2021 was metallic, but not superconducting down to 4 K. No intergrowths were observed in either of the Tl2021 polymorphs examined by Beyers *et al.*[366] The structural differences between the 0, 20, and 80 K Tl2021 superconductors may provide important clues to the origin of superconductivity in these oxides. Wide variations in the transition temperatures in materials with the Tl1021 structure may also occur: Beyers *et al.*[366] found Tl1021 was not superconducting down to 4 K, whereas Haldar *et al.*[379] reported a transition temperature of 50 K in $(Tl, Bi)_1(Sr, Ca)_2Cu_1O_{4.5+x}$, which has the Tl1021 structure.

It is an idealization to treat the thallium-containing superconductors as line compounds (see Table VI).[366,367,368,370,382,383] The stacking defects are one way to accommodate off-stoichiometry in the metal cations. Microprobe analysis consistently shows thallium deficiency in the Tl–O bilayer phases, possibly indicating Tl–O monolayer intergrowths, whereas the reverse is found in the Tl–O monolayer phases.[366,367] Additionally, there may be deficiencies or substitutions on certain cation sites.[368,370,382,383] Diffraction studies of large single crystals are required before any definitive conclusions regarding site occupancy can be drawn. Furthermore, neutron diffraction and thermogravimetric studies of single phase or single crystal samples are needed to determine the absolute oxygen content in these oxides and its variation with processing. These

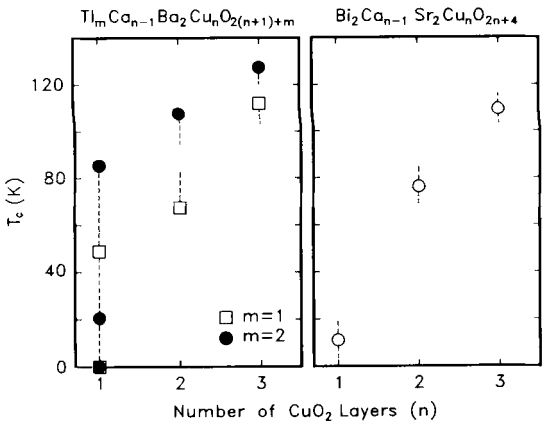

FIG. 28. Superconducting transition temperature versus the number of CuO_2 layers in the thallium- and bismuth-containing superconductors.

studies are required before more can be said about the average Cu oxidation state. Note, however, that the average Cu oxidation state in the ideal Tl–O monolayer structures varies from +3 in Tl1021 (not superconducting) to +2.33 in 1223 ($T_c = 110$ K), whereas the average Cu oxidation state is +2 for all of the ideal Tl–O bilayer structures.

In both the bismuth- and thallium-containing superconductors, the most obvious correlation between structure and properties is that the superconducting transition temperature increases with the number of CuO_2 layers in the perovskite-like unit (Fig. 28). Earlier comparisons of the 123 and $La_{2-x}M_xCuO_{4-y}$ structures led to speculation that this might be the case. Theorists are currently trying to determine if this trend can be explained by a simple density of states argument—i.e., increasing the number of CuO_2 layers increases the electronic density of states, which in turn increases T_c in a BCS formalism[385,386]—or if more elaborate explanations are required. The wide variation in superconducting properties in the Tl2021 phase alone implies that more than just the number of CuO_2 layers must be included in a rigorous theory. Experimentalists, on the other hand, are trying to fabricate materials with greater than three CuO_2 layers, such as $Tl_1Ca_3Ba_2Cu_4O_{11}$ and $Tl_2Ca_3Ba_2Cu_4O_{12}$. The observation of isolated intergrowths with greater than three CuO_2 layers in high-resolution images offers some hope that these structures may yet

[385]F. Herman, R. V. Kasowski, and W. Y. Hsu, *Phys. Rev. B* **38,** 204 (1988).
[386]R. V. Kasowski, W. Y. Hsu, and F. Herman, *Phys. Rev. B* **38,** 6470 (1988).

be formed in bulk quantities. Indeed, Ihara *et al.*[387,388] recently reported forming $Tl_1Ca_3Ba_2Cu_4O_{11}$ as a bulk, 122 K superconductor.

VII. Summary and Future Work

It is evident from the variety of behaviors exhibited by 123 after different processing conditions that the structure has considerable flexibility. The oxygen stoichiometry can be varied over a wide range, and different cations can be substituted at least partially into every site. Certain cation substitutions have extensive solid solution ranges. Structural and physical changes occur on heating and cooling, and numerous structural defects form. Because of this variability in the 123 structure, it is not surprising that a considerable amount of the experimental data from different researchers is quantitatively and in some cases qualitatively in conflict. The variability of the structure highlights the need for carefully controlled experiments to resolve these conflicts. The complexity of the structure renders difficult, if not impossible, the preparation of a series of samples in which a single aspect of the structure is changed. For example, substitution of even small amounts of iron can change the oxygen ordering, oxygen content, twin structure, and magnetic ordering in the structure. Thus characterization of only one aspect of the material can lead to misleading correlations. There is a clear need for further studies in which several complementary characterization techniques are applied to each sample in the study.

In spite of these difficulties, many aspects of the 123 structure have been resolved. The basic structure is well understood. The mechanism of the high-temperature orthorhombic-to-tetragonal transformation has been determined. The major defects in the structure have been identified and characterized.

A major challenge has been to link the basic features of the structure to the superconducting behavior. Most work in this area has focussed on determining the role of the chains versus the planes in superconductivity. Early speculation, based on the observation that only the orthorhombic form of $Y_1Ba_2Cu_3O_{7-\delta}$ is superconducting, suggested that continuous copper oxygen chains in the basal plane of the 123 structure were essential for superconductivity. It is now known that tetragonal forms of

[387]H. Ihara, R. Sugise, M. Hirabayashi, N. Terada, M. Jo, K. Hayashi, A. Negishi, M. Tokumoto, Y. Kimura, and T. Shimomura, *Nature* **334**, 510 (1988).

[388]H. Ihara, R. Sugise, K. Hayashi, N. Terada, M. Jo, M. Hirabayashi, A. Negishi, N. Atoda, H. Oyanagi, T. Shimomura, and S. Ohashi, *Phys. Rev. B* (1988) (in press).

the 123 structure can superconduct. Although short copper oxygen chains may still exist in the basal copper planes of the tetragonal 123 superconductors, they are probably not essential for superconductivity. The discovery of tetragonal 123 superconductors implies that it is the two-dimensional CuO_2 planes that are the essential structural feature needed for superconductivity. This conclusion is strongly supported by the observation of high-temperature superconductivity in the Bi–Ca-Sr–Cu–O and Tl–Ca–Ba–Cu–O structures, which contain copper-oxygen planes but no chains. A particularly compelling observation in this respect is the finding of 80 K superconductivity in the $Tl_1Ca_1Ba_2Cu_2O_7$ structure, which is essentially identical to the 123 structure except for the substitution of Tl for Cu in the basal plane sites and the replacement of Y by Ca.

The question remains as to what role the chains play in superconductivity. The experiments on reduced or cation-substituted materials show that the major structural effect of reduction or substitution is to change the oxygen arrangement in the basal copper plane. The structure of the CuO_2 planes remains unchanged unless direct substitution for copper in the planes occurs. These observations imply that the chains' role in superconductivity is primarily electronic. The problem, then, is to determine the mechanisms by which changes in oxygen content or substitution of aliovalent cations are electronically compensated for. Hole formation, oxygen intercalation, and peroxide formation have all been implicated as possible compensation mechanisms. Of these only hole concentration has been linked directly to T_c. Analysis of the total hole concentration requires independent measurements of each of these quantities. The problem is further complicated by the fact that there are two copper sites in the structure whose oxidation states can vary independently. Compensation for a substituted cation might change the concentration of holes in one location in the structure but not the other. Tokura *et al.*[223] used this possibility to rationalize the transition temperatures observed in samples with a wide range of oxygen contents and total charge on the non-copper cations. They suggested that hole formation occurs more easily in the basal copper plane so that the basal plane acts as a reservoir for charge at low hole concentrations. Only after a threshold concentration of holes forms is superconductivity induced in the CuO_2 planes.

The possibility that certain cation substitutions have a direct structural effect on superconductivity can not be completely ruled out. For example, the rapid suppression of T_c by the substitution of isovalent cations such as Zn or Ni suggests that they directly influence T_c by replacing the Cu in the CuO_2 planes. However, the conflicting reports

about the location of Zn in the structure need to be resolved. The decrease in T_c caused by the substitution of Sr for Ba also appears to be structural in origin, although an alternate explanation in which the difference in polarizability of the Ba and Sr ions changes the interaction between holes in the structure has been suggested.[389] Strong correlations between changes in certain bond lengths and T_c that occur with oxygen intercalation or cobalt substitution have also been noted. It is unclear, however, whether these changes are coincidental or are directly linked to T_c, since the charge compensation in the structure also changes in each case. The nature of any such direct structural effect remains unknown.

Defects in the structure, especially the twins, have been speculated to be directly linked to the superconducting behavior. This speculation seems unfounded, given the observation of superconductivity in untwinned tetragonal crystals. Defects, however, clearly influence secondary superconducting properties. In particular, the grain boundaries are responsible for the low critical current densities observed in polycrystalline 123. The sensitivity of critical current densities to defects probably results from the short coherence length in these materials. The disruption of superconductivity by grain boundaries is probably further aggravated by the large unit cell that necessitates the formation of defects with large cores of distorted structure. The challenge now is to develop fabrication techniques that minimize these detrimental effects. Twins and faults distort the structure less severely, and it seems likely that their influence on critical current densities will be small. Experiments in which the twin or fault densities are varied in materials with constant composition and oxygen content are needed to determine what effect these defects have on superconducting properties. It is also important to recognize that variations in defect structure and microstructure can influence the behavior during heat or oxygen treatments and possibly alter the distribution of substituted elements. Characterization of defect structures is therefore also essential in preparing materials for controlled experiments.

The same types of experiments used to determine the relationships among processing, structure, and superconductivity in 123 will surely be performed on the bismuth- and thallium-containing superconductors. For these quinary oxides, the preparation of samples under reproducible, thermodynamically well-defined conditions will be especially difficult. Consequently, the need to use complementary characterization techniques to derive quantitative processing-structure-property relationships will become all the more essential.

[389]M. Ronay and D. M. Newns, *Phys. Rev. B* (1988) (submitted).

ACKNOWLEDGMENTS

We thank our many colleagues within IBM Research for their stimulating discussions and collaborations throughout the past two years. We thank David Clarke, Frank Herman, Sam LaPlaca, Merril Shafer, and Jerry Torrance for their comments on the manuscript. One of the authors (R.B.) thanks Byung Tae Ahn, Turgut Gür, and Robert Huggins at Stanford University for their invaluable collaboration on the solid-state ionic studies and Robert Sinclair, also at Stanford, for his advice and for the use of his electron microscope.

Notes Added in Proof

Three new oxides have been discovered that may provide important clues to the role of various structural features in high-temperature superconductivity. First, Mattheiss *et al.*[1] and Cava *et al.*[2] found superconductivity near 30 K in a copperless oxide, $Ba_{1-x}K_xBiO_{3-\delta}$ ($x \sim 0.4$). This oxide has a cubic perovskite structure, with none of the two-dimensional features observed in the copper-based superconducting oxides. In $Ba_{1-x}K_xBiO_{3-\delta}$, potassium substitution on the barium site is used to dope the parent compound, $BaBiO_3$, whereas lead substitution on the bismuth site had been used previously to make the first known superconducting oxide, $BaPb_xBi_{1-x}O_3$ ($T_c = 13$ K).[3] It remains an open question whether the pairing mechanism in these oxides is the same as that in the copper-containing oxides.[4–7] The lack of magnetic ordering in $Ba_{1-x}K_xBiO_{3-\delta}$ appears to rule out a magnetically mediated pairing mechanism in the material.[7]

Second, Siegrist *et al.*[8] synthesized $Ca_{0.88}Sr_{0.14}CuO_2$, a structure that consists of infinite CuO_2 planes separated by Ca and Sr atoms. Its copper valence is +2 and the material is an insulator. It remains to be seen whether this material can be made metallic or superconducting by

[1]L. F. Mattheiss, E. M. Gyorgy, and D. W. Johnson Jr., *Phys. Rev. B* **37,** 3745 (1988).
[2]R. J. Cava, B. Batlogg, J. J. Krajewski, R. C. Farrow, L. W. Rupp, Jr., A. E. White, K. T. Short, W. F. Peck, Jr., and T. Y. Kometani, *Nature* **332,** 814 (1988).
[3]A. W. Sleight, J. L. Gillson, and P. E. Bierstedt, *Solid State Commun.* **17,** 27 (1975).
[4]T. M. Rice, *Nature* **332,** 780 (1988).
[5]D. G. Hinks, B. Dabrowski, J. D. Jorgensen, A. W. Mitchell, D. R. Richards, Shiyou Pei, and Donglu Shi, *Nature* **333,** 836 (1988).
[6]Shiyou Pei, N. J. Zaluzec, J. D. Jorgensen, B. Dabrowski, D. G. Hinks, A. W. Mitchell, and D. R. Richards, *Phys. Rev. B* (1988) (in press).
[7]Y. J. Uemura, B. J. Sternlieb, D. E. Cox, J. H. Brewer, R. Kadono, J. R. Kempton, R. F. Kiefl, S. R. Kreitzman, G. M. Luke, P. Mulhern, T. Riseman, D. L. Williams, W. J. Kossler, X. H. Yu, C. E. Stronach, M. A. Subramanian, J. Gopalakrishnan, and A. W. Sleight, *Nature* **335,** 151 (1988).
[8]T. Siegrist, S. M. Zahurak, D. W. Murphy, and R. S. Roth, *Nature* **334,** 231 (1988).

doping. If the material can be doped but does not become superconducting, then this result would imply that five- or six-coordinated, Jahn-Teller distorted copper ions, not just CuO_2 planes per se, are an essential structural feature for high-temperature superconductivity.[9]

Third, Cava *et al.*[10] discovered superconductivity near 70 K in a series of copper oxides with the general formula $Pb_2Sr_2ACu_3O_{8+\delta}$ where A = Y, La, Pr, Nd, Eu, Dy, Ho, Tm, or Lu plus Sr or Ca. This structure contains the same square pyramidal copper-oxygen planes that are found in 123 and in the bismuth- and thallium- containing superconductors.

[9]C. Greaves, *Nature* **334,** 193 (1988).

[10]R. J. Cava, B. Batlogg, J. J. Krajewski, L. W. Rupp, Jr., L. F. Schneemeyer, T. Siegrist, R. B. van Dover, P. Marsh, W. F. Peck, Jr., P. K. Gallagher, S. H. Glarum, J. H. Marshall, R. C. Farrow, J. V. Waszczak, R. Hull, and P. Trevor, *Nature* **336,** 211 (1988).